Survey of the high resolution infrared spectrum of methane (12CH4 and 13CH4): Partial vibrational assignment extended towards 12 000 cm−1

O. N. Ulenikov, E. S. Bekhtereva, S. Albert, S. Bauerecker, H. M. Niederer, and M. Quack

Citation: The Journal of Chemical Physics **141**, 234302 (2014); doi: 10.1063/1.4899263
View online: http://dx.doi.org/10.1063/1.4899263
View Table of Contents: http://scitation.aip.org/content/aip/journal/jcp/141/23?ver=pdfcov
Published by the AIP Publishing

Articles you may be interested in

Accurate first-principles calculations for 12CH3D infrared spectra from isotopic and symmetry transformations
J. Chem. Phys. **141**, 044316 (2014); 10.1063/1.4890956

Synchrotron-based far infrared study of the rotation-vibration-inversion spectrum of silacyclobutane below 500 cm−1: The v29 and v30 bands
J. Chem. Phys. **139**, 244305 (2013); 10.1063/1.4848676

The high-resolution infrared spectrum of DC4H from 450 to 1100 cm−1: Overtone, combination, and hot bands
J. Chem. Phys. **139**, 154308 (2013); 10.1063/1.4824656

Anharmonic force field and vibrational dynamics of CH2F2 up to 5000 cm−1 studied by Fourier transform infrared spectroscopy and state-of-the-art ab initio calculations
J. Chem. Phys. **136**, 214302 (2012); 10.1063/1.4720502

High-resolution Fourier transform infrared and cw-diode laser cavity ringdown spectroscopy of the v 2 +2v 3 band of methane near 7510 cm −1 in slit jet expansions and at room temperature
J. Chem. Phys. **116**, 6045 (2002); 10.1063/1.1433505

This article is copyrighted as indicated in the article. Reuse of AIP content is subject to the terms at: http://scitation.aip.org/termsconditions. Downloaded to IP: 129.132.218.57 On: Tue, 16 Dec 2014 16:10:57

Survey of the high resolution infrared spectrum of methane ($^{12}CH_4$ and $^{13}CH_4$): Partial vibrational assignment extended towards 12 000 cm^{-1}

O. N. Ulenikov,[1,2] E. S. Bekhtereva,[1,2] S. Albert,[1,3] S. Bauerecker,[1,4] H. M. Niederer,[1] and M. Quack[1,a)]

[1]*Physical Chemistry, ETH Zürich, CH-8093 Zürich, Switzerland*
[2]*Institute of Physics and Technology National Research, Tomsk Polytechnic University, Tomsk 634050, Russia*
[3]*Swiss Light Source, Paul-Scherrer-Institute, CH-5232 Villigen, Switzerland*
[4]*Institut für Physikalische und Theoretische Chemie, Technische Universität Braunschweig, D-38106 Braunschweig, Germany*

(Received 8 August 2014; accepted 2 October 2014; published online 16 December 2014)

We have recorded the complete infrared spectrum of methane $^{12}CH_4$ and its second most abundant isotopomer $^{13}CH_4$ extending from the fundamental range starting at 1000 cm^{-1} up to the overtone region near 12 000 cm^{-1} in the near infrared at the limit towards the visible range, at temperatures of about 80 K and also at 298 K with Doppler limited resolution in the gas phase by means of interferometric Fourier transform spectroscopy using the Bruker IFS 125 HR prototype (ZP 2001) of the ETH Zürich laboratory. This provides the so far most complete data set on methane spectra in this range at high resolution. In the present work we report in particular those results, where the partial rovibrational analysis allows for the direct assignment of pure ($J = 0$) vibrational levels including high excitation. These results substantially extend the accurate knowledge of vibrational band centers to higher energies and provide a benchmark for both the comparison with theoretical results on the one hand and atmospheric spectroscopy on the other hand. We also present a simple effective Hamiltonian analysis, which is discussed in terms of vibrational level assignments and ^{13}C isotope effects. © *2014 AIP Publishing LLC*. [http://dx.doi.org/10.1063/1.4899263]

I. INTRODUCTION

Methane is the prototypical hydrocarbon and of great importance for our understanding of chemical bonding, structure, and reactivity from the early days of chemistry.[1–7] Its current interest ranges from quantum dynamics and chemical reactions on potential hypersurfaces on the one hand[8–20] to atmospheric and astrophysical spectroscopy including its effects as a greenhouse gas on the other hand.[21–34] Methane combustion with a reaction enthalpy $\Delta_R H_0^0 \simeq -800$ kJ mol^{-1} is also among the largest chemical processes of mankind at a technical scale for energy production in the TJ range per year. On the other hand, the tiny energetic effects of parity violating potentials in the methane molecule in the range of fJ mol^{-1} have been discussed to be of interest for fundamental physics as well.[35,36]

Although there has been substantial spectroscopic work on methane for more than a century (see below), due to its obvious importance, the understanding of the high resolution infrared spectrum is incomplete to a surprising degree, particularly as far as the higher energy ranges of overtone absorption are concerned. Therefore, we have started some time ago, a major experimental effort to measure at high resolution the complete infrared spectrum of methane CH_4 and its stable isotopomers, and several aspects of our previous work on the spectra on various partially deuterated isotopomers have been reported in recent previous publications from this effort.[37–42] The analysis of the infrared spectrum of $^{12}CH_4$ and $^{13}CH_4$ is now fairly complete up to the energy range of the octad (i.e., below about 5000 cm^{-1}).[41–44] In the present work we carry out a partial analysis extending towards 12 000 cm^{-1}. Apart from the fundamental interest, the spectra of these two isotopomers are of obvious importance for the spectroscopy of the earth's atmosphere as well as the atmospheres of the other planets and some of their moons (in particular Titan[27–31]), as $^{12}CH_4$ and $^{13}CH_4$ are the two by far most abundant isotopomers of methane in a natural environment (with a ratio $[^{12}CH_4]$: $[^{13}CH_4] \simeq 99{:}1$).

Early infrared spectra of methane were already reported in the nineteenth and early twentieth century.[45–47] Rotationally resolved spectra of methane were recorded by Cooley in 1925.[48] In 1935, Nielsen and Nielsen reported the fine structure of rovibrational transitions in methane,[49] analyzed theoretically by Jahn in several papers.[50–53] Also higher overtone spectra were reported at high resolution in the "photographic infrared" above 8000 cm^{-1} and the early history is well told in Herzberg's book.[54]

Further experimental and theoretical progress was made in the early 1960s,[55–58] when there was also substantial effort towards the theory of spectra of spherical top molecules in general.[57–64] This work was extended towards analyses of the spectra of methane notably in Refs. 65–69. For the substantial body of subsequent work we refer to the recent paper of Albert *et al.*[43] as well as several articles in the *Handbook of High-Resolution Spectroscopy*[70–75] and Niederer's thesis.[41]

a)Author to whom correspondence should be addressed. Electronic mail: Martin@Quack.ch. Fax: 0041-44-6321021. Mailing address: ETH Zürich, Lab. für Physikalische Chemie, CH-8093 Zürich, Switzerland.

 © 2014 AIP Publishing LLC

This article is copyrighted as indicated in the article. Reuse of AIP content is subject to the terms at: http://scitation.aip.org/termsconditions. Downloaded to IP: 129.132.218.57 On: Tue, 16 Dec 2014 16:10:57

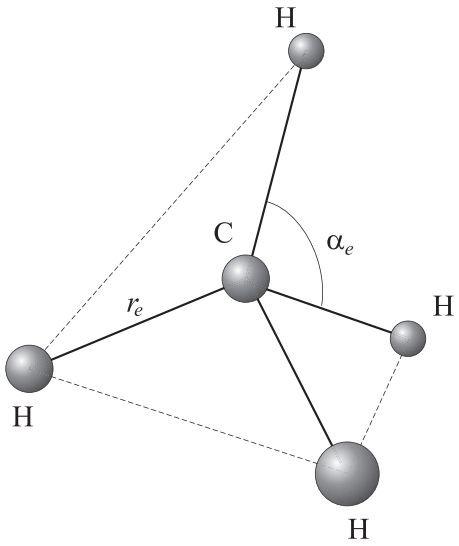

FIG. 1. Equilibrium structure of the CH_4 molecule with the equilibrium bond length r_e and angle α_e.

Methane CH_4 (Fig. 1) has tetrahedral symmetry with point group T_d and nine vibrational degrees of freedom corresponding to four normal frequencies. Two of these correspond to CH stretching ν_1 (A_1) nondegenerate and $\nu_3(F_2)$ triply degenerate and two of these to deformation (bending) vibrations, ν_2 (E) doubly degenerate, and ν_4 (F_2) triply degenerate. Because of the approximate relationship of fundamental wavenumbers $\tilde{\nu}_1 \simeq \tilde{\nu}_3 \simeq 2\tilde{\nu}_2 \simeq 2\tilde{\nu}_4 \simeq 3000$ cm^{-1} (see Table I) the fundamental and overtone and vibrational combination spectra can be grouped into polyads of interacting vibrational levels of similar energy. These polyads are characterized either by symbol P_n with the integer index n given by the sum[43]

$$n = 2v_1 + v_2 + 2v_3 + v_4 \quad (1)$$

which also can be represented as $(2, 1, 2, 1)(v_1, v_2, v_3, v_4)^t$, where (2,1,2,1) is then the "polyadstructure," or by polyad quantum number N defined by the sum[8,70,76]

$$N = v_1 + (v_2/2) + v_3 + (v_4/2) = n/2 \quad (2)$$

including integer and half odd integer polyad quantum numbers N. The v_i are the vibrational quantum numbers of the vibrational mode ν_i. The polyads are further named by greek prefixes corresponding to the number of overtone and combination levels, which they comprise (the ground state "monad" P_0, the dyad P_1 with 2 levels, the pentad P_2 with 5 levels, the octad P_3 with 8 levels, the tetradecad P_4 with 14 levels and the icosad P_5 with 20 levels, see Table I). Figure 2 provides an instructive survey of the clearly visible polyad structure of the absorption spectrum of methane in the range from 1000 cm^{-1} to 12 000 cm^{-1}. Up to the icosad the polyads are rather well separated in energy from each other, whereas there is increasingly important overlap for the higher polyads. Because the maximum degeneracy in T_d is 3 for sublevels of F symmetry, the more highly excited degenerate levels are further split into sublevels of well defined symmetry species in T_d (9 sublevels for the pentad, 24 for the octad, 60 for the tetradecad, 134 for the icosad, etc., see Table I). As Table I shows, the sublevels of a given symmetry species approximately approach a regular representation for large N (m(A_1):m(A_2):m(E):m(F_1):m(F_2) = 1:1:2:3:3) a result consistent with more general symmetry properties of the densities of states of polyatomic molecules at higher energy.[77] The spectrum of levels thus obviously gets very rich in the higher energy ranges. Strongly allowed transitions from the A_1 ground state occur to the F_2 sublevels. Due to the large rotational constant and due to vibrational and rovibrational interactions between sublevels, an exceedingly rich rovibrational structure is generated in the overtone and combination spectral region of the infrared spectrum of methane. A complete rovibrational assignment thus becomes a formidable task, so far completed for the $^{12}CH_4$ isotopomer up to the octad[43] and up to the pentad[44] for $^{13}CH_4$, now extended towards the octad.[41,42] While extension to higher polyads is possible, and recent work along these lines addresses the range of the tetradecad,[78] it is increasingly difficult to achieve similarly complete analyses for the higher polyads at the moment.

We have shown, however, that an alternative approach is possible to specifically address the assignment of excited vibrational levels without rotational excitation, if spectra at sufficiently low temperatures are available in order to unambiguously assign the $J' = 0 \leftarrow J'' = 1$ transition from the

TABLE I. Number of the vibrational states of different symmetry in the polyads $N \leq 4$.

n(P_n)	N	m(A_1)	m(A_2)	m(E)	m(F_1)	m(F_2)	Name of polyad[a]	m[b]	Range for $^{12}CH_4$[c]	Range for $^{13}CH_4$[c]
0	0	1	0	0	0	0	Monad (1)	1	0	0
1	1/2	0	0	1	0	1	Dyad (2)	2	1200–1630	1200–1630
2	1	3	0	2	1	3	Pentad (5)	9	2490–3170	2470–3170
3	3/2	4	2	5	5	8	Octad (8)	24	3770–4700	3750–4700
4	2	11	2	14	13	20	Tetradecad (14)	60	5020–6230	5000–6230
5	5/2	18	11	28	34	43	Icosad (20)	134	6270–7700	6230–7700
6	3	41	20	58	71	90	Triacontad (30)	280	7500–9250	7450–9250
7	7/2	64	45	112	148	169	Tetracontad (40)	538	8720–10 770	8660–10 770
8	4	126	81	204	272	313	Pentacontakaipentad (55)	996	9920–12 200	9850–12 200

[a]Numbers of levels in parentheses.
[b]Total number of sublevels.
[c]In cm^{-1}, fundamentals for $^{12}CH_4$ ($^{13}CH_4$) are $\tilde{\nu}_1(A_1) = 2916.481$ (2915.442) cm^{-1}, $\tilde{\nu}_2(E) = 1533.333$ (1533.493) cm^{-1}, $\tilde{\nu}_3(F_2) = 3019.493$ (3009.545) cm^{-1}, $\tilde{\nu}_4(F_2) = 1310.761$ (1302.781) cm^{-1}.

This article is copyrighted as indicated in the article. Reuse of AIP content is subject to the terms at: http://scitation.aip.org/termsconditions. Downloaded to IP: 129.132.218.57 On: Tue, 16 Dec 2014 16:10:57

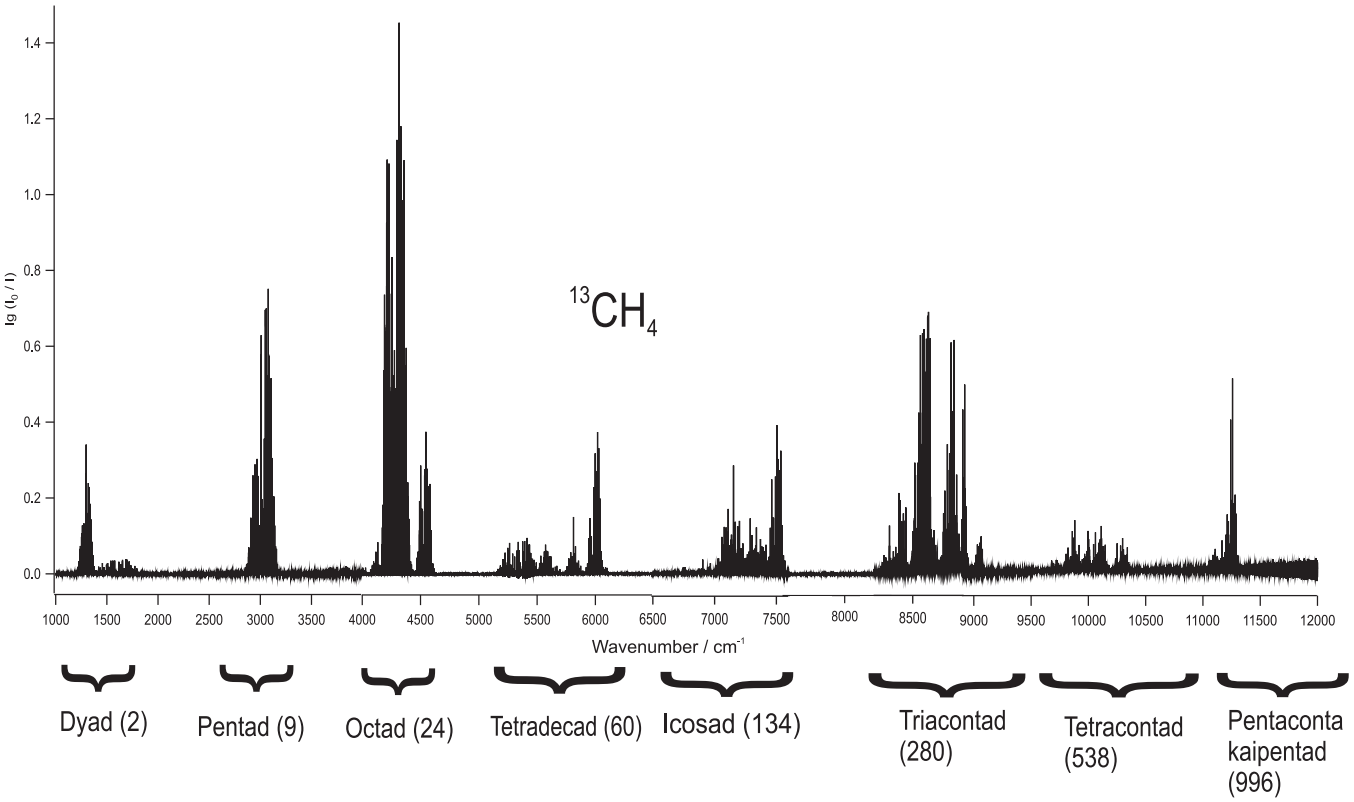

FIG. 2. Overview spectrum of $^{13}CH_4$ including the polyad structure of the spectrum shown as decadic absorbance $\lg(I_0/I)$. (1000–3600 cm^{-1}, dyad and pentad: l = 20 cm, p = 80 Pa, T = 298 K, 3600–6500 cm^{-1}, octad and tetradecad: l = 10 m, p = 280 Pa at mixing ratio $x = [CH_4]/([CH_4] + [He]) \approx 0.1$ and T = 80 K, 6500–8000 cm^{-1}, icosad: l = 10 m, p = 280 Pa at $x \approx 0.1$, T = 80 K, 8000–9500 cm^{-1}, triacontad: l = 15 m, p = 280 Pa at $x = \approx 0.5$, T = 80 K, 9500–12 000 cm^{-1}, tetracontad and pentacontakaipentad: l = 15 m, p = 480 Pa at $x \approx 0.1$, T = 80 K.) Under the conditions given here, the absorption patterns for the different polyads are well separated with "windows" in between. The numbers given in parenthesis after the polyad name indicate here the number of sublevels (Table I).

vibrational ground state to the vibrational level considered, as the energy of the $J'' = 1$ level in the ground state is well known.[42,67] This method of assignment has been used to assign the $\nu_2 + 2\nu_3$ vibrational level of $^{12}CH_4$ ($J = 0$, F_2 in T_d or F_1^- in S_4^*)[79–82] in the icosad (at 7510.3378 ± 0.003 cm^{-1}) on the basis of supersonic jet, continuous wave laser cavity ring down spectra.[80,82] We have more recently used this approach to assign a very large number of vibrational levels for CH_2D_2[39] as well as CH_3D and CHD_3[40] up to energies of about $E = (hc)12\,000$ cm^{-1}, using high resolution Fourier transform infrared (FTIR) spectroscopy of methane using enclosive flow cooling down to 80 K and He as a buffer gas.

In the present work, we extend this approach to the isotopomers $^{12}CH_4$ and $^{13}CH_4$ complementing the wavenumber range studied for these molecules up to 12 000 cm^{-1} (or about 1.5 eV of vibrational energy). A preliminary report on the present work was included in Refs. 41, 83, and 84. The outline of the present paper is roughly as follows. After a description of the experiments in Sec. II, we discuss briefly the symmetry properties of methane energy levels in Sec. III defining also our notation followed by a discussion of the approach used to assign the $J = 0$ pure vibrational levels from the spectra with some characteristic illustrations in Sec. IV. Section V describes the theoretical background for the effective Hamiltonian used in the vibrational analysis, based largely on the approach of Hecht.[57,58] Section VI provides the analysis and discussion for $^{12}CH_4$, and Sec. VII for $^{13}CH_4$. The conclusions from the present work are summarized in Sec. VIII.

II. EXPERIMENTAL

The FTIR spectra of $^{12}CH_4$ and $^{13}CH_4$ have been recorded in the wavenumber range from 1000 to 12 500 cm^{-1} with the Zürich FTIR spectrometer Bruker IFS 125 prototype 2001.[71,85–89] The nominal instrumental resolution, defined by $1/d_{MOPD}$ (maximum optical path difference) ranged from 0.0027 to 0.01 cm^{-1} resulting in almost Doppler limited spectra. The Doppler widths at 78 K range from about 0.004 cm^{-1} at 2800 cm^{-1} to 0.02 cm^{-1} at 12 500 cm^{-1}. About 100 to 1000 spectra were typically added in each spectral region. A multireflection collisional cooling cell based on White optics and embedded in a Dewar filled with liquid nitrogen was used for recording the cold spectra.[90] This cell is similar in design to the one described in Refs. 91–93. Optical path lengths ranging from 5 m to 15 m were used for the measurements. An InSb nitrogen cooled detector was used for the measurements between 2800 and 9000 cm^{-1} and a Si diode working at room temperature for the spectral range 9000–12 500 cm^{-1}. More details of the experimental setup and procedures can be found in Ref. 90.

This article is copyrighted as indicated in the article. Reuse of AIP content is subject to the terms at: http://scitation.aip.org/termsconditions. Downloaded to IP: 129.132.218.57 On: Tue, 16 Dec 2014 16:10:57

TABLE II. Experimental setup for the regions 1200–12 500 cm $^{-1}$ of the infrared spectrum of $^{12}CH_4$ and $^{13}CH_4$ (nominal resolution defined by $1/d_{MOPD}$).

Opt. filter (cm^{-1})	Resolution (cm^{-1})	Windows	Light source	Detector	Beamsplitter	Aperture (mm)	ν_{mirror} (kHz)	Electr. filter (cm^{-1})	Calib. gas
1200–1800	0.0015	KBr	Globar	MCT	KBr	1.0	40	500–3700	OCS[94]
1800–2300	0.0015	KBr	Globar	InSb	KBr	0.8	40	500–3700	OCS[94]
2300–2900	0.0015	KBr	Globar	InSb	CaF_2	0.8	40	500–3700	OCS[94]
2800–3600	0.0027	KBr	Globar	InSb	CaF_2	1.0	40	2600–3700	OCS[94]
3400–4400	0.0033	KBr	Tungsten	InSb	CaF_2	1.0	40	2800–5500	CH_4[95]
4100–6000	0.0033	KBr	Tungsten	InSb	CaF_2	1.0	40	3200–6300	CH_4[95]
5500–6200	0.0048	KBr	Tungsten	InSb	CaF_2	1.0	40	3600–7800	CH_4[95]
6100–8100	0.0037	KBr	Tungsten	InSb	CaF_2	0.8	40	3950–13800	CH_4[95]
8000–9500	0.01	KBr	Tungsten	InSb	CaF_2	1.15	40	3950–19740	CH_4[95]
8400–12500	0.01	KBr	Tungsten	Si diode	CaF_2	1.15	20	7840–39495	CH_4[95]

The $^{12}CH_4$ or $^{13}CH_4$ spectra assigned here were taken at about 80 K but we have also carried out measurements at room temperature for comparison. The total sample pressure of a mixture of $^{12}CH_4$ or $^{13}CH_4$ with He in the cell ranged from 2 to 4 mbar where the partial pressure of methane was in the order of 0.05–0.5 mbar to record weak absorption features in the spectra on the one hand and to take spectra without saturation of the strong absorption features on the other hand. Pressure broadening can be neglected under these conditions. All spectra were self-apodized. The aperture was in the range from 0.8 to 1.15 mm. Table II summarizes the experimental parameters. The spectra were calibrated with OCS at room temperature (2900–3600 cm^{-1})[94] and with $^{12}CH_4$ from 3000 to 12 500 cm^{-1}.[95,96] Methane, CH_4, as natural isotope mixture was obtained from PanGas with specified 99% chemical purity. The $^{13}CH_4$ sample was purchased from Cambridge Isotope Laboratories. The identity, chemical and isotopic purity (specified to be better than 98%) was obvious from the spectra.

The absolute wavenumber accuracy of nonblended, unsaturated and not too weak lines can be estimated to be about 10^{-4} cm^{-1} for the range from 2800 to 6600 cm^{-1} and about 10^{-3} cm^{-1} for the range from 6600 to 12 500 cm^{-1}, being limited essentially by the limited availability of sufficiently precise and accurate calibration spectra. The relative wavenumber accuracy is better than 10^{-6} cm^{-1} below 2000 cm^{-1} and between 10^{-5} cm^{-1} and 10^{-4} cm^{-1}, above 2000 cm^{-1}, depending upon the detailed spectral range and conditions. The graphs of the spectra shown are uncalibrated, the shift being hardly visible on this scale. The line positions reported here, however, correspond to calibrated values, which have adequate accuracy for the purpose of the present analysis. Figure 3 shows, as an example, the line shape of the isolated P(1) line and the corresponding part of the $\nu_2 + 2\nu_3$ (F_2) vibrational subband of the icosad near 7500 cm^{-1} for $^{13}CH_4$, indicating the level of very small pressure broadening, Doppler broadening, and self-apodisation in this spectral range.

III. SYMMETRY ASSIGNMENTS AND NOTATION

While vibrational and electronic wave functions can be conveniently assigned to the T_d point group symmetry species[54] and this is possible also for rovibrational levels,[97,98] a further reaching assignment is possible using the full permutation inversion group S_4^* following Longuet-Higgins.[74,79,82,99] $S_4^* = S_4 \otimes S^*$ is the direct product of the symmetric group S_4 of permutations of the four protons and the space inversion group S^* with elements E, E^* (or E, P), where E^* denotes the reflection of all coordinates at the origin (also denoted as parity operation P). Thus in S_4^* every species can be assigned a well defined parity (+ or −), whether the wave function is symmetric [+] or antisymmetric [−] with respect to reflection. Following Longuet-Higgins[99] the point group T_d can be associated with a subgroup of S_4^*, the molecular symmetry group M_{S24}. If the stereomutation tunneling of methane is very slow because of the high barrier of about 400 kJ mol^{-1},[11,12,35] the inversion sublevels occur as nearly degenerate pairs which, when classified in T_d or M_{S24}, generate an induced representation $\Gamma(M_{S24}) \uparrow S_4^*$ which defines the symmetry structure of the nearly degenerate sublevels (see Refs. 74, 77, and 79 for a detailed discussion).

Table III summarizes for convenience the symmetry species Γ in T_d and M_{S24} as being related to the subgroup T. It also gives the tunneling sublevel structure in terms of the induced representation $\Gamma(M_{S24}) \uparrow S_4^\star$. Here we use the standard point group character tables and notation for T and T_d[54] and the notation and character tables for M_{S24} and $S_4^\star$ from Refs. 74 and 79 which agrees with Ref. 100 but differs from Ref. 101 (for a critical discussion of different notations see Ref. 74). In our notation parity is given as a superscript (+ or –) and the species in the permutation group S_4 is given either in "spectroscopic" notation A_1, A_2, E, F_1, F_2 or in the group theoretical notation in terms of the partition [...,...] (see Refs. 74 and 102).

Further considerations arise through application of the generalized Pauli-principle to the four identical protons with nuclear spin $I_H = 1/2$. The corresponding $2^4 = 16$ nuclear spin functions generate a reducible representation $^5A_1^+(I = 2)$, $^1E^+(I = 0)$, $^3F_2^+(I = 1)$ where the upper left index indicates both the frequency of the corresponding species in the reduction and the M degeneracy relating to the combined total nuclear spin I of the four protons indicated in parentheses. Because of the approximate conservation of nuclear spin symmetry[79] one can identify three "nuclear spin isomers" in methane conventionally denoted as ortho ($^3F_2^+$, $I = 1$), meta

This article is copyrighted as indicated in the article. Reuse of AIP content is subject to the terms at: http://scitation.aip.org/termsconditions. Downloaded to IP: 129.132.218.57 On: Tue, 16 Dec 2014 16:10:57

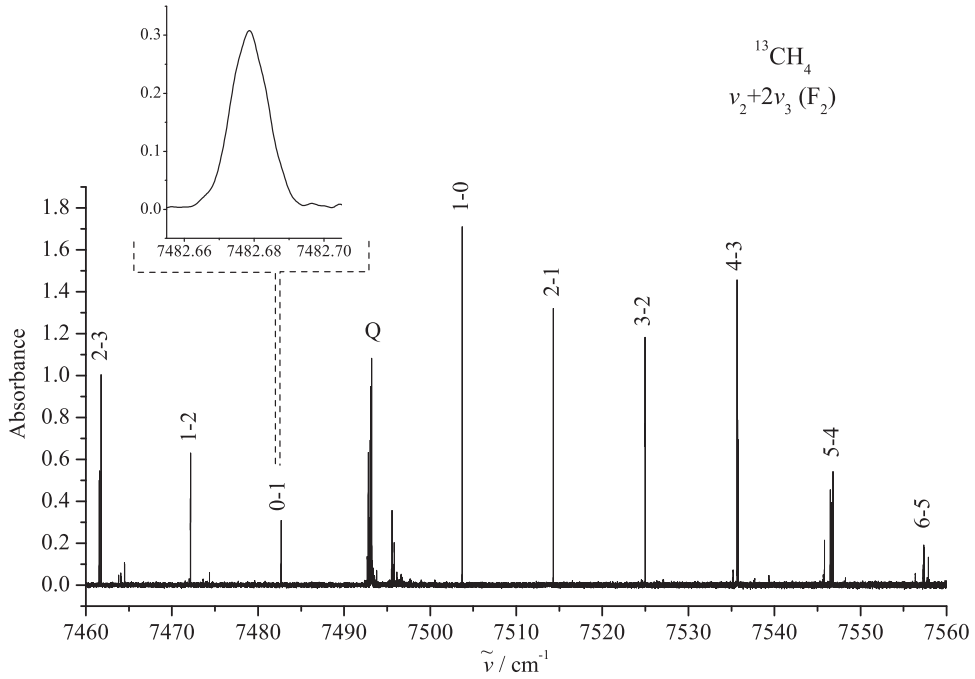

FIG. 3. High resolution spectrum of $^{13}CH_4$ as decadic absorbance $\lg(I_0/I)$ in the region of the $\nu_2 + 2\nu_3$ (F_2) band. The rotational quantum numbers, $J' \leftarrow J''$, connected by the transitions are indicated in the assignments on top of the lines. The transition $J' = 0 \leftarrow J'' = 1$ is easily visible which allows one to determine a highly accurate "experimental" value of the center of the $\nu_2 + 2\nu_3$ (F_2) band at 7510.337 cm^{-1} (see text). The total gas pressure is 280 Pa at a mixing ratio $x = [CH_4]/([CH_4] + [He])$ of about 0.1 and the optical path length is 10 m (T = 80 K).

($^5A_1^+$, $I = 2$), and para ($^1E^+$, $I = 0$). These spin isomers interconvert only slowly under ordinary conditions,[82,103,104] which justifies the name "isomer" (similar to ortho and para hydrogen[74,105,106]). The parity of the proton is positive, thus one has positive parity for the overall nuclear spin wave function as well. According to the generalized Pauli-Principle only nurovibrational states (i.e., complete states including nuclear spin, rotational, vibrational, and electronic wave functions) which transform as A_2^+ or A_2^- are allowed for the fermionic protons and thus the rovibrational states of the ortho isomer transform as F_1^+ or F_1^-, those of the meta isomer transform as A_2^+ or A_2^- and those of the para isomer as E^+ or E^- as also summarized in Table III.

It can be useful to take the parity of the carbon nucleus into account in the representation of the overall parity of the wave function. $^{12}_6C^{6+}$ has positive parity and nuclear spin zero, whereas $^{13}_6C^{6+}$ has negative parity and nuclear spin 1/2. Including this in the notation for Pauli allowed rovibrational symmetries one obtains the corresponding columns Γ_P in Table III. $^{13}CH_4$ levels have reversed parity compared to the corresponding $^{12}CH_4$ levels. We give also the overall degeneracies g_{12} and g_{13} of the levels under our conditions, where the hyperfine structure and the splittings of the E^+ and E^- levels are not resolved in the spectra commonly called "nuclear spin statistical weights," although the double weight for E^+/E^- pairs arises from parity doublets (not from nuclear spin). The electric dipole selection rules imply approximate conservation of nuclear spin symmetry and change of parity, thus one has the allowed transitions in S_4^* for CH_4

$$A_2^+ \leftrightarrow A_2^-, \tag{3}$$

$$E^+ \leftrightarrow E^-, \tag{4}$$

$$F_1^+ \leftrightarrow F_1^-. \tag{5}$$

TABLE III. Symmetry assignments for $^{12}CH_4$ and $^{13}CH_4$ in the groups T, T_d, M_{S24}, S_4^*.[a]

$\Gamma(T)$	$\Gamma(T_d)$	$\Gamma(M_{S24}) \uparrow S_4^*$	$[partition]^{Parity}$	$I(\Gamma_S)$	$\Gamma_P(^{12}CH_4)$	g_{12}	$\Gamma_P(^{13}CH_4)$	g_{13}
A	A_1	$A_1^+ + A_2^-$	$[4]^+ + [1^4]^-$	$2(A_1^+)$	A_2^-	5	A_2^+	10
A	A_2	$A_2^+ + A_1^-$	$[1^4]^+ + [4]^-$	$2(A_1^+)$	A_2^+	5	A_2^-	10
E	E	$E^+ + E^-$	$[2^2]^+ + [2^2]^-$	$0(E^+)$	$E^+ + E^-$	2	$E^+ + E^-$	4
F	F_1	$F_1^+ + F_2^-$	$[2, 1^2]^+ + [3, 1]^-$	$1(F_2^+)$	F_1^+	3	F_1^-	6
F	F_2	$F_2^+ + F_1^-$	$[3, 1]^+ + [2, 1^2]^-$	$1(F_2^+)$	F_1^-	3	F_1^+	6

[a] $\Gamma(T)$, $\Gamma(T_d)$, and $\Gamma(M_{S24})$ are the species in the corresponding groups, $\Gamma(M_{S24}) \uparrow S_4^*$ is the induced representation and tunneling sublevel structure, $[partition]^{Parity}$ gives the partition of the permutation and parity (+ and –) as right exponent, $I(\Gamma_S)$ gives the total nuclear spin for the 4 protons and the species of the nuclear spin wave function, $\Gamma_P(^{12}CH_4)$ and $\Gamma_P(^{13}CH_4)$ give the Pauli allowed rovibrational species including the parity of the carbon nucleus for $^{12}CH_4$ and $^{13}CH_4$ (thus also overall parity), g_{12} and g_{13} give statistical weights of the levels with unresolved hyperfine and parity doublet splittings for $^{12}CH_4$ and $^{13}CH_4$.

This article is copyrighted as indicated in the article. Reuse of AIP content is subject to the terms at: http://scitation.aip.org/termsconditions. Downloaded to IP: 129.132.218.57 On: Tue, 16 Dec 2014 16:10:57

Table III summarizes all the relevant information concerning symmetry selection rules and statistical weights for $^{12}CH_4$ and $^{13}CH_4$.

IV. ANALYSIS OF THE ($J' = 0$) LEVELS

Figures 4–7 show more detailed survey spectra of $^{12}CH_4$ and $^{13}CH_4$, in the region 1200 to 12 000 cm^{-1} at 80 K. In the higher wavenumber ranges, one can see very strong absorption in the regions 5500–6200 and 6800–7600 cm^{-1} where the bands of the polyads $N = 2$ and 2.5 are located. Pronounced absorption lines can also be seen in the regions of location of the polyads $N = 3$, 3.5, and 4, in the ranges 8300–9000 cm^{-1}, 9700–10 500 cm^{-1}, and around 11 300 cm^{-1}. Figures 3, 8, and 9 illustrate also the differences between the $^{12}CH_4$ and $^{13}CH_4$ spectra visible as a shift of the $^{13}CH_4$ lines compared to the $^{12}CH_4$ lines, although also the rovibrational fine structure may differ significantly for the two isotopomers.

From the ground state only vibrational transitions to levels of F_2 symmetry species are strongly allowed in absorption. However, one expects numerous resonance interactions as found in the lower *N*-polyads (see, e.g., Ref. 43 and references cited therein). These can perturb the rotational structure of the allowed F_2 bands, but also contribute to the appearance of bands with A_1, A_2, E, or F_1 vibrational symmetry in the upper level, by rovibrational interactions. Therefore, in general, an assignment of all lines is needed in a careful step-by-step rovibrational analysis in order to obtain the vibrational band centers and rovibrational parameters. However, in some spectral regions, where the spectrum is not too complex, even a simple approximate assignment provides the possibility to obtain beyond doubt the centers ($J = 0$ energy levels) of the F_2-type vibrational bands.

Figures 3 and 10 illustrate the assignment procedure, for instance, for the $\nu_2 + 2\nu_3(F_2)$ combination band of $^{13}CH_4$ which follows the corresponding study for $^{12}CH_4$ in a supersonic jet.[80,82] The line series in Figure 3 is first approximately assigned with the main goal of identifying the isolated $P(1)$ line, corresponding to the $J' = 0 \leftarrow J'' = 1$ transition to the relevant vibrational level. Using the level scheme of Figure 10 one obtains the upper level by adding the very well known ground state energy, $E = (hc) \cdot 10.48164867$ cm^{-1} ($^{12}CH_4$) or $E = (hc) \cdot 10.48213260$ cm^{-1} (for $^{13}CH_4$), Refs. 41, 42, and 107. It may be noted here that the total parities are reverted here compared to the similar diagram in Refs. 80 and 81, because the ^{13}C nucleus has negative parity, whereas the ^{12}C nucleus has positive parity as have also the protons (see Ref. 74).

Figure 8 gives for comparison a similar survey for the $^{12}CH_4$ isotopomer, which illustrates very nicely the $^{13}C/^{12}C$ isotope shift for the $\nu_2 + 2\nu_3$ (F_2) bands. It should be noted here that the vibrational labeling using the normal modes ν_1, ν_2, ν_3, ν_4 is only an approximate assignment due to the strong interaction between several vibrational states.

Figure 9 shows the central part of the $2\nu_3$ (F_2) band of $^{12}CH_4$ and $^{13}CH_4$ as a further example for the assignment. These bands provide an excellent illustration of the fairly simple and regular structures which can be used in the assignments of further bands. This type of band is characterized by a fairly pronounced and dense set of *Q* branch lines and a regular structure of patterns separated by approximately $2B$ in the *P* and *R* branches. The $P(1)$ line is isolated and weaker than the cluster of *Q* branch lines and the cluster of $P(2)$ and $P(3)$ lines. These features are frequently sufficient to provide an unambiguous assignment of the $P(1)$ line, even if the *Q* branch lines and the higher $P(J'')$ and $R(J'')$ line clusters are complex and not easily assigned in detail. Obviously low temperature spectra greatly simplify the assignments.

For low *J*, the transition wavenumber can be expressed approximately as[54]

$$\tilde{\nu} = \tilde{\nu}_0 - (B' + B'' - 2B'\theta)m + (B' - B'')m^2, \qquad (6)$$

where B' is the rotational constant for the upper and B'' for the lower state and where $m = J + 1$ for the R branch and $m = -J$ for the P branch. The Coriolis coefficient (θ) describes the Coriolis interaction between the F sublevels. If the Coriolis interaction can be neglected, the spacing between the levels is just twice the rotational constant to a first approximation and the line structure is relatively simple which is mostly the case upon excitation of ν_1, ν_2, and ν_3 as shown in Figures 3, 8, and 9.

However, if the Coriolis interaction cannot be neglected ($\theta \neq 0$) the absorption patterns are more complicated as is the case upon excitation of ν_4. As an example we present here the fundamental ν_4 in Figure 11. As one can see the identification of the P(1) line is much more difficult but still possible. For a more detailed description we refer to Refs. 51 and 108.

When the ν_4 mode is excited, the θ_4-dependent contributions according to Eq. (6) are important, and the spectrum shows patterns as the ones shown in Figure 11. In this case, the distance between the centers of multiplets in the *R*-branch is decreased approximately by a factor of 2. The *Q*-branch is not as narrow as for the first type of F_2 bands, and it is overlapped considerably with the *P*-branch.

As further examples, now for high vibrational excitations, we present the $2\nu_1 + \nu_3$ (F_2) bands of $^{12}CH_4$ and $^{13}CH_4$ in Fig. 12 as well as the $\nu_1 + \nu_2 + 2\nu_3$ (F_2) bands of $^{12}CH_4$ (Fig. 13) and $^{13}CH_4$ (Fig. 14). As one can see the spectrum above 10 000 cm^{-1} is rather congested. In addition, due to the use of the Si diode the noise level at wavnumbers above 10 000 cm^{-1} is higher than at the lower wavenumbers. Appendix A gives a complete set of spectra and assignments as obtained in the present work and published in detail in the supplementary material.[109]

As a result of the analysis we identified numerous vibrational levels for both isotopomers $^{12}CH_4$ and $^{13}CH_4$. Their band centers as determined using the P(1) line assignment are summarized in Tables IV and V together with further band centers previously obtained from rotational analyses using effective Hamiltonians, as specified in the references given in the tables.

As mentioned before the values of the band centers at $J' = 0$ (upper vibrational energy levels) have been determined from the experimental ($J' = 0 \leftarrow J'' = 1$) transitions by adding the rotational ground state energy value $E_{(J=1,F_1)}$

This article is copyrighted as indicated in the article. Reuse of AIP content is subject to the terms at: http://scitation.aip.org/termsconditions. Downloaded to IP: 129.132.218.57 On: Tue, 16 Dec 2014 16:10:57

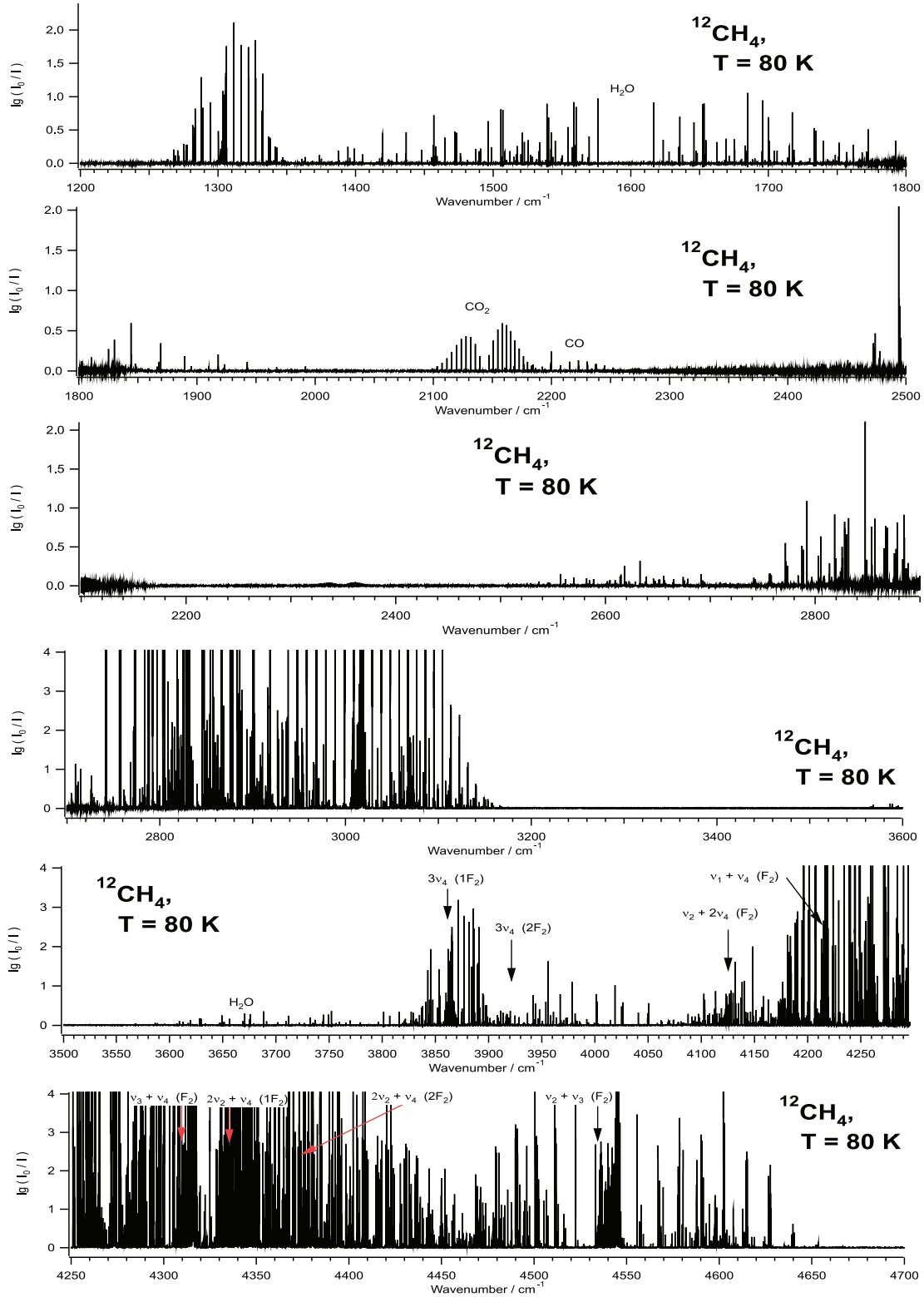

FIG. 4. Survey spectrum as decadic absorbance $\lg(I_0/I)$ of $^{12}CH_4$ in the region 1200–4700 cm^{-1}. Experimental conditions are presented in Table II. The total gas pressure is 280 Pa at mixing ratios $x = [CH_4]/([CH_4] + [He])$ of about 0.005 and 0.1 and the optical path length is 5 m. Some ranges show strongly saturated spectra in order to make weak lines appear (T = 80 K).

equal to 10.48164867 cm^{-1} for $^{12}CH_4$ or 10.48213260 cm^{-1} for $^{13}CH_4$. The list of the P(1) lines of $^{12}CH_4$ obtained from the analysis of the experimental data is presented in column 2 of Table IV. Column 4 of that table gives the values of the corresponding vibrational term values calculated from ($J' = 0 \leftarrow J'' = 1$) transitions by adding the rotational ground state energy for $J'' = 1$. In addition, results from previous work are provided in columns 3 and 5.

Appendix A with the supplementary material[109] presents the central parts of all bands from Table IV ($J' \leftarrow J''$

This article is copyrighted as indicated in the article. Reuse of AIP content is subject to the terms at: http://scitation.aip.org/termsconditions. Downloaded to IP: 129.132.218.57 On: Tue, 16 Dec 2014 16:10:57

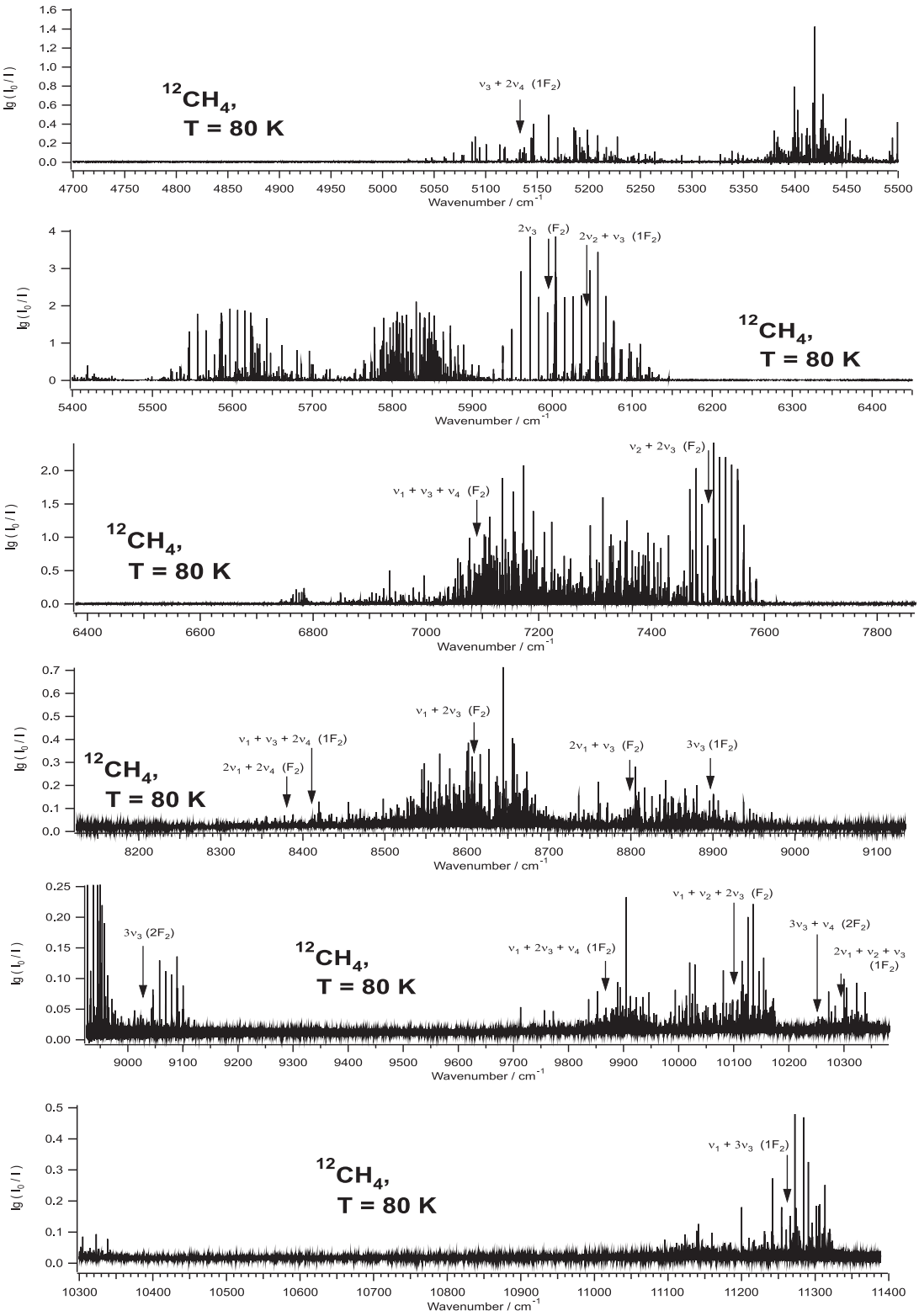

FIG. 5. Survey spectrum as decadic absorbance $\lg(I_0/I)$ of $^{12}CH_4$ in the region 4700–11 400 cm^{-1}. Experimental conditions are presented in Table II. The total gas pressure is 280 Pa and 480 Pa at mixing ratios $x = [CH_4]/([CH_4] + [He])$ of about 0.1 and the optical path length is 10 and 15 m. Some ranges show strongly saturated spectra in order to make weak lines appear (T = 80 K).

transitions with low values of quantum number J are marked in some cases also). In all figures which correspond to the bands located in the region above 5000 cm^{-1}, one can see clearly the pronounced structures discussed above, which characterize the F_2-type bands of the CH_4 spectra. Of course, the presence of strong resonance interactions with numerous other vibrational states, may considerably complicate the picture of the central part of the F_2 bands (there are 615 levels of

This article is copyrighted as indicated in the article. Reuse of AIP content is subject to the terms at: http://scitation.aip.org/termsconditions. Downloaded to IP: 129.132.218.57 On: Tue, 16 Dec 2014 16:10:57

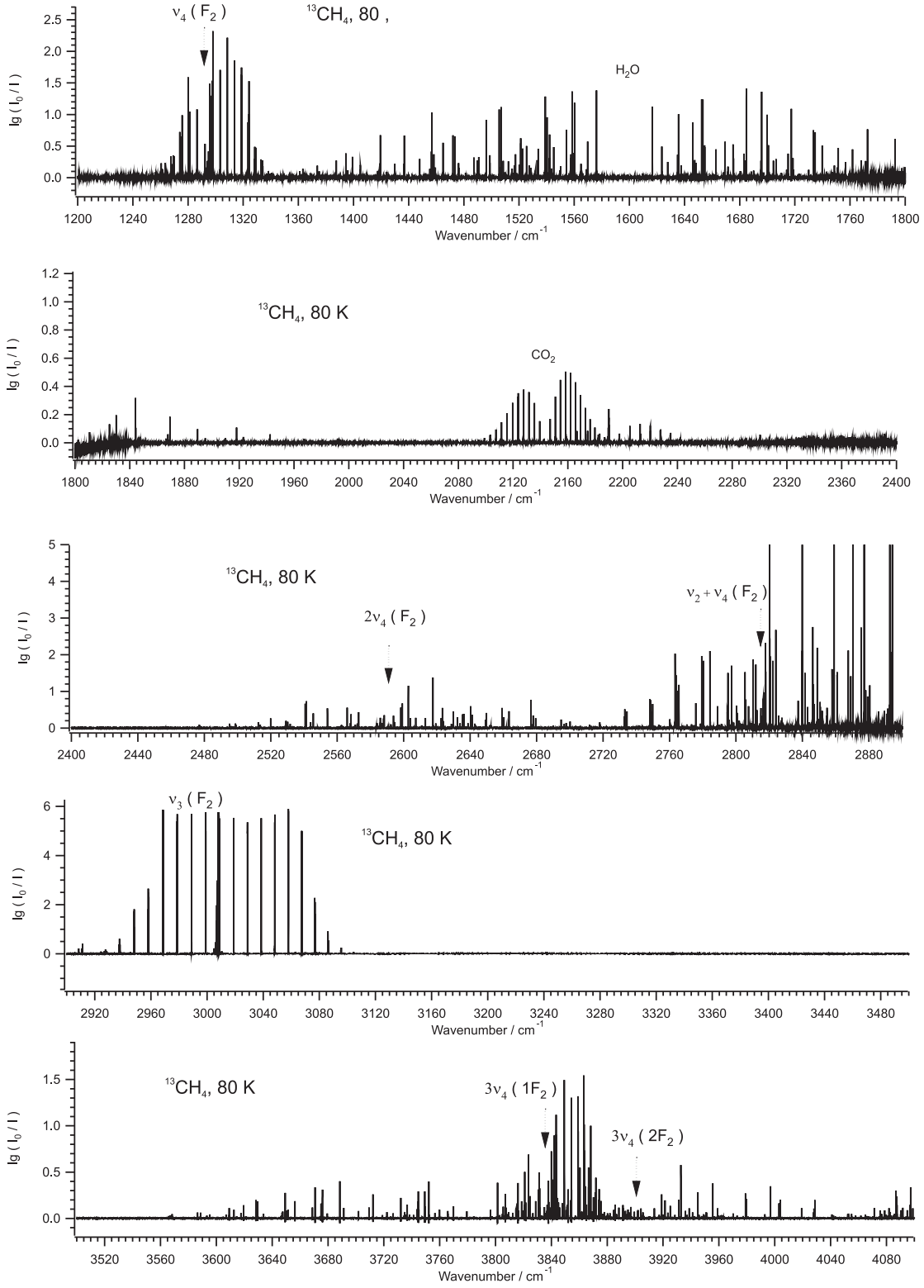

FIG. 6. Survey spectrum as decadic absorbance $\lg(I_0/I)$ of $^{13}CH_4$ in the region 1200–4100 cm^{-1}. Experimental conditions are presented in Table II. The total gas pressure is 280 Pa at mixing ratios $x = [CH_4]/([CH_4] + [He])$ of about 0.005 and 0.1 and the optical path length is 5 m. Some ranges show strongly saturated spectra in order to make weak lines appear (T = 80 K).

F_2 symmetry and 1333 levels of A_1, A_2, E, and F_1 symmetry in the polyads $2.5 \leq N \leq 4$; for more details, see Table I). Nevertheless, both the central parts of the bands, and their ($J' = 0 \leftarrow J'' = 1$) transitions can be clearly recognized for the bands listed in Table IV.

For some bands reproduced in Table IV the $J' = 0 \leftarrow J'' = 1$ transitions were assigned on the basis of the band centers from Ref. 43. For the $2\nu_2 + \nu_4$ band, which is quite weak, we used a more complete rovibrational analysis for the assignment of the P(1) line.[41]

This article is copyrighted as indicated in the article. Reuse of AIP content is subject to the terms at: http://scitation.aip.org/termsconditions. Downloaded to IP: 129.132.218.57 On: Tue, 16 Dec 2014 16:10:57

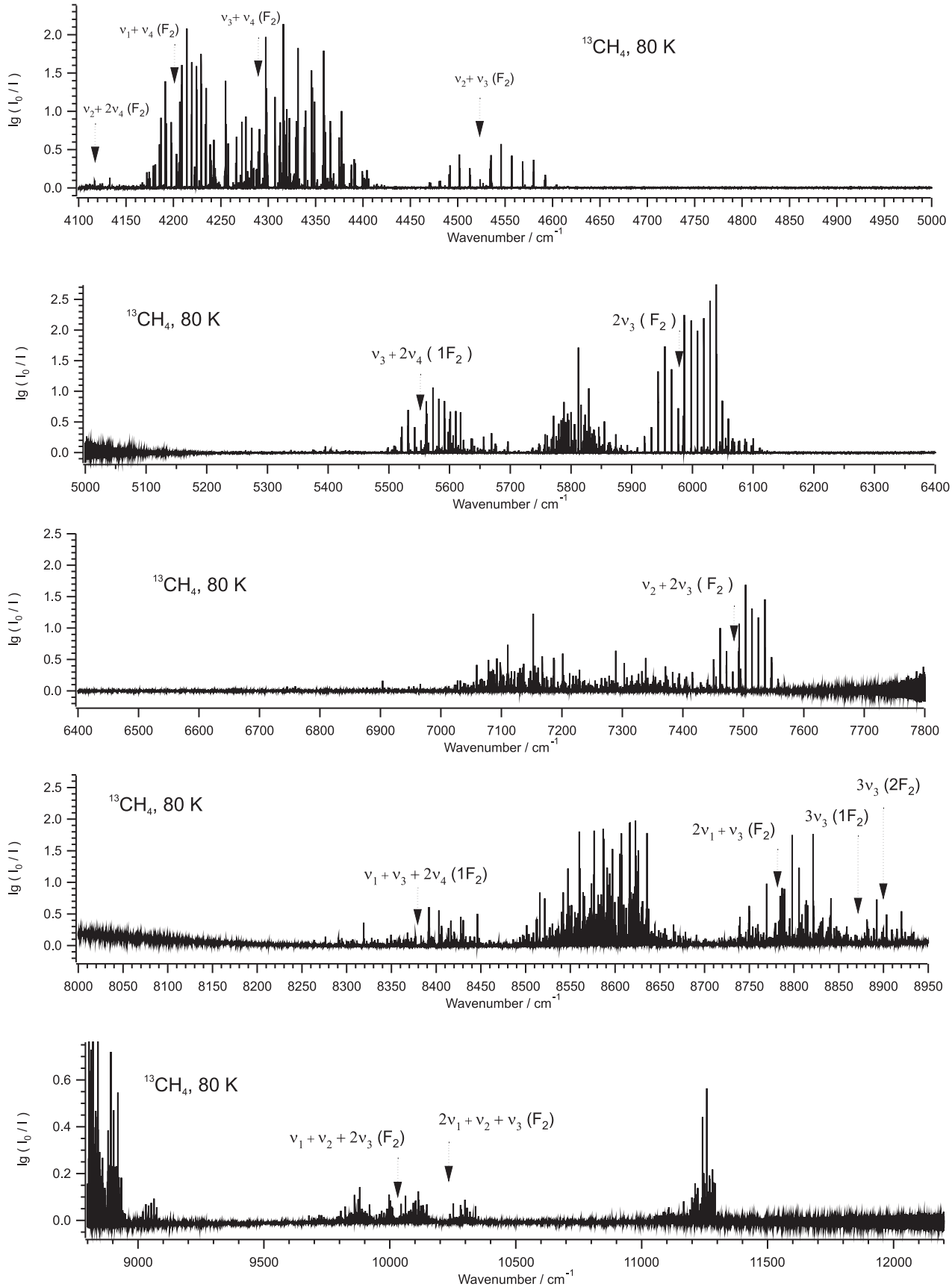

FIG. 7. Survey spectrum as decadic absorbance $\lg(I_0/I)$ of $^{13}CH_4$ in the region 4100–12 000 cm^{-1}. Experimental conditions are presented in Table II. The total gas pressure is 280 Pa and 480 Pa at mixing ratios $x = [CH_4]/([CH_4] + [He])$ of about 0.1 and the optical path length is 10 and 15 m. Some ranges show strongly saturated spectra in order to make weak lines appear (T = 80 K).

This article is copyrighted as indicated in the article. Reuse of AIP content is subject to the terms at: http://scitation.aip.org/termsconditions. Downloaded to IP: 129.132.218.57 On: Tue, 16 Dec 2014 16:10:57

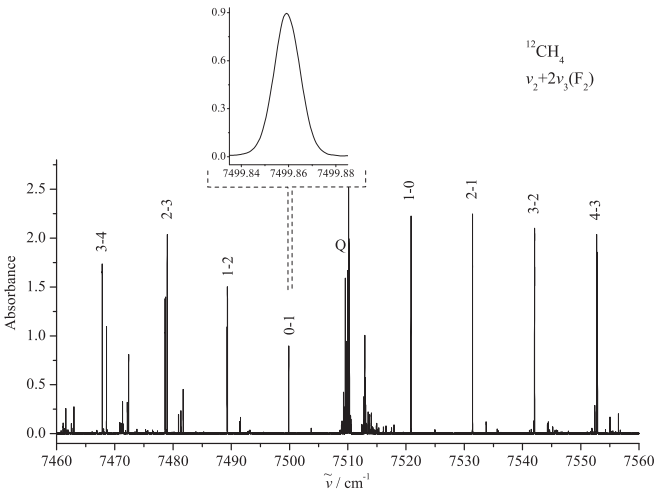

FIG. 8. High resolution spectrum shown as decadic absorbance $\lg(I_0/I)$ of the $^{12}CH_4$ isotopomer in the region of the $\nu_2 + 2\nu_3$ (F_2) band. The strongest lines in this spectrum are close to saturation.The total gas pressure is 280 Pa at a mixing ratio $x = [CH_4]/([CH_4] + [He])$ of about 0.1 and the optical path length is 10 m (T = 80 K, see also caption to Fig. 3).

V. THEORETICAL BACKGROUND FOR THE EFFECTIVE HAMILTONIAN USED IN THE VIBRATIONAL ANALYSIS

To put the analysis of newly assigned bands of the $^{12}CH_4$ and $^{13}CH_4$ isotopomers into a broader perspective, we have conducted a vibrational analysis of experimentally known vibrational band centers of both isotopomers using an effective Hamiltonian. It was possible to determine the harmonic wavenumber, ω_i, the anharmonic coefficients, x_{ij}, and the vibrational tetrahedral splitting coefficients, $G_{\dots}$, $T_{\dots}$, and $S_{\dots}$. Using our analysis we are able to predict the band centers of further vibrational bands with satisfactory accuracy as will be

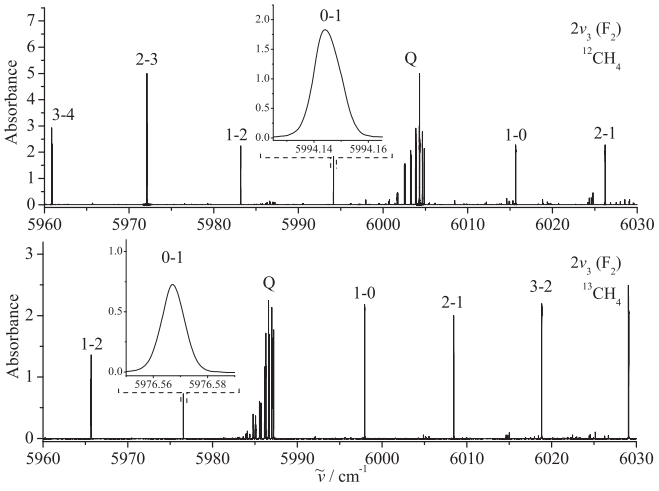

FIG. 9. High resolution spectrum shown as decadic absorbance $\lg(I_0/I)$ of the central part of the $2\nu_3$ (F_2) band of $^{12}CH_4$ (top) and $^{13}CH_4$ (bottom). The P(1) line of $^{12}CH_4$ (top) and $^{13}CH_4$ (bottom) is rather close to saturation while many other lines are clearly saturated above $\lg(I_0/I) = 2$, where intensities have no quantitative significance. The total gas pressure is 280 Pa at a mixing ratio $x = [CH_4]/([CH_4] + [He])$ of about 0.1 and the optical path length is 10 m (T = 80 K, see also caption to Fig. 3).

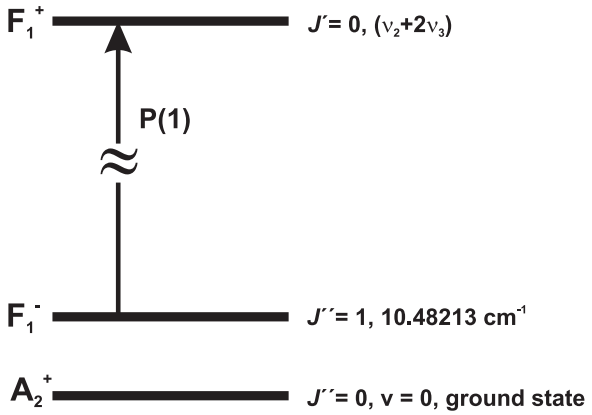

FIG. 10. Term value level scheme for the determination of the $P(1)$ rovibrational transition of the $\nu_2 + 2\nu_3$ (F_2) subband of $^{13}CH_4$ shown in Figure 3 as an example. The symmetry labels include the parity from the nucleus $^{13}_{6}C^{6+}$ (see Sec. III).

discussed below in more detail. We describe the theoretical background for this analysis in Subsections V A–V G.

A. Description of the vibrational spectrum using spectroscopic parameters

Within the framework of an effective Hamiltonian description from vibration-rotation theory (see, e.g., Refs. 39, 40, 54, and 110), the vibrational energies of the methane molecule can be obtained as a result of a diagonalization of the matrix $H^{vib.}$ consisting of off-diagonal elements $H_{v\tilde{v}}$ ($v \neq \tilde{v}$) describing the relevant resonance interactions. These interactions will be discussed in detail later. The diagonal elements H_{vv} can be written as sums of two terms:

$$H_{vv} = E_v + W_v \equiv E_v + W(v_1 v_2 v_3 v_4 n \Gamma_v). \quad (7)$$

The first term E_v in the diagonal elements H_{vv} represents usually the unperturbed vibrational energies according to

$$(E_v/hc) = \sum_i \omega_i \left(v_i + \frac{d_i}{2}\right) + \sum_{i,j \geq i} x_{ij} \left(v_i + \frac{d_i}{2}\right) \times \left(v_j + \frac{d_j}{2}\right) + \dots . \quad (8)$$

Here, the indices i and j enumerate the vibrational modes of CH_4; the ω_i are the harmonic wavenumbers and the x_{ij} the anharmonic coefficients; $d_i = 1$ for the nondegenerate ($i = 1$), $d_i = 2$ for doubly degenerate ($i = 2$), and $d_i = 3$ for triply degenerate ($i = 3$ or 4) vibrational states. The terms $W(v_1 v_2 v_3 v_4 n \Gamma_v)$, describe the so-called tetrahedral splittings of specific vibrational states $(v) \equiv (v_1 v_2 v_3 v_4)$ and, in general, these terms are complicated functions of the vibrational quantum numbers v_1, v_2, v_3, v_4 and of the symmetry species Γ_v of the vibrational states in the T_d point group. The index n distinguishes states with the same values of the quantum numbers v_1, v_2, v_3, v_4 and symmetries Γ_v. (We use italics n here to distinguish it from the polyad quantum number n, but there can hardly arise confusion for these two quantities.) The calculation of the tetrahedral splittings according to Eq. (7) is nontrivial. Earlier results for $W(v_1 v_2 v_3 v_4 n \Gamma_v)$ have been

This article is copyrighted as indicated in the article. Reuse of AIP content is subject to the terms at: http://scitation.aip.org/termsconditions. Downloaded to IP: 129.132.218.57 On: Tue, 16 Dec 2014 16:10:57

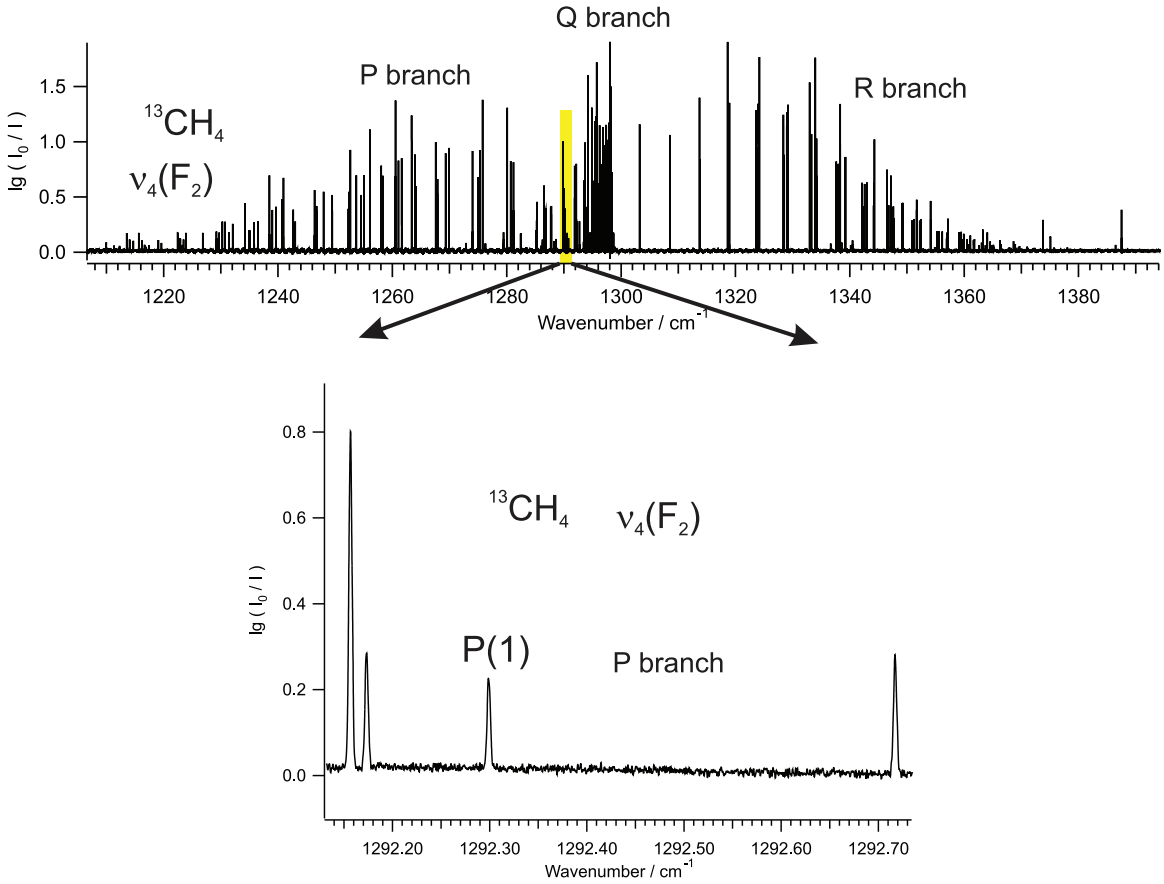

FIG. 11. Illustration of peculiarities of the second (F_2)-type absorption bands of $^{13}CH_4$. The central part of the ν_2 (F_2) band of $^{13}CH_4$ is shown in the figure. The *R*-branch is clearly separated, while the *Q*- and *P*-branches are strongly overlapped. The total gas pressure is 280 Pa at mixing ratio $x = [CH_4]/([CH_4] + [He])$ about 0.005 and the optical path length is 5 m (T = 80 K).

presented only for states with low quantum numbers, v_2, v_3, and v_4.[57] In order to describe the vibrational spectrum of CH_4 up to high excitations (up to 12 000 cm^{-1} in our work) it is necessary to derive the corresponding equations for the tetrahedral splittings, $W(v_1 v_2 v_3 v_4 n \Gamma_v)$. This problem can be solved using a calculation of the matrix elements of vibrational operators responsible for the tetrahedral splittings for the relevant wave functions. For this purpose it is convenient to use the irreducible tensor representation of both the operators and wave functions making use of the high symmetry of CH_4.

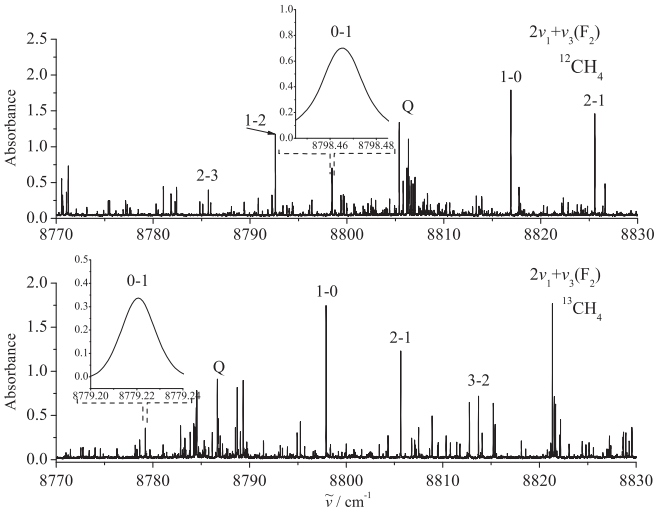

FIG. 12. The high resolution FTIR spectrum shown as decadic absorbance $\lg(I_0/I)$ of $^{12}CH_4$ (top) and $^{13}CH_4$ (bottom) isotopomers in the region of the high-frequency band $2\nu_1 + \nu_3$ (F_2). The total gas pressure is 280 Pa at mixing ratios $x = [CH_4]/([CH_4] + [He])$ of about 0.5 and the optical path length is 15 m (T = 80 K, see also caption to Fig. 3).

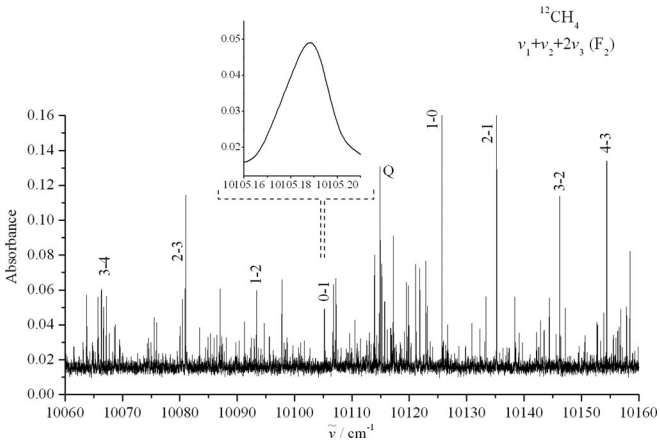

FIG. 13. High resolution spectrum shown as decadic absorbance $\lg(I_0/I)$ of $^{12}CH_4$ molecule near 10 100 cm^{-1}, the $\nu_1 + \nu_2 + 2\nu_3$ (F_2) band. The total gas pressure is 480 Pa at a mixing ratio $x = [CH_4]/([CH_4] + [He])$ of about 0.1 and the optical path length is 15 m (T = 80 K, see also caption to Fig. 3).

This article is copyrighted as indicated in the article. Reuse of AIP content is subject to the terms at: http://scitation.aip.org/termsconditions. Downloaded to IP: 129.132.218.57 On: Tue, 16 Dec 2014 16:10:57

B. Irreducible tensor representation of the vibrational wave functions of CH_4

According to the theory of Irreducible Tensorial Sets (see, e.g., Refs. 111 and 112), the symmetrized vibrational wave functions of the CH_4 (T_d-symmetry) molecule can be presented in the following form:

$$|v_1; v_2 l_2 \gamma_2; v_3 l_3, v_4 l_4, l n_l \gamma_{34}; n\gamma\sigma\rangle = |v_1\rangle(|v_2 l_2 \gamma_2\rangle \otimes |v_3 l_3, v_4 l_4, l n_l \gamma_{34}\rangle)^{n\gamma}_{\sigma}. \quad (9)$$

Here the $|v_1\rangle$ are the elementary nondegenerate vibrational functions (see, e.g., Ref. 113). The $|v_2 l_2 \gamma_2 \sigma_2\rangle$ are symmetrized functions of the doubly degenerate harmonic oscillator. They can be connected easily (see Appendix B for details) with the vibrational basis functions of the doubly degenerate harmonic oscillator.[113] In this case, γ_2 is the symmetry of the $|v_2 l_2 \gamma_2 \sigma_2\rangle$-function. The symbol $\otimes$ denotes the tensorial product; γ and σ are the indices of the corresponding irreducible representation of the symmetry group T_d and its line, respectively; and the third wave function, $|v_3 l_3, v_4 l_4, l n_l \gamma_{34} \sigma_{34}\rangle$, in Eq. (6) has the following form:

$$|v_3 l_3, v_4 l_4, l n_l \gamma_{34} \sigma_{34}\rangle = \sum_{m=-l}^{l} {}^{l}G^{m}_{n_l \gamma_{34} \sigma_{34}} \sum_{|l_3 - l_4| \le l \le l_3 + l_4} (|v_3 l_3\rangle \otimes |v_4 l_4\rangle)^{l}_{m} = \sum_{m=-l}^{l} {}^{l}G^{m}_{n_l \gamma_{34} \sigma_{34}} \sum_{|l_3 - l_4| \le l \le l_3 + l_4} C^{lm}_{l_3 m_3 l_4 m_4} |v_3 l_3 m_3\rangle |v_4 l_4 m_4\rangle. \quad (10)$$

The functions $|v_3 l_3 m_3\rangle$ and $|v_4 l_4 m_4\rangle$ in Eq. (10) are the elementary vibrational functions of triply degenerate harmonic oscillators;[113] the coefficients $C^{lm}_{l_3 m_3 l_4 m_4}$ are the well known Clebsch-Gordan coefficients (see, e.g., Refs. 114 and 115); and the coefficients ${}^{l}G^{m}_{n_l \gamma_{34} \sigma_{34}}$ are the G-matrix elements which provide a reduction of the irreducible representations, $D^{(J)}$, of the rotational symmetry group, $SO(3)$, to the irreducible representations, Γ ($\Gamma = A_1, A_2, E, F_1, F_2$), of T_d.

All the quantities used to construct symmetrized vibrational wave functions are known as analytical forms with exception of the G-matrix elements.

C. Analytical representation of the *G*-matrix elements for the T_d symmetry group

For the calculation of the G-matrix elements, we use the results given in Ref. 116 and, for the convenience of the reader, we will derive from this reference the general expressions that allow us to obtain analytical expressions for the G-matrix elements used.

As shown in Ref. 116, the elements of the G-matrix for a molecule with T_d symmetry can be determined from the following analytical expressions ($i = \sqrt{-1}$):

$${}^{J}G^{m}_{kF_{\lambda}z} = \frac{\exp(i\phi_J)}{2\sqrt{2}} \frac{[1-(-1)^J \delta_{k0}]}{(1+\delta_{k0})^{3/2}} [1-(-1)^{\lambda+k/2}][\delta_{km} - (-1)^J \delta_{-km}], \quad (11)$$

$${}^{J}G^{m}_{kF_{\lambda}y} = \frac{\exp(i\phi_J)}{2\sqrt{2}} \frac{[1-(-1)^J \delta_{k0}]}{(1+\delta_{k0})^{3/2}} [1-(-1)^{\lambda+k/2}](-i)^m [1-(-1)^m] d^{J}_{km}(\pi/2), \quad (12)$$

$${}^{J}G^{m}_{kF_{\lambda}x} = (-1)^{\lambda+1} \frac{\exp(i\phi_J)}{2\sqrt{2}} \frac{[1-(-1)^J \delta_{k0}]}{(1+\delta_{k0})^{3/2}} [1-(-1)^{\lambda+k/2}][1-(-1)^m] d^{J}_{km}(\pi/2), \quad (13)$$

$${}^{J}G^{m}_{kA_{\lambda}} = \sum_{n=L}^{k} \alpha^{JA_{\lambda}}_{kn} \frac{\exp(i\chi_J)}{2\sqrt{6}} [1-(-1)^{\lambda+n/2}] \times \{[1+(-1)^m][1-(-1)^{\lambda+m/2}] d^{J}_{nm}(\pi/2) - (-1)^{\lambda} \delta_{nm} - (-1)^{\lambda+J} \delta_{-nm}\}, \quad (14)$$

and

$${}^{J}G^{m}_{kE_{\lambda}} = (-1)^{\lambda+1} \sum_{n=L}^{k} \alpha^{JE}_{kn} \frac{\exp(i\chi_J)}{4(1+2\delta_{\lambda 1})^{1/2}} [1+(-1)^{n/2}] \times \{[1+(-1)^m][1-(-1)^{\lambda+m/2}] d^{J}_{nm}(\pi/2) - 2\delta_{\lambda 1}[\delta_{nm} + (-1)^J \delta_{-nm}]\}. \quad (15)$$

This article is copyrighted as indicated in the article. Reuse of AIP content is subject to the terms at: http://scitation.aip.org/termsconditions. Downloaded to IP: 129.132.218.57 On: Tue, 16 Dec 2014 16:10:57

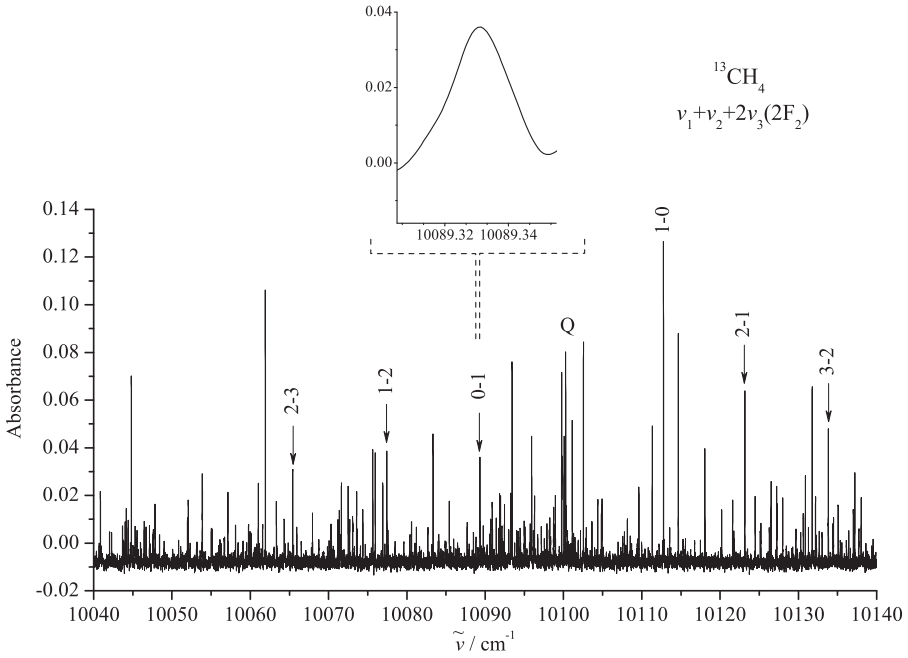

FIG. 14. High resolution spectrum shown as decadic absorbance $\lg(I_0/I)$ of $^{13}CH_4$ in the region of the band $\nu_1 + \nu_2 + 2\nu_3$ (F_2). The total gas pressure is 480 Pa at a mixing ratio $x = [CH_4]/([CH_4] + [He])$ of about 0.1 and the optical path length is 15 m (T = 80 K, see also caption to Fig. 3).

In Eqs. (11)–(15) $\lambda = 1$ or 2, and the phases $\exp(i\phi_J)$ and $\exp(i\chi_J)$ are chosen in such a way that $\exp(i\phi_J) = -i\exp(i\chi_J) = 1$ for odd J and $\exp(i\phi_J) = i\exp(i\chi_J) = i$ for even J. This choice satisfies the relations ${}^J G^{-m}_{k\gamma\sigma} = (-1)^{m\,J} G^{-m*}_{k\gamma\sigma}$ and returns real values of the Hamiltonian matrix as described in, e.g., Ref. 68. The quantities $d^J_{km}(\pi/2)$ are known from angular momentum theory, Ref. 114:

$$d^J_{km}(\pi/2) = (-1)^{k+m}\frac{1}{2^J}\left(\frac{(J+k)!(J-k)!}{(J+m)!(J-m)!}\right)^{1/2} \times \sum_r (-1)^r \binom{J+m}{r}\binom{J-m}{\tau+k-m}. \quad (16)$$

The index k in Eqs. (11)–(16) takes the values $0, 2, 4, \ldots, J$ (or $J-1$) only. In Eqs. (14) and (15) $n = L, L+4, L+8, \ldots, k$ and $L = 0$ for $\Gamma = A_1$ or E, $L = 2$ for $\Gamma = A_2$. The coefficients $\alpha^{J\Gamma}_{kn}$ can be obtained from the recurrence relations:

$$\left(\alpha^{J\Gamma}_{kk}\right)^{-1/2} = 1 + \delta_{k0}(-1)^J + [4(-1)^\Gamma - 6\delta_{\Gamma E}]d^J_{kk}(\pi/2) - \sum_{l=L}^{k-4}\sum_{i\le l, j\le l}\alpha^{J\Gamma}_{li}\alpha^{J\Gamma}_{lj}[4(-1)^\Gamma - 6\delta_{\Gamma E}]^2 \times d^J_{ki}(\pi/2)d^J_{kj}(\pi/2), \quad (17)$$

and

$$\alpha^{J\Gamma}_{kn} = -\alpha^{J\Gamma}_{kk}\sum_{i\ge n}^{k-4}\sum_{j\le i}\alpha^{J\Gamma}_{ij}\alpha^{J\Gamma}_{in}[4(-1)^\Gamma - 6\delta_{\Gamma E}]d^J_{kj}(\pi/2). \quad (18)$$

In Eqs. (17) and (18) the numbers k, n, i, j, and l are multiples of 4 when $\Gamma = A_1$ or E, and are even but not multiples of 4 when $\Gamma = A_2$.

If the recurrence relations (17) and (18) are used one can encounter problems because for some combinations k_a, J_a, and Γ_a of the indices k, J, and Γ, the expression on the right-hand side of Eq. (17) will vanish. In this case, one must proceed as described in the following. As an example, it can be seen that if one follows the above scheme and tries to construct the function of symmetry $\Gamma_a\sigma_a = E_2$ for $J_a = 5$ (that is, ${}^5G^m_{kE_2}$), then with $k_a = 0$ the right-hand side of Eq. (17) becomes zero. This problem can be solved as follows: As discussed in Ref. 117, for a given irreducible representation $D^{(J)}$, the number of G-matrix elements of a given symmetry ($\Gamma_a = A_1$, A_2 or E) determined using Eqs. (14)–(18) is always larger than the real number of irreducible representations of this symmetry to which the representation $D^{(J)}$ is reduced. Therefore, when the situation mentioned above occurs, one must use, in the general equation (17), the value of k which follows from the value k_a, namely, $k_b = k_a + 4$. In this case, one must take into account that in Eqs. (17) and (18), $k \neq k_a$. In particular, in the above example one must take $k = 4$ in order to construct the G-matrix elements of E symmetry. It may easily be seen that in this case, Eqs. (14)–(18) give

$${}^5G^m_{E_2} \equiv {}^5G^m_{4E_2} = i2^{-1/2}(\delta_{2m} - \delta_{-2m}). \quad (19)$$

The direct use of the general equations (11)–(18) allows one to obtain whatever is necessary for a further analysis of the G-matrix elements. The results of such calculations are shown in Table VI, where we present (a) all nonzero ${}^JG$-matrix elements for values of $0 \le J \le 4$, and (b) the ${}^JG^m_{nF_{\lambda z}}$-matrix elements for $5 \le J \le 8$ as necessary for further discussion.

This article is copyrighted as indicated in the article. Reuse of AIP content is subject to the terms at: http://scitation.aip.org/termsconditions. Downloaded to IP: 129.132.218.57 On: Tue, 16 Dec 2014 16:10:57

TABLE IV. Band centers for $^{12}CH_4$ identified in the region of 3800–12 000 cm^{-1}.

	$(J' = 0 \leftarrow J'' = 1)$		Band center (level position)	
Band[a]	This work[b]	Previous work	This work[c]	Previous work
1	2	3	4	5
$3\nu_4(1F_2)$	3860.0045[b]	3860.004160[d]	3870.4862[c]	3870.488[d,e]
$3\nu_4(2F_2)$	3920.4408[b]	3920.438008[d]	3930.9225[c]	3930.923[d,e]
$\nu_2 + 2\nu_4(F_2)$	4132.3802[b]	4132.379922[d]	4142.8619[c]	4142.865[d,e]
$\nu_1 + \nu_4(F_2)$	4212.9805[b]		4223.4621[c]	4223.462[d,e]
$\nu_3 + \nu_4(F_2)$	4308.7276[b]	4308.728063[d]	4319.2093[c]	4319.212[d,e]
$2\nu_2 + \nu_4(1F_2)$	4338.2349[b]	4338.234877[d]	4348.7166[c]	4348.716[d,e]
$2\nu_2 + \nu_4(2F_2)$	4368.4674[b]		4378.9491[c]	4378.947[d,e]
$\nu_2 + \nu_3(F_2)$	4533.2800[b]	4533.280334[d]	4543.7617[c]	4543.757[d,e]
$\nu_3 + 2\nu_4(1F_2)$	5577.4948[b]		5587.9764[c]	5587.967[e,f]
$2\nu_3(F_2)$	5994.1441[b]		6004.6258[c]	6004.621[e,f]
$2\nu_2 + \nu_3(1F_2)$	6044.1245[b]	6044.1452[g]	6054.6061[c]	6054.609[e,f]
$\nu_1 + \nu_3 + \nu_4(F_2)$	7146.2331[b]		7156.7148[c]	
$\nu_2 + 2\nu_3(F_2)$	7499.8556[b]	7499.8562[h]	7510.3373[c]	7510.3378[h,i]
$2\nu_1 + 2\nu_4(F_2)$	8377.517(2)[b]		8387.999[c]	
$\nu_1 + \nu_3 + 2\nu_4(1F_2)$	8410.514(2)[b]		8420.996[c]	
$\nu_1 + 2\nu_3(F_2)$	8608.189(2)[b]		8618.671[c]	
$2\nu_1 + \nu_3(F_2)$	8798.465(2)[b]		8808.947[c]	
$3\nu_3(1F_2)$	8896.815(2)[b]	8896.815[j]	8907.297[c]	8907.30[e,j]
$3\nu_3(2F_2)$	9035.474(2)[b]	9035.465[k]	9045.956[c]	9045.92[e,k]
$\nu_1 + 2\nu_3 + \nu_4(1F_2)$	9877.993(2)[b]		9888.475[c]	
$\nu_1 + \nu_2 + 2\nu_3(F_2)$	10105.188(2)[b]		10115.670[c]	
$3\nu_3 + \nu_4(2F_2)$	10255.104(2)[b]		10265.586[c]	
$2\nu_1 + \nu_2 + \nu_3(F_2)$	10291.692(2)[b]		10302.174[c]	
$\nu_1 + 3\nu_3(1F_2)$	11265.827(2)[b]		11276.309[c]	

[a]We give in the first column an approximate vibrational assignment and the symmetry species F_2 with a number indicating the sublevel index in the polyad in order of increasing energy for this species.
[b]Position of the $(J' = 0 \leftarrow J'' = 1)$ transition assigned in our experimental spectra.
[c]Position of the $(J' = 0)$ vibrational level obtained from the direct experimental line position presented in the column 2 of this table and adding the ground state $(J'' = 1)$ wavenumber.
[d]S. Albert, S. Bauerecker, V. Boudon, L. R. Brown, J.-P. Champion, M. Loëte, A. Nikitin, and M. Quack, Chem. Phys. **356**, 131–146 (2009).[43] The lower vibrational levels have been summarized therein.
[e]Obtained from a fit of rovibrational lines to an effective Hamiltonian.
[f]A. Nikitin, V. Boudon, C. Wenger, S. Albert, L. R. Brown, S. Bauerecker, and M. Quack, Phys. Chem. Chem. Phys. **15**, 10071–10093 (2013).[78]
[g]The value of the unclear origin in the HITRAN database is 6044.1452 cm^{-1}.[95]
[h]M. Hippler and M. Quack, J. Chem. Phys. **116**, 6045–6055 (2002).[80]
[i]Obtained from the direct experimental line position presented in the column 3 of this table and adding the ground state $(J'' = 1)$ wavenumber.
[j]A. De Martino, R. Frey, and F. Pradere, Mol. Phys. **55**, 731–749 (1985).[132]
[k]G. Pierre, J.-C. Hilico, C. de Bergh, and J.-P. Maillard, J. Mol. Spectrosc. **82**, 379–393 (1980).[143]

The reason for such a presentation will be discussed in Subsection V D.

D. Symmetrized vibrational wave functions

The *G*-matrix elements obtained in Sec. V C can be used directly in Eqs. (9) and (10) for the construction of symmetrized vibrational wave functions of CH_4. The wave functions constructed here can be used in a further construction and diagonalization of the Hamiltonian matrix. By symmetry,[111,112] the Hamiltonian matrix is divided into sets of equivalent sub-matrixes for which the basis functions, Eq. (9), differ from each other only by the index σ of the line of corresponding irreducible representation. Therefore, in the Hamiltonian matrix it is possible to consider only the "E_1" sub-matrix and, similarly, only the "F_1z" and "F_2z" sub-matrixes and omit the "E_2," "F_1x," "F_1y," "F_2x," and "F_2y" sub-matrixes. Thus, in Table VI we omitted the corresponding *G*-matrix elements for $5 \leq J \leq 8$. As discussed below, for the polyads $N = 2.5$, 3, 3.5, and 4 we calculated and analyzed only the vibrational states of F_2 symmetry. For this reason, only the ${}^{J}G^{m}_{nF_\lambda z}$-matrix elements with $5 \leq J \leq 8$ were calculated and are presented in Table VI.

Because the number of different symmetrized vibrational functions is large, on the one hand, and the knowledge of the general equations (9) and (10), and the necessary *G*-matrix elements make the procedure of construction of the corresponding functions a routine procedure, on the other hand, we do not present here all the results obtained, but show as examples only some of them for the polyads $N = 2$ and 4:

This article is copyrighted as indicated in the article. Reuse of AIP content is subject to the terms at: http://scitation.aip.org/termsconditions. Downloaded to IP: 129.132.218.57 On: Tue, 16 Dec 2014 16:10:57

TABLE V. Band centers for $^{13}CH_4$ (in cm^{-1}).

Band	$(J' = 0 \leftarrow J'' = 1)$[a]	Band[a]	Predict.-I[b]	Predict.-II[c]	Fit.-III[d]
1	2	3	5	6	7
$\nu_4(F_2)$	1292.2987	1302.7808	1302.56	1302.57	1302.1291
$2\nu_4(F_2)$	2588.1588	2598.6409	2597.91	2597.72	2598.2363
$\nu_2 + \nu_4(F_2)$	2811.9798	2822.4519	2823.33	2823.35	2822.7670
$\nu_1(A_1)$	2915.4426[e]	2915.4426	2916.93	2916.84	2916.2625
$\nu_3(F_2)$	2999.0634	3009.5455	3009.01	3008.96	3009.4484
$2\nu_2(A_1)$	3064.9640[e]	3063.9640	3063.85	3063.85	3063.5661
$3\nu_4(1F_2)$	3837.9048	3848.3869	3847.25	3848.74	3848.1799
$3\nu_4(2F_2)$	3897.0171	3907.4992	3907.18	3906.46	3907.4321
$\nu_2 + 2\nu_4(F_2)$	4116.8742	4127.3563	4127.47	4127.38	4127.7480
$\nu_1 + \nu_4(F_2)$	4203.3420	4213.8241	4216.23	4216.12	4214.5730
$\nu_3 + \nu_4(F_2)$	4290.8152	4301.2972	4301.43	4301.46	4301.5000
$2\nu_2 + \nu_4(F_2)$	4340.9084	4340.9084	4341.73	4341.73	4341.0005
$\nu_2 + \nu_3(F_2)$	4523.5725	4534.0546	4533.44	4533.44	4533.7800
$\nu_3 + 2\nu_4(1F_2)$	5552.9355	5563.4176	5564.49	5565.36	5564.3582
$2\nu_3(F_2)$	5976.5658	5987.0479	5986.22	5986.25	5986.2802
$\nu_2 + 2\nu_3(F_2)$	7482.6763	7493.1584	7493.52	7493.59	7493.3622
$\nu_1 + \nu_3 + 2\nu_4(1F_2)$	8383.139(2)	8393.621(2)	8394.37	8394.98	8393.1580
$2\nu_1 + \nu_3(F_2)$	8779.221(2)	8789.703(2)	8792.75	8792.68	8790.0344
$3\nu_3(1F_2)$	8870.391(2)	8880.873(2)	8880.92	8880.92	8880.8272
$3\nu_3(2F_2)$	9009.109(2)	9019.591(2)	9016.17	9016.36	9019.7292
$\nu_1 + \nu_2 + 2\nu_3(F_2)$	10089.331(2)	10099.813(2)	10098.11	10098.11	10099.8375
$2\nu_1 + \nu_2 + \nu_3(F_2)$	10273.831(2)	10284.313(2)	10287.56	10287.60	10284.2582

[a]This work, see also caption to Table IV for further explanations.
[b]Predicted with the parameters from column 4 of Table XII.
[c]Predicted with the parameters from column 7 of Table XII.
[d]Calculated with fitted parameters from column 9 of Table XII.
[e]Value from Raman spectroscopy[144] (see also Ref. 42).

TABLE VI. Quantities for the calculations of nonzero G-matrix elements for T_d symmetry group ($J \le 8$).[a]

J	k	$\Gamma\sigma$	m	${}^J G^m_{k\Gamma\sigma}$	J	k	$\Gamma\sigma$	m	${}^J G^m_{k\Gamma\sigma}$
1	0	F_1z	0	1	5	2	F_2z	2	$1/\sqrt{2}$
2	2	F_2z	2	$i/\sqrt{2}$	5	2	F_2z	−2	$1/\sqrt{2}$
2	2	F_2z	−2	$-i/\sqrt{2}$	6	4	F_1z	4	$i/\sqrt{2}$
2	0	E_1	0	−1	6	4	F_1z	−4	$-i/\sqrt{2}$
2	0	E_2	−2	$-1/\sqrt{2}$	6	2	F_2z	2	$i/\sqrt{2}$
2	0	E_2	2	$-1/\sqrt{2}$	6	2	F_2z	−2	$-i/\sqrt{2}$
3	0	F_1z	0	1	6	6	F_2z	6	$i/\sqrt{2}$
3	2	F_2z	2	$1/\sqrt{2}$	6	6	F_2z	−6	$-i/\sqrt{2}$
3	2	F_2z	−2	$1/\sqrt{2}$	7	0	F_1z	0	1
3	2	A_2	2	$-i/\sqrt{2}$	7	4	F_1z	4	$1/\sqrt{2}$
3	2	A_2	−2	$i/\sqrt{2}$	7	4	F_1z	−4	$1/\sqrt{2}$
4	0	A_1	0	$\sqrt{21}/6$	7	2	F_2z	2	$1/\sqrt{2}$
4	0	A_1	4	$\sqrt{5}/2\sqrt{6}$	7	2	F_2z	−2	$1/\sqrt{2}$
4	0	A_1	−4	$\sqrt{5}/2\sqrt{6}$	7	6	F_2z	6	$1/\sqrt{2}$
4	0	E_1	0	$-\sqrt{15}/6$	7	6	F_2z	−6	$1/\sqrt{2}$
4	0	E_1	4	$\sqrt{7/24}$	8	4	F_1z	4	$i/\sqrt{2}$
4	0	E_1	−4	$\sqrt{7/24}$	8	4	F_1z	−4	$-i/\sqrt{2}$
4	4	F_1z	4	$i/\sqrt{2}$	8	8	F_1z	8	$i/\sqrt{2}$
4	4	F_1z	−4	$-i/\sqrt{2}$	8	8	F_1z	−8	$-i/\sqrt{2}$
4	2	F_2z	2	$i/\sqrt{2}$	8	2	F_2z	2	$i/\sqrt{2}$
4	2	F_2z	−2	$-i/\sqrt{2}$	8	2	F_2z	−2	$-i/\sqrt{2}$
5	0	F_1z	0	1	8	6	F_2z	6	$i/\sqrt{2}$
5	4	F_1z	4	$1/\sqrt{2}$	8	6	F_2z	−6	$-i/\sqrt{2}$
5	4	F_1z	−4	$1/\sqrt{2}$					

[a]See text in Sec. V for details.

This article is copyrighted as indicated in the article. Reuse of AIP content is subject to the terms at: http://scitation.aip.org/termsconditions. Downloaded to IP: 129.132.218.57 On: Tue, 16 Dec 2014 16:10:57

These symmetrized wave functions are

$$(4\nu_4, 2A_1) \equiv |v_1 = 0; v_2 = l_2 = 0; v_3 = l_3 = 0, v_4 = l_4 = 4; n = 2\gamma = A_1\rangle$$
$$= \frac{\sqrt{21}}{6}|v_4 = l_4 = 4m_4 = 0\rangle$$
$$+\sqrt{\frac{5}{24}}\{|v_4 = l_4 = 4m_4 = 4\rangle + |v_4 = l_4 = 4m_4 = -4\rangle\}, \quad (20)$$

$$(\nu_2 + 3\nu_3 + \nu_4, 7F_2z) \equiv |v_1 = 0; v_2 = l_2 = 1; v_3 = l_3 = 3, v_4 = l_4 = 1; n = 7\gamma = F_2\sigma = z\rangle$$
$$= -\frac{i}{4\sqrt{7}}\{|v_2 = 1l_2 = 1\rangle + |v_2 = 1l_2 = -1\rangle\}$$
$$\times\{|v_3 = l_3 = 3m_3 = 3\rangle|v_4 = l_4 = 1m_4 = -1\rangle - |v_3 = l_3 = 3m_3 = -3\rangle|v_4 = l_4 = 1m_4 = 1\rangle\}$$
$$-\frac{i\sqrt{3}}{2\sqrt{7}}\{|v_2 = 1l_2 = 1\rangle + |v_2 = 1l_2 = -1\rangle\}$$
$$\times\{|v_3 = l_3 = 3m_3 = 2\rangle|v_4 = l_4 = 1m_4 = 0\rangle - |v_3 = l_3 = 3m_3 = -2\rangle|v_4 = l_4 = 1m_4 = 0\rangle\}$$
$$-\frac{i\sqrt{15}}{4\sqrt{7}}\{|v_2 = 1l_2 = 1\rangle + |v_2 = 1l_2 = -1\rangle\}$$
$$\times\{|v_3 = l_3 = 3m_3 = 1\rangle|v_4 = l_4 = 1m_4 = 1\rangle - |v_3 = l_3 = 3m_3 = -1\rangle|v_4 = l_4 = 1m_4 = -1\rangle\}. \quad (21)$$

The functions on the right-hand sides of Eqs. (20) and (21) are the elementary vibrational functions of the doubly and triply degenerate harmonic oscillators.

E. Vibrational Hamiltonian of CH_4 including tetrahedral splittings

The vibrational Hamiltonian of a polyatomic molecule can be written in the following form (see, e.g., Refs. 110 and 118):

$$H^{vib.} = H^{harm.} + H^{cor.} + V. \quad (22)$$

In Eq. (22) $H^{harm.}$ is the harmonic part of the Hamiltonian:

$$H^{harm.} = \frac{1}{2}\sum_{\lambda} P_\lambda^2 + \frac{(2\pi c)^2}{2}\sum_{\lambda}\omega_\lambda^2 Q_\lambda^2, \quad (23)$$

where $P_\lambda = -i\hbar\frac{\partial}{\partial Q_\lambda}$. The operator $H^{cor.}$ has the following form:

$$H^{cor.} = \frac{1}{2}\sum_{\alpha\beta}\mu_{\alpha\beta}G_\alpha G_\beta. \quad (24)$$

Here $\alpha, \beta = x, y, z$, and $\mu_{\alpha\beta}$ are the elements of the matrix of the inverse moments of inertia and G_α the vibrational angular momentum operators (see Refs. 110 and 118). The operator V corresponds to the anharmonic part of the intramolecular potential function:

$$V = \sum_{\lambda\mu\nu} K_{\lambda\mu\nu} Q_\lambda Q_\mu Q_\nu + \sum_{\lambda\mu\nu\xi} K_{\lambda\mu\nu\xi} Q_\lambda Q_\mu Q_\nu Q_\xi + \ldots. \quad (25)$$

Equations (23)–(25) provide good approximations for a "normal" (semirigid) polyatomic molecule. In the case of XY_4 (T_d) molecules, the general relations (23)–(25) should be reconstructed using the symmetry properties of CH_4. We shall, however, not consider here the total Hamiltonian, Eqs. (22)–(25), but will pay attention only to those parts of the Hamiltonian which are responsible for the tetrahedral splittings of the vibrational levels. Following Ref. 57 we notice that ten tetrahedral splitting parameters, G_{22}, G_{33}, G_{34}, G_{44}, S_{34}, T_{33}, T_{34}, T_{44}, T_{23}, and T_{24}, have the form given in Ref. 57 as reproduced in Appendix C. Using the symmetry properties of CH_4 it is possible to show that the parts of the Hamiltonian given by Eqs. (23)–(25), responsible for the ten mentioned tetrahedral "effects," have the following form:

1. The parts of the expression $W(v_1v_2v_3v_4n\Gamma_v)$ in Eq. (7) which are connected with the parameters G_{33} and G_{44} arise from the operators

$$\hat{H}_1 = B\zeta_\lambda^2\sum_{\mu\nu}\epsilon_{\lambda\mu\nu}(Q_\mu P_\nu - Q_\nu P_\mu)^2$$
$$+ d_{\lambda\lambda\lambda\lambda_s}\left(Q_{\lambda x}^2 + Q_{\lambda y}^2 + Q_{\lambda z}^2\right)^2 + V_3, \quad (26)$$

where $\lambda = 3$ or 4; B is the equilibrium rotational constant; the symbol V_3 in Eqs. (26)–(32) denotes the cubic part of the intramolecular potential function V; $\epsilon_{\lambda\mu\nu}$ in Eq. (26) is a totally antisymmetric tensor. The notations of the d-parameters correspond to notations of Ref. 57.

2. The operator responsible for the G_{22}-type splittings is

$$\hat{H}_2 = d_{2222}\left(Q_{2_1}^2 + Q_{2_2}^2\right)^2 + V_3. \quad (27)$$

This article is copyrighted as indicated in the article. Reuse of AIP content is subject to the terms at: http://scitation.aip.org/termsconditions. Downloaded to IP: 129.132.218.57 On: Tue, 16 Dec 2014 16:10:57

3. The splittings connected with the parameter G_{34} arise from the operator

$$\hat{H}_3 = \frac{B}{2}\zeta_{34}^2 + 2B\zeta_3\zeta_4 + V_3. \quad (28)$$

4. The operator responsible for the T_{33} and T_{44} splittings has the more complicated form:

$$\hat{H}_4 = d_{\lambda\lambda\lambda\lambda_t}\left(Q_{\lambda x}^4 + Q_{\lambda y}^4 + Q_{\lambda z}^4 - 3Q_{\lambda x}^2 Q_{\lambda y}^2 - 3Q_{\lambda x}^2 Q_{\lambda z}^2 - 3Q_{\lambda y}^2 Q_{\lambda z}^2\right) + V_3 \quad (29)$$

again $\lambda = 3, 4$.

5. Similarly, we have for the operators producing the T_{34} and $T_{2\lambda}$ ($\lambda = 3, 4$) splittings:

$$\hat{H}_{5_a} = d_{3344_t}\left[3Q_{3x}^2 Q_{4x}^2 + 3Q_{3y}^2 Q_{4y}^2 + 3Q_{3z}^2 Q_{4z}^2 - \left(Q_{3x}^2 + Q_{3y}^2 + Q_{3z}^2\right)\left(Q_{4x}^2 + Q_{4y}^2 + Q_{4z}^2\right) - 4Q_{3x}Q_{3y}Q_{4x}Q_{4y} - 4Q_{3x}Q_{3z}Q_{4x}Q_{4z} - 4Q_{3y}Q_{3z}Q_{4y}Q_{4z}\right] + V_3 \quad (30)$$

and

$$\hat{H}_{5_b} = d_{22\lambda\lambda_t}\left[Q_{2_1}Q_{2_2}\left(Q_{\lambda x}^2 - Q_{\lambda y}^2\right) + \left(Q_{2_1}^2 - Q_{2_2}^2\right) \times \left(Q_{\lambda x}^2 + Q_{\lambda y}^2 - 2Q_{\lambda z}^2\right)/2\sqrt{3}\right] + V_3. \quad (31)$$

6. For the S_{34}-type splittings, the corresponding operator has the form:

$$\hat{H}_6 = d_{3344_{sb}}\left[\left(Q_{3x}Q_{4x} + Q_{3y}Q_{4y} + Q_{3z}Q_{4z}\right)^2 - \frac{1}{3}\left(Q_{3x}^2 + Q_{3y}^2 + Q_{3z}^2\right)\left(Q_{4x}^2 + Q_{4y}^2 + Q_{4z}^2\right)\right] + V_3. \quad (32)$$

If we now use perturbation theory up to the second order to obtain corrections by means of the symmetrized wave functions derived in Subsection V D, and the operators given in Eqs. (26)–(32), and compare the results with the equations for splitting parameters presented in Appendix C, then it is possible to derive the corresponding tetrahedral splittings $W(v_1v_2v_3v_4n\Gamma_v)$ for every vibrational term. It is necessary to take into account that the vibrational levels E_v, Eqs. (7) and (8), can comprise more than one sublevel of the same symmetry Γ. In this case, the splittings are not determined by the simple expression, $W(v_1v_2v_3v_4n\Gamma_v)$, but result from a diagonalisation of matrices obtained from the corresponding $W(v_1v_2v_3v_4n\Gamma_v)$ having the same index Γ (see also, Ref. 57). The dimension of such a matrix is equal to the number of sublevels of a specific symmetry.

F. Vibrational resonance interactions in the CH_4 molecule

The last step in the calculation of the vibrational structure of CH_4 is the analysis of possible vibrational resonance interactions. As will be discussed in Sec. VI, for the correct description of the vibrational spectrum of the CH_4 molecule by spectroscopic parameters one can restrict the consideration of vibrational resonance effects to two main types of interactions:

1. Darling–Dennison interactions between the states $|v_1; v_2l_2; v_3l_3, v_4l_4; n\gamma\sigma\rangle$ and $|v_1 \pm 2; v_2l_2; v_3 \mp 2l_3, v_4l_4; n'\gamma\sigma\rangle$ (n' may be different from n). In this case, the part of the Hamiltonian responsible for such interactions is

$$\hat{H}_{DD} = d_{1133}Q_1^2\left(Q_{3x}^2 + Q_{3y}^2 + Q_{3z}^2\right) + V_3. \quad (33)$$

2. Anharmonic-resonance interactions between the states $|v_1; v_2l_2; v_3l_3, v_4l_4; n\gamma\sigma\rangle$ and $|v_1 \pm 1; v_2l_2; v_3 \mp 1l_3 \mp 1(\mp 3), v_4l_4; n'\gamma\sigma\rangle$. The corresponding vibrational operator has the following form:

$$\hat{H}_F = d_{1333}Q_1Q_{3x}Q_{3y}Q_{3z} + V_3. \quad (34)$$

The matrix elements of the operators in Eqs. (33) and (34) with the symmetrized wave functions, Eqs. (9)–(13), allow one take into account some of the dominant interactions between different vibrational states of CH_4. One might consider also the CH stretching-CH bending Fermi-type interactions in the future, as such interactions are known to be quite strong. However, the present effective Hamiltonian provides already a good description of the experimental data as will be seen from the results discussed below. As discussed in Ref. 76 the inclusion of the Fermi-resonance may become more important, when considering also intensity information and such work is in progress. While such a change is not expected to improve the quality of the fit by much, it should increase the predictive power of the model and may be needed when more data become available.

G. Results of calculation of tetrahedral splittings

The considerations of Secs. V A–V F were used for practical computations of the values $W(v_1v_2v_3v_4n\Gamma_v)$ from Eq. (7) and of the matrix elements which provide vibrational resonance interactions. We performed calculations for all vibrational states which are comprised in the polyads $N = 0.5$, 1, 1.5, and 2. For the polyads $N = 2.5$, 3, 3.5, and 4 calculations have been performed for the F_2-type vibrational states only.

To check the validity of the scheme of calculations derived here, we first reproduced the results for the states analyzed already in Ref. 57 and found that our calculations (realized with analytical language MAPLE) exactly agreed with Table III from Ref. 57. This perfect consistency can be considered as a confirmation of our scheme of calculation and the computer code generated on that basis, as well as an independent confirmation of the results of Ref. 57.

In a second step, we have computed the tetrahedral splitting for all vibrational states discussed above. Due to the large volume of information, we present here, as an illustration, results only for two sets of vibrational bands:

1. The bands $\nu_3 + 5\nu_4$ and $\nu_1 + 5\nu_4$.

This article is copyrighted as indicated in the article. Reuse of AIP content is subject to the terms at: http://scitation.aip.org/termsconditions. Downloaded to IP: 129.132.218.57 On: Tue, 16 Dec 2014 16:10:57

Tetrahedral splittings and resonance interactions of the bands $\nu_3 + 5\nu_4$ and $\nu_1 + 5\nu_4$.

	$\nu_3 + 5\nu_4$								$\nu_1 + 5\nu_4$			
	$l_3 = 1$ $l_4 = 1$	$l_3 = 1$ $l_4 = 3$	$l_3 = 1$ $l_4 = 3$	$l_3 = 1$ $l_4 = 3$	$l_3 = 1$ $l_4 = 5$	$l_3 = 1$ $l_4 = 5$	$l_3 = 1$ $l_4 = 5$	$l_3 = 1$ $l_4 = 5$	$l_3 = 0$ $l_4 = 1$	$l_3 = 0$ $l_4 = 3$	$l_3 = 0$ $l_4 = 5$	$l_3 = 0$ $l_4 = 5$
	1	2	3	4	5	6	7	8	9	10	11	12
1	$W_{1,1}$	$W_{1,2}$	$W_{1,3}$	$W_{1,4}$	$W_{1,5}$	$W_{1,6}$	$W_{1,7}$	$W_{1,8}$	0	0	0	0
2		$W_{2,2}$	$W_{2,3}$	$W_{2,4}$	$W_{2,5}$	$W_{2,6}$	$W_{2,7}$	$W_{2,8}$	0	0	0	0
3			$W_{3,3}$	$W_{3,4}$	$W_{3,5}$	$W_{3,6}$	$W_{3,7}$	$W_{3,8}$	0	0	0	0
4				$W_{4,4}$	$W_{4,5}$	$W_{4,6}$	$W_{4,7}$	$W_{4,8}$	0	0	0	0
5					$W_{5,5}$	$W_{5,6}$	$W_{5,7}$	$W_{5,8}$	0	0	0	0
6						$W_{6,6}$	$W_{6,7}$	$W_{6,8}$	0	0	0	0
7							$W_{7,7}$	$W_{7,8}$	0	0	0	0
8								$W_{8,8}$	0	0	0	0
9									$W_{9,9}$	$W_{9,10}$	$W_{9,11}$	$W_{9,12}$
10										$W_{10,10}$	$W_{10,11}$	$W_{10,12}$
11											$W_{11,11}$	$W_{11,12}$
12												$W_{12,12}$

FIG. 15. Tetrahedral splitting matrix for the set of F_2-type sub-bands of the bands $\nu_3 + 5\nu_4$ and $\nu_1 + 5\nu_4$ of the CH_4 molecule.

2. The set of interacting bands $\nu_2 + 2\nu_3 + 2\nu_4$, $\nu_1 + \nu_2 + \nu_3 + 2\nu_4$ and $2\nu_1 + \nu_2 + 2\nu_4$ from the polyad $N = 3.5$ (the complete results for all polyads, $0.5 \leq N = \leq 4$ are presented in Appendix D, as part of the supplementary material[109]).

Because the bands $\nu_3 + 5\nu_4$ and $\nu_1 + 5\nu_4$ comprise 8 and 4 subbands of F_2 symmetry, respectively, the tetrahedral splittings are determined by a matrix of the dimension 12 × 12. The structure of this matrix is shown in Fig. 15 (see also Table VII). Similarly, the interacting bands $\nu_2 + 2\nu_3 + 2\nu_4$, $\nu_1 + \nu_2 + \nu_3 + 2\nu_4$, and $2\nu_1 + \nu_2 + 2\nu_4$, comprise 8, 3, and 1 sub-bands of F_2 symmetry, respectively. The corresponding matrix is shown in Fig. 16 and Table VIII and has also the dimension of 12 × 12.

VI. VIBRATIONAL ANALYSIS FOR $^{12}CH_4$ UP TO 12 000 cm^{-1}: SPECTROSCOPIC PARAMETERS AND ENERGY LEVELS

As initial data we used experimental values of the band centers taken both from the earlier references,[43,78,80,119] and the new results from Table IV. The experimental band centers used are summarized in Table IX (columns 1 and 2). Column 3 indicates the origin of the experimental data.

For practical reasons we do not use the energy terms $E_v + W(v_1v_2v_3v_4n\Gamma_v)$, Eq. (7) but the values of the band centers, $E_v + W(v_1v_2v_3v_4n\Gamma_v) - E_{gr.}$, with the ground state energy $E_{gr.}$ which leads to simpler expressions than given by Eqs. (7) and (8)

$$\tilde{H}_{vv} = \tilde{\nu}_v + W(v_1v_2v_3v_4n\Gamma_v)/(hc). \tag{35}$$

where

$$\tilde{\nu}_v = \sum_i \tilde{\omega}_i v_i + \sum_{i,j\geq i} \tilde{x}_{ij} v_i v_j. \tag{36}$$

It is easy to show that two sets of parameters, ω_i, x_{ij} and $\tilde{\omega}_i$, $\tilde{x}_{ij}$, provide equivalent representations of energy levels and, if one does not take into account the third order anharmonic coefficients y_{ijk}, simple relations between the two sets of parameters are valid:

$$\tilde{\omega}_i = \omega_i + x_{ii}d_i + \frac{1}{2}\sum_{j\neq i} x_{ij}d_j \tag{37}$$

and

$$\tilde{x}_{ij} = x_{ij}. \tag{38}$$

The problem of determining the spectroscopic parameters (harmonic wavenumbers, ω, anharmonic coefficients, x, and parameters of tetrahedral splittings) was solved in three steps. At first, we used as starting values the highly accurate values of the 18 band centers marked by an asterisk, *, in the column 2 of Table IX) and obtained values of the same number, 18, of spectroscopic parameters: $\tilde{\omega}_2$, $\tilde{\omega}_4$, x_{22},x_{24}, x_{44}, G_{22}, G_{44}, T_{24}, T_{44}, and $\tilde{\omega}_1$, $\tilde{\omega}_3$, x_{14}, x_{23},x_{34}, G_{34}, T_{23}, T_{34}, S_{34}. The first nine parameters of the eighteen parameters can be

This article is copyrighted as indicated in the article. Reuse of AIP content is subject to the terms at: http://scitation.aip.org/termsconditions. Downloaded to IP: 129.132.218.57 On: Tue, 16 Dec 2014 16:10:57

TABLE VII. Non-zero elements of the matrix of tetrahedral splittings and resonance interactions for the set of bands $\nu_3 + 5\nu_4$ and $\nu_1 + 5\nu_4$.

i, j	v_1	v_2	l_2	v_3	l_3	v_4	l_4	v_1'	v_2'	l_2'	v_3'	l_3'	v_4'	l_4'	$W_{i,j}$
1, 1	0	0	0	1	1	5	1	0	0	0	1	1	5	1	$2(G_{33}+G_{44})+G_{34}+\frac{26}{5}(\frac{1}{3}S_{34}-2T_{34})$
1, 2	0	0	0	1	1	5	1	0	0	0	1	1	5	3	$\sqrt{6}(\frac{6}{5}S_{34}-\frac{208}{21}T_{44}-\frac{8}{35}T_{34})$
1, 3	0	0	0	1	1	5	1	0	0	0	1	1	5	3	$2\sqrt{\frac{30}{7}}(T_{34}-\frac{26}{3}T_{44})$
1, 4	0	0	0	1	1	5	1	0	0	0	1	1	5	3	$2\frac{\sqrt{30}}{7}(\frac{26}{3}T_{44}+3T_{34})$
1, 5	0	0	0	1	1	5	1	0	0	0	1	1	5	5	$\frac{32}{\sqrt{33}}T_{44}$
1, 6	0	0	0	1	1	5	1	0	0	0	1	1	5	5	$-64\sqrt{\frac{2}{21}}T44$
1, 7	0	0	0	1	1	5	1	0	0	0	1	1	5	5	$104\sqrt{\frac{5}{231}}T44$
1, 8	0	0	0	1	1	5	1	0	0	0	1	1	5	5	$40\sqrt{\frac{3}{7}}T44$
2, 2	0	0	0	1	1	5	3	0	0	0	1	1	5	3	$2G_{33}+12G_{44}-\frac{88}{9}T_{44}+\frac{104}{15}S_{34}-\frac{104}{315}T_{34}-4G_{34}$
2, 3	0	0	0	1	1	5	3	0	0	0	1	1	5	3	$\frac{2\sqrt{35}}{9}(22T_{44}+\frac{13}{7}T_{34})$
2, 4	0	0	0	1	1	5	3	0	0	0	1	1	5	3	$2\sqrt{5}(2T_{44}+\frac{13}{21}T_{34})$
2, 5	0	0	0	1	1	5	3	0	0	0	1	1	5	5	$\frac{4\sqrt{22}}{77}(52T_{44}+\frac{5}{3}T_{34})$
2, 6	0	0	0	1	1	5	3	0	0	0	1	1	5	5	$\frac{16}{9\sqrt{7}}(26T_{44}+5T_{34})$
2, 7	0	0	0	1	1	5	3	0	0	0	1	1	5	5	$\frac{2\sqrt{770}}{693}(26T_{44}+65T_{34})$
2, 8	0	0	0	1	1	5	3	0	0	0	1	1	5	5	$\frac{10}{3}\sqrt{\frac{2}{7}}(2T_{44}+5T_{34})$
3, 3	0	0	0	1	1	5	3	0	0	0	1	1	5	3	$2G_{33}+12G_{44}-\frac{14}{9}T_{44}-\frac{26}{3}S_{34}+\frac{13}{9}T_{34}-G_{34}$
3, 4	0	0	0	1	1	5	3	0	0	0	1	1	5	3	$-\sqrt{7}(10T_{44}-\frac{65}{21}T_{34})$
3, 5	0	0	0	1	1	5	3	0	0	0	1	1	5	5	$2\sqrt{\frac{10}{77}}(26T_{44}+\frac{5}{3}T_{34})$
3, 6	0	0	0	1	1	5	3	0	0	0	1	1	5	5	$\frac{2\sqrt{5}}{9}(22T_{44}-5T_{34})$
3, 7	0	0	0	1	1	5	3	0	0	0	1	1	5	5	$-\frac{115\sqrt{22}}{99}(T_{34}-2T_{44})$
3, 8	0	0	0	1	1	5	3	0	0	0	1	1	5	5	$-\frac{5\sqrt{10}}{3}(2T_{44}-T_{34})$
4, 4	0	0	0	1	1	5	3	0	0	0	1	1	5	3	$2G_{33}+12G_{44}-26T_{44}+\frac{26}{9}S_{34}-\frac{169}{21}T_{34}+3G_{34}$
4, 5	0	0	0	1	1	5	3	0	0	0	1	1	5	5	$\frac{\sqrt{110}}{7}(\frac{14}{9}S_{34}-\frac{52}{11}T_{44}-\frac{26}{33}T_{34})$
4, 6	0	0	0	1	1	5	3	0	0	0	1	1	5	5	$2\sqrt{\frac{5}{7}}(2T_{44}-\frac{1}{3}T_{34})$
4, 7	0	0	0	1	1	5	3	0	0	0	1	1	5	5	$-25\sqrt{\frac{2}{77}}(2T_{44}+\frac{1}{3}T_{34})$
4, 8	0	0	0	1	1	5	3	0	0	0	1	1	5	5	$5\sqrt{\frac{10}{7}}(2T_{44}+\frac{1}{3}T_{34})$
5, 5	0	0	0	1	1	5	5	0	0	0	1	1	5	5	$2G_{33}+30G_{44}-\frac{260}{11}T_{44}+\frac{52}{9}S_{34}-\frac{52}{33}T_{34}-6G_{34}$
5, 6	0	0	0	1	1	5	5	0	0	0	1	1	5	5	$-2\sqrt{154}(\frac{10}{77}T_{44}+\frac{1}{33}T_{34})$
5, 7	0	0	0	1	1	5	5	0	0	0	1	1	5	5	$-10\sqrt{35}(\frac{2}{77}T_{44}+\frac{1}{33}T_{34})$
5, 8	0	0	0	1	1	5	5	0	0	0	1	1	5	5	$10\sqrt{77}(\frac{2}{77}T_{44}+\frac{1}{33}T_{34})$
6, 6	0	0	0	1	1	5	5	0	0	0	1	1	5	5	$2G_{33}+30G_{44}+\frac{80}{9}T_{44}-\frac{26}{3}S_{34}-\frac{28}{9}T_{34}-G_{34}$
6, 7	0	0	0	1	1	5	5	0	0	0	1	1	5	5	$-\frac{85\sqrt{110}}{99}(2T_{44}-T_{34})$
6, 8	0	0	0	1	1	5	5	0	0	0	1	1	5	5	$-\frac{5\sqrt{2}}{3}(2T_{44}-T_{34})$
7, 7	0	0	0	1	1	5	5	0	0	0	1	1	5	5	$2G_{33}+30G_{44}-\frac{1180}{99}T_{44}+\frac{10}{3}S_{34}-\frac{295}{99}T_{34}+5G_{34}$
7, 8	0	0	0	1	1	5	5	0	0	0	1	1	5	5	$\frac{5\sqrt{55}}{33}(4T_{44}+T_{34})$
8, 8	0	0	0	1	1	5	5	0	0	0	1	1	5	5	$2G_{33}+30G_{44}+20T_{44}+\frac{10}{3}S_{34}+5T_{34}+5G_{34}$
9, 9	1	0	0	0	0	5	1	1	0	0	0	0	5	1	$2G_{44}$
9, 10	1	0	0	0	0	5	1	1	0	0	0	0	5	3	$-\frac{208}{\sqrt{21}}T_{44}$
9, 11	1	0	0	0	0	5	1	1	0	0	0	0	5	5	$40\sqrt{\frac{2}{3}}T_{44}$
9, 12	1	0	0	0	0	5	1	1	0	0	0	0	5	5	$8\sqrt{\frac{30}{7}}T_{44}$
10, 10	1	0	0	0	0	5	3	1	0	0	0	0	5	3	$12G_{44}+28T_{44}$
10, 11	1	0	0	0	0	5	3	1	0	0	0	0	5	5	$-40\sqrt{\frac{2}{7}}T_{44}$
10, 12	1	0	0	0	0	5	3	1	0	0	0	0	5	5	$8\sqrt{10}T_{44}$

This article is copyrighted as indicated in the article. Reuse of AIP content is subject to the terms at: http://scitation.aip.org/termsconditions. Downloaded to IP: 129.132.218.57 On: Tue, 16 Dec 2014 16:10:57

TABLE VII. (*Continued.*)

i,j	v_1	v_2	l_2	v_3	l_3	v_4	l_4	v'_1	v'_2	l'_2	v'_3	l'_3	v'_4	l'_4	$W_{i,j}$
11, 11	1	0	0	0	0	5	5	1	0	0	0	0	5	5	$30G_{44} + 20T_{44}$
11, 12	1	0	0	0	0	5	5	1	0	0	0	0	5	5	$20\sqrt{\frac{5}{7}}T_{44}$
12, 12	1	0	0	0	0	5	5	1	0	0	0	0	5	5	$30G_{44} - 20T_{44}$

described as pure deformation parameters, the last nine parameters can be described as stretch-deformation parameters. As one can see from the column 2 of Table IX, the 18 initial bands can also be divided in two groups: the 9 bands of pure deformation and 9 stretch-deformation bands with a single excitation of stretch quanta. These 18 parameters have been used afterwards for an estimation of the band centers of the higher pure deformation and stretch-deformation levels with a single excitation of a stretching quantum. The 34 additional higher experimental band centers known from previous work are predicted using the set of parameters obtained with the mean accuracy better than 1.5 cm^{-1}. Considering this accuracy we can claim first that 18 spectroscopic parameters are sufficient for a reliable prediction and that, second, interactions can be neglected at this point.

In a second step of the vibrational analysis we added four pure stretching parameters: x_{11}, x_{33}, G_{33}, and T_{33}, and the initial values of four band centers: $2\nu_1(A_1)$, $2\nu_3(A_1)$, $2\nu_3(E)$, and $2\nu_3(F_2)$ (they are marked in the column 2 of Table VIII by a double asterisk, (**)). After this step we were able to assign all the bands listed in Table IV. However, we found that the accuracy of the prediction of the centers of those bands which correspond to two and more excitations of stretching quanta is less good than for the first set of the bands discussed above because we neglected the strong resonance interactions discussed in Sec. V F.

The final step of the analysis was the joint fit of 26 spectroscopic parameters (two interaction parameters, F_{1133} and F_{1333}, and two anharmonic coefficients, x_{12} and x_{13}, were added to the 22 parameters) of the experimental band centers from Table IX. Band centers from Ref. 78, which were based on less than 5 (and sometimes zero) rovibrational lines for the given band, were not included in the fit and therefore not listed. We refer also to Table IX, where the results of the band center estimations from previous work are presented. One can see that the results of all theoretical calculations for the bands mentioned agree with satisfactory accuracy.

The parameters obtained from the fit are presented in Table X column 2 together with their 1σ statistical confidence intervals. They reproduce 52 initial experimental term values (without the band centers from Ref. 78) with a $d_{rms} = 0.64$ cm^{-1}. In this case, as was mentioned above, the calculations for comparison with the recent data from Ref. 78 can be considered as a prediction.

After our analysis had been largely completed, we also learned from Ref. 120 which contains the results of an analysis of the set of sub-bands of the $5\nu_4$ band (they are reproduced in column 2 of Table IX around 6500 cm^{-1}). In the initial fit (results are presented in column 2 of Table IX) we did not take into account the values of these four sub-band centers. As a consequence the corresponding values of the centers of sub-bands, $5\nu_4$, in column 4 of Table IX should be consid-

Tetrahedral splittings and resonance interactions of the bands $\nu_2 + 2\nu_3 + 2\nu_4$, $\nu_1 + \nu_2 + \nu_3 + 2\nu_4$ and $2\nu_1 + \nu_2 + 2\nu_4$.

	$\nu_2 + 2\nu_3 + 2\nu_4$							$\nu_1 + \nu_2 + \nu_3 + 2\nu_4$				$\nu_2 + 2\nu_1 + 2\nu_4$
	1	2	3	4	5	6	7	8	9	10	11	12
	$l_2 = 1$ $l_3 = 0$ $l_4 = 2$	$l_2 = 1$ $l_3 = 2$ $l_4 = 0$	$l_2 = 1$ $l_3 = 2$ $l_4 = 2$	$l_2 = 1$ $l_3 = 2$ $l_4 = 2$	$l_2 = 1$ $l_3 = 2$ $l_4 = 2$	$l_2 = 1$ $l_3 = 2$ $l_4 = 2$	$l_2 = 1$ $l_3 = 2$ $l_4 = 2$	$l_2 = 1$ $l_3 = 2$ $l_4 = 2$	$l_2 = 1$ $l_3 = 1$ $l_4 = 0$	$l_2 = 1$ $l_3 = 1$ $l_4 = 2$	$l_2 = 1$ $l_3 = 1$ $l_4 = 2$	$l_2 = 1$ $l_3 = 0$ $l_4 = 2$
1	$W_{1,1}$	$W_{1,2}$	$W_{1,3}$	$W_{1,4}$	$W_{1,5}$	$W_{1,6}$	$W_{1,7}$	$W_{1,8}$	0	0	0	$W_{1,12}$
2		$W_{2,2}$	$W_{2,3}$	$W_{2,4}$	$W_{2,5}$	$W_{2,6}$	$W_{2,7}$	$W_{2,8}$	$W_{2,9}$	0	0	0
3			$W_{3,3}$	$W_{3,4}$	$W_{3,5}$	$W_{3,6}$	$W_{3,7}$	0	0	0	0	0
4				$W_{4,4}$	$W_{4,5}$	$W_{4,6}$	$W_{4,7}$	$W_{4,8}$	0	0	0	0
5					$W_{5,5}$	$W_{5,6}$	$W_{5,7}$	$W_{5,8}$	0	0	0	0
6						$W_{6,6}$	$W_{6,7}$	$W_{6,8}$	0	$W_{6,10}$	$W_{6,11}$	0
7							$W_{7,7}$	$W_{7,8}$	0	$W_{7,10}$	$W_{7,11}$	0
8								$W_{8,8}$	0	$W_{8,10}$	$W_{8,11}$	0
9									$W_{9,9}$	$W_{9,10}$	$W_{9,11}$	0
10										$W_{10,10}$	$W_{10,11}$	0
11											$W_{11,11}$	0
12												$W_{12,12}$

FIG. 16. Tetrahedral splitting matrix for the set of F_2-type sub-band of the bands $\nu_2 + 2\nu_3 + 2\nu_4$, $\nu_1 + \nu_2 + \nu_3 + 2\nu_4$, and $2\nu_1 + \nu_2 + 2\nu_4$. Resonance interactions between all three sets of sub-bands are also taken into account.

This article is copyrighted as indicated in the article. Reuse of AIP content is subject to the terms at: http://scitation.aip.org/termsconditions. Downloaded to IP: 129.132.218.57 On: Tue, 16 Dec 2014 16:10:57

TABLE VIII. Non-zero elements of the matrix of tetrahedral splittings and resonance interactions for the set of bands $\nu_2 + 2\nu_3 + 2\nu_4$ / $\nu_1 + \nu_2 + \nu_3 + 2\nu_4$/ $2\nu_1 + \nu_2 + 2\nu_4$.

i, j	v_1	v_2	l_2	v_3	l_3	v_4	l_4	v_1'	v_2'	l_2'	v_3'	l_3'	v_4'	l_4'	W
1, 1	0	1	1	2	0	2	2	0	1	1	2	0	2	2	$G_{22} + 6G_{44} - 8T_{24} - 8T_{44}$
1, 2	0	1	1	2	0	2	2	0	1	1	2	2	2	0	$\frac{4}{3}(S_{34} - 4T_{34})$
1, 3	0	1	1	2	0	2	2	0	1	1	2	2	2	2	$-\frac{16}{\sqrt{5}}T_{23}$
1, 4	0	1	1	2	0	2	2	0	1	1	2	2	2	2	$-\frac{8}{\sqrt{5}}T_{23}$
1, 5	0	1	1	2	0	2	2	0	1	1	2	2	2	2	$-8T_{23}$
1, 6	0	1	1	2	0	2	2	0	1	1	2	2	2	2	$(\frac{2}{3}S_{34} - \frac{16}{7}T_{23} - \frac{16}{21}T_{34})\sqrt{7}$
1, 7	0	1	1	2	0	2	2	0	1	1	2	2	2	2	$4(\frac{5}{3}T_{34} - 2T_{23})$
1, 8	0	1	1	2	0	2	2	0	1	1	2	2	2	2	$\sqrt{2}1(\frac{20}{21}T_{34} - \frac{8}{7}T_{23})$
1, 12	0	1	1	2	0	2	2	2	1	1	0	0	2	2	$\frac{\sqrt{3}}{2}F_{1133}$
2, 2	0	1	1	2	2	2	0	0	1	1	2	2	2	0	$G_{22} + 6G_{33} - 8T_{23} - 8T_{33}$
2, 3	0	1	1	2	2	2	0	0	1	1	2	2	2	2	$\frac{16}{\sqrt{5}}T_{24}$
2, 4	0	1	1	2	2	2	0	0	1	1	2	2	2	2	$\frac{8}{\sqrt{5}}T_{24}$
2, 5	0	1	1	2	2	2	0	0	1	1	2	2	2	2	$-8T_{24}$
2, 6	0	1	1	2	2	2	0	0	1	1	2	2	2	2	$2\sqrt{7}(\frac{1}{3}S_{34} - \frac{8}{7}T_{24} - \frac{8}{21}T_{34})$
2, 7	0	1	1	2	2	2	0	0	1	1	2	2	2	2	$4(2T_{24} - \frac{5}{3}T_{34})$
2, 8	0	1	1	2	2	2	0	0	1	1	2	2	2	2	$\sqrt{2}1(\frac{20}{21}T_{34} - \frac{8}{7}T_{24})$
2, 9	0	1	1	2	2	2	0	1	1	1	1	1	2	0	$\frac{1}{4}F_{1333}$
3, 3	0	1	1	2	2	2	2	0	1	1	2	2	2	2	$G_{22} + 6G_{33} + 6G_{44} + \frac{28}{5}T_{23} + \frac{28}{5}T_{24} + \frac{14}{3}S_{34} - 5G_{34}$
3, 4	0	1	1	2	2	2	2	0	1	1	2	2	2	2	$4(\frac{6}{5}T_{23} + \frac{6}{5}T_{24} + T_{33} + T_{44} + T_{34})$
3, 5	0	1	1	2	2	2	2	0	1	1	2	2	2	2	$-4\sqrt{5}(T_{44} - T_{33})$
3, 6	0	1	1	2	2	2	2	0	1	1	2	2	2	2	$-4\sqrt{\frac{7}{5}}(T_{23} - T_{24})$
3, 7	0	1	1	2	2	2	2	0	1	1	2	2	2	2	$-\frac{8}{\sqrt{5}}(T_{23} + T_{24})$
4, 4	0	1	1	2	2	2	2	0	1	1	2	2	2	2	$G_{22} + 6G_{33} + 6G_{44} - \frac{8}{5}T_{23} - \frac{8}{5}T_{24}$ $-6T_{33} - 6T_{44} - \frac{16}{3}S_{34} + 4T_{34}$
4, 5	0	1	1	2	2	2	2	0	1	1	2	2	2	2	$-2\sqrt{5}(T_{44} - T_{33})$
4, 6	0	1	1	2	2	2	2	0	1	1	2	2	2	2	$-\frac{16}{\sqrt{35}}(T_{24} - T_{23})$
4, 7	0	1	1	2	2	2	2	0	1	1	2	2	2	2	$-\frac{4}{\sqrt{5}}(T_{23} + T_{24})$
4, 8	0	1	1	2	2	2	2	0	1	1	2	2	2	2	$-4\sqrt{\frac{15}{7}}(T_{23} - T_{24})$
5, 5	0	1	1	2	2	2	2	0	1	1	2	2	2	2	$G_{22} + 6G_{33} + 6G_{44} + 8T_{23} + 8T_{24} + 2T_{33} + 2T_{44}$ $+\frac{8}{3}S_{34} + 4T_{34} + 4G_{34}$
5, 6	0	1	1	2	2	2	2	0	1	1	2	2	2	2	$-\frac{8}{\sqrt{7}}(T_{23} + T_{24})$
5, 7	0	1	1	2	2	2	2	0	1	1	2	2	2	2	$4(T_{24} - T_{23})$
5, 8	0	1	1	2	2	2	2	0	1	1	2	2	2	2	$-4\sqrt{\frac{3}{7}}(T_{23} + T_{24})$
6, 6	0	1	1	2	2	2	2	0	1	1	2	2	2	2	$G_{22} + 6G_{33} + 6G_{44} + \frac{12}{7}T_{23} + \frac{12}{7}T_{24}$ $-\frac{16}{7}T_{33} - \frac{16}{7}T_{44} - 2S_{34} - \frac{68}{21}T_{34} - 3G_{34}$
6, 7	0	1	1	2	2	2	2	0	1	1	2	2	2	2	$\frac{4}{\sqrt{7}}(4T_{23} - 4T_{24} + 5T_{33} - 5T_{44})$
6, 8	0	1	1	2	2	2	2	0	1	1	2	2	2	2	$\frac{4\sqrt{3}}{7}(5T_{33} + 5T_{44} - \frac{5}{3}T_{34} - 2T_{23} - 2T_{24})$
6, 10	0	1	1	2	2	2	2	1	1	1	1	1	2	2	$\frac{1}{4\sqrt{35}}F_{1333}$
6, 11	0	1	1	2	2	2	2	1	1	1	1	1	2	2	$\sqrt{\frac{3}{70}}F_{1333}$
7, 7	0	1	1	2	2	2	2	0	1	1	2	2	2	2	$G_{22} + 6G_{33} + 6G_{44} + 2T_{33} + 2T_{44} - \frac{16}{3}S_{34} - \frac{4}{3}T_{34}$
7, 8	0	1	1	2	2	2	2	0	1	1	2	2	2	2	$-2\sqrt{\frac{3}{7}}(4T_{24} - 4T_{23} + 5T_{44} - 5T_{33})$
7, 10	0	1	1	2	2	2	2	1	1	1	1	1	2	2	$\frac{1}{4\sqrt{5}}F_{1333}$
7, 11	0	1	1	2	2	2	2	1	1	1	1	1	2	2	$-\frac{1}{4}\sqrt{\frac{3}{10}}F_{1333}$

This article is copyrighted as indicated in the article. Reuse of AIP content is subject to the terms at: http://scitation.aip.org/termsconditions. Downloaded to IP: 129.132.218.57 On: Tue, 16 Dec 2014 16:10:57

TABLE VIII. (*Continued.*)

i, j	v_1	v_2	l_2	v_3	l_3	v_4	l_4	v'_1	v'_2	l'_2	v'_3	l'_3	v'_4	l'_4	W
8, 8	0	1	1	2	2	2	2	0	1	1	2	2	2	2	$G_{22}+6G_{33}+6G_{44}+\frac{16}{7}T_{23}+\frac{16}{7}T_{24}$ $-\frac{26}{7}T_{33}-\frac{26}{7}T_{44}+\frac{8}{3}S_{34}-\frac{52}{7}T_{34}+4G_{34}$
8, 10	0	1	1	2	2	2	2	1	1	1	1	1	2	2	$-\frac{3}{4}\sqrt{\frac{3}{35}}F_{1333}$
8, 11	0	1	1	2	2	2	2	1	1	1	1	1	2	2	$-\frac{1}{4\sqrt{70}}F_{1333}$
9, 9	1	1	1	1	1	2	0	1	1	1	1	1	2	0	$G_{22}+2G_{33}+8T_{23}$
9, 10	1	1	1	1	1	2	0	1	1	1	1	1	2	2	$\sqrt{5}(\frac{16}{5}T_{24}+\frac{2}{3}S_{34})$
9, 11	1	1	1	1	1	2	0	1	1	1	1	1	2	2	$-4\sqrt{30}(\frac{2}{5}T_{24}+\frac{1}{3}T_{34})$
0, 10	1	1	1	1	1	2	2	1	1	1	1	1	2	2	$G_{22}+2G_{33}+6G_{44}+\frac{4}{5}T_{23}+\frac{28}{5}T_{24}+\frac{14}{3}S_{34}-3G_{34}$
11, 10	1	1	1	1	1	2	2	1	1	1	1	1	2	2	$-\frac{4\sqrt{6}}{5}(3T_{23}+T_{24})-\frac{4}{\sqrt{6}}(6T_{44}+T_{34})$
11, 11	1	1	1	1	1	2	2	1	1	1	1	1	2	2	$G_{22}+2G_{33}+6G_{44}+\frac{16}{5}T_{23}+\frac{32}{5}T_{24}$ $+4T_{44}+\frac{4}{3}S_{34}+4T_{34}+2G_{34}$
12, 12	2	1	1	0	0	2	2	2	1	1	0	0	2	2	$G_{22}+6G_{44}-8T_{24}-8T_{44}$

ered as a prediction, which is considerably better than analogous predictions with other sets of data (see, for comparison, corresponding results from columns 6–11 of Table IX).

Column 5 of Table IX presents results of the fit with the four additional terms being included. Of course, in this case, the agreement between the experimental data and the results from the fit is much better. However, even in the second fit, the results for the $5\nu_4$ subbands are less good than for the other undoubtedly correct band centers. This effect is perhaps due to the high excitations with five bending vibrational quanta of the $5\nu_4$ band. For a more correct description of the vibrational structure it is necessary to consider tetrahedral splitting of higher order (similar to higher anharmonicities in the description of unperturbed vibrational energies, and perhaps also include the CH stretching-bending Fermi resonance explicitly in the model). To confirm this observation we note that for the four subbands of the $5\nu_4$ band the largest differences Δ between the experimental and calculated values have different signs. Thus, this discrepancy cannot be removed just by adding higher order anharmonicity, but one needs higher order tetrahedral interactions.

As for the initial fit, the results of the second fit are presented in Table X (column 3). Comparison with the values from column 2 of Table X shows that the values of parameters fitted are not changed very much.

The values of the band centers calculated with the parameters from columns 2 and 3 of Table X are shown in columns 4 and 5 of Table IX. There is good agreement between the experimental and calculated band centers.

As a further test of our results, we compare the values obtained for the "stretching" parameters with the general relations which have been derived in the local mode model for the CH_4 −type molecules, see, e.g., Ref. 121. According to Ref. 121, the following relations apply for some of the spectroscopic parameters for CH_4:

$$x_{11} = \frac{1}{4}x_{13} = \frac{5}{9}x_{33} = -\frac{5}{3}G_{33} = -5T_{33} = \frac{1}{4}F_{1133} = \frac{1}{16}F_{1333}. \quad (39)$$

Table XI presents a test of these relations as applied to the set of parameters obtained from the fit of the experimental data. One finds reasonable consistency as expressed in terms of the values equivalent to x_{33} in Table XI.

We also compare our results with the results of previous calculations for methane. We calculated the band centers from Table IX on the basis of the set of spectroscopic parameters given by Lee, Martin, and Taylor (LMT,[122] we reproduce these parameters in column 4 of Table X). The results of the two calculations are shown in columns 6 and 7 of Table IX. In column 6 calculations were made directly with the parameters from Ref. 122. For the results presented in column 7 we added two resonance interaction parameters F_{1133} and F_{1333} from column 2 of Table X to the *LMT*-parameters. Also for comparison, the columns 8–11 of Table IX give the values of the band centers estimated in Refs. 19 and 123–125. Columns 8 and 9 present calculations with two different basis sets from Refs. 19 and 123. One can see that all the results agree with each other more or less, but our present results are closer to the experimental values of the band centers, and they cover a larger spectral range up to higher frequencies.

We have also checked the efficiency of our model by the fit of an alternative set of energy levels. The column 5 of Table X gives also the results of such a test. The parameters presented in column 5 were obtained from the fit of "*ab initio*" energies from Ref. 123 (they are reproduced also in column 4 of Table S1 of the supplementary material;[109] see also Appendix E). As one can see they agree approximately with our data in columns 2-3 of Table X. The d_{rms} deviation is 3.03 cm^{-1} for the 142 energies used for the parameters from column 5, Table X. Also as an illustration, column 5 of Table S1 (supplementary material[109]) presents the differences $\Delta = E - E^{(fit)}$ (in cm^{-1}) for the set of data from Ref. 123.

The set of spectroscopic parameters from column 2 of Table X was used for estimating the vibrational band centers up to 12 000 cm^{-1}. The results and a comparison with results from Ref. 123 are presented in Table S1 (compare column 2–3 and 4).

This article is copyrighted as indicated in the article. Reuse of AIP content is subject to the terms at: http://scitation.aip.org/termsconditions. Downloaded to IP: 129.132.218.57 On: Tue, 16 Dec 2014 16:10:57

TABLE IX. Band centers for $^{12}CH_4$ (in cm^{-1}).

Band	Exp.	Ref.	Δ,[a] –I, tw[b]	Δ,[a] –II, tw[b]	Δ,[a] –1, Ref. 122[c]	Δ,[a] –2, Ref. 122[c]	Δ,[a] –1, Ref. 19[d]	Δ,[a] –2, Ref. 123[d]	Δ,[a] Ref. 124	Δ,[a] Ref. 125
1	2	3	4	5	6	7	8	9	10	11
$\nu_4(F_2)$	1310.76(*)[e]	43	0.29	0.26	− 1.93	− 1.93	− 0.98	− 0.98	− 0.99	0.26
$\nu_2(E)$	1533.33(*)[e]	43	− 0.02	0.28	0.20	0.20	0.08	0.08	0.08	− 0.69
$2\nu_4(A_1)$	2587.04(*)[e]	43	− 0.71	− 1.41	− 6.68	− 6.68	− 2.73	− 2.73	− 2.73	− 0.41
$2\nu_4(F_2)$	2614.26(*)[e]	43	0.64	0.68	− 5.18	− 5.18	− 1.98	− 1.98	− 1.98	0.16
$2\nu_4(E)$	2624.62(*)[e]	43	0.16	0.38	− 5.52	− 5.52	− 2.68	− 2.67	− 2.68	0.21
$\nu_2 + \nu_4(F_2)$	2830.32(*)[e]	43	− 0.72	− 0.07	− 3.02	− 3.02	− 1.21	− 1.20	− 1.21	− 0.04
$\nu_2 + \nu_4(F_1)$	2846.07(*)[e]	43	0.61	0.90	− 1.76	− 1.76	− 0.83	− 0.83	− 0.83	− 0.25
$\nu_1(A_1)$	2916.48(*)[e]	43	− 0.15	− 0.56	5.20	5.20	2.55	2.55	2.69	− 1.46
$\nu_3(F_2)$	3019.49(*)[e]	43	0.25	0.12	7.84	7.84	5.89	5.89	6.06	− 0.46
$2\nu_2(A_1)$	3063.65(*)[e]	43	0.03	− 0.42	− 2.72	− 2.72	0.16	0.17	0.16	− 0.29
$2\nu_2(E)$	3065.14(*)[e]	43	0.07	0.35	0.33	0.33	0.13	0.13	0.13	− 0.67
$3\nu_4(1F_2)$	3870.49	tw	0.28	− 0.66	− 0.69	− 10.71	− 4.26	− 4.25	− 4.24	− 1.06
$3\nu_4(A_1)$	3909.20	43	− 0.26	− 0.06	− 11.05	− 11.05	− 3.09	− 3.08	− 3.08	− 0.85
$3\nu_4(F_1)$	3920.51	43	0.21	0.59	− 10.42	− 10.42	− 3.58	− 3.57	− 3.57	− 0.13
$3\nu_4(2F_2)$	3930.92	tw	0.03	0.75	0.57	− 10.47	− 4.42	− 4.40	− 4.42	− 0.11
$\nu_2 + 2\nu_4(1E)$	4101.393	43	− 3.59	− 3.26	− 6.71	− 6.71	0.67	0.71	0.74	2.72
$\nu_2 + 2\nu_4(F_1)$	4128.76	43	0.13	1.05	− 6.13	− 6.13	− 2.74	− 2.69	− 2.68	0.46
$\nu_2 + 2\nu_4(A_1)$	4132.86	43	0.60	1.88	− 5.29	− 5.29	− 2.81	− 2.77	− 2.77	1.04
$\nu_2 + 2\nu_4(F_2)$	4142.86	tw	− 0.19	− 0.12	0.36	− 6.49	− 2.02	− 1.97	− 1.99	− 0.54
$\nu_2 + 2\nu_4(2E)$	4151.21	43	− 0.46	0.13	− 6.87	− 6.87	− 2.54	− 2.50	− 2.52	− 0.11
$\nu_2 + 2\nu_4(A_2)$	4161.85	43	0.75	1.30	− 5.39	− 5.39	− 2.49	− 2.45	− 2.46	− 0.13
$\nu_1 + \nu_4(F_2)$	4223.46(*)[e]	tw	− 0.35	− 0.87	0.47	0.47	1.61	1.62	1.74	− 3.05
$\nu_3 + \nu_4(F_2)$	4319.21(*)[e]	43	− 0.26	0.81	4.60	4.60	4.98	4.98	5.15	− 0.49
$\nu_3 + \nu_4(E)$	4322.18(*)[e]	43	0.14	− 0.32	5.70	5.70	4.56	4.56	4.73	0.14
$\nu_3 + \nu_4(F_1)$	4322.59(*)[e]	43	0.62	0.27	5.80	5.80	4.75	4.75	4.92	− 0.22
$\nu_3 + \nu_4(A_1)$	4322.70(*)[e]	43	− 0.12	0.63	4.97	4.97	4.30	4.30	4.46	− 4.47
$2\nu_2 + \nu_4(1F_2)$	4348.72	tw	− 0.53	0.11	0.07	− 4.60	− 1.33	− 1.30	− 1.30	0.32
$2\nu_2 + \nu_4(F_1)$	4363.61	43	− 0.15	− 0.19	− 3.45	− 3.45	− 1.43	− 1.40	− 1.41	− 0.11
$2\nu_2 + \nu_4(2F_2)$	4378.95	tw	0.83	0.76	0.72	− 3.36	− 0.67	− 0.64	− 0.65	0.17
$\nu_1 + \nu_2(E)$	4435.12	43	− 0.35	− 0.15	9.28	9.28	2.90	2.90	3.01	− 3.42
$\nu_2 + \nu_3(F_1)$	4537.55(*)[e]	43	0.19	0.39	8.87	8.87	6.20	6.20	6.35	− 0.90
$\nu_2 + \nu_3(F_2)$	4543.76(*)[e]	43	0.32	0.39	8.56	8.56	5.94	5.94	6.09	− 0.42
$3\nu_2(E)$	4592.03	43	− 0.24	− 1.75	− 6.16	− 6.16	0.09	0.11	0.10	0.59
$3\nu_2(A_2)$	4595.27	43	0.11	0.06	0.23	0.23	0.15	0.16	0.16	− 0.04
$3\nu_2(A_1)$	4595.50	43	0.34	0.29	0.41	0.41	0.12	0.13	0.13	0.19
$4\nu_4(1F_2)$	5143.36	78	2.41	1.22	− 15.03	− 15.03	− 7.20	− 5.84	− 5.77	
$4\nu_4(1E)$	5167.20	78	− 0.05	− 0.77	− 17.17	− 17.17	− 8.22	− 6.81	− 6.77	
$4\nu_4(2F_2)$	5210.74	78	− 1.90	− 1.29	− 18.92	− 18.92	− 6.24	− 4.94	− 4.92	
$4\nu_4(2E)$	5228.74	78	− 1.05	− 0.10	− 17.73	− 17.73	− 7.34	− 6.02	− 6.03	
$4\nu_4(F_1)$	5230.58	78	0.74	1.08	− 15.95	− 15.95	− 6.49	− 5.20	− 5.20	
$\nu_2 + 3\nu_4(1F_2)$	5370.49	78	− 4.29	− 3.93	− 9.50	− 15.96	− 12.16	− 5.17	− 5.09	
$\nu_2 + 3\nu_4(1F_1)$	5389.73	78	− 1.98	− 1.87	− 13.74	− 13.74	− 11.91	− 4.48	− 4.42	
$\nu_2 + 3\nu_4(E)$	5424.78	78	− 1.34	− 0.23	− 12.90	− 12.90	− 10.66	− 3.78	− 3.71	
$\nu_2 + 3\nu_4(2F_2)$	5429.87	78	1.99	3.74	− 9.28	− 9.28	− 10.80	− 4.35	− 4.47	
$\nu_2 + 3\nu_4(2F_1)$	5437.30	78	− 0.51	0.56	− 11.97	− 11.97	− 10.79	− 4.12	− 4.28	
$\nu_2 + 3\nu_4(3F_2)$	5444.80	78	− 2.28	− 1.15	− 13.71	− 13.71	− 10.26	− 3.69	− 3.89	
$\nu_2 + 3\nu_4(3F_1)$	5462.90	78	− 0.57	0.38	− 11.95	− 11.95	− 10.63	− 4.23	− 4.40	
$\nu_3 + 2\nu_4(1F_2)$	5587.98	[tw]	− 1.97	− 2.21	− 0.84	− 0.84	2.62	2.99	3.18	− 0.66
$\nu_3 + 2\nu_4(2F_1)$	5615.41	78	− 0.47	0.08	3.63	1.05	2.97	3.30	3.46	
$\nu_3 + 2\nu_4(2F_2)$	5615.99	78	− 0.61	− 0.07	0.76	0.76	3.72	4.20	4.36	− 1.52
$\nu_3 + 2\nu_4(E)$	5618.24	78	2.11	1.53	3.36	3.36	4.59	5.53	5.63	
$\nu_3 + 2\nu_4(1F_1)$	5626.11	78	0.07	− 0.05	1.38	1.38	2.69	6.42	6.42	
$\nu_3 + 2\nu_4(3F_2)$	5627.34	78	− 0.72	− 0.41	0.99	0.99	2.02	4.29	4.23	− 3.02
$2\nu_2 + 2\nu_4(1F_2)$	5641.86	78	0.58	1.70	− 36.77	− 36.77	− 9.26	− 3.45	− 3.42	
$2\nu_2 + 2\nu_4(F_1)$	5655.76	78	− 0.67	0.45	− 7.57	− 7.57	− 8.44	− 2.61	− 2.60	
$2\nu_2 + 2\nu_4(2F_2)$	5668.35	78	− 1.79	− 1.39	18.76	18.76	− 8.28	− 2.40	− 2.41	
$2\nu_1(A_1)$	5790.25(**)[e]	145	0.30	0.12	− 6.84	9.62	8.00	8.07	8.89	− 3.30

This article is copyrighted as indicated in the article. Reuse of AIP content is subject to the terms at: http://scitation.aip.org/termsconditions. Downloaded to IP: 129.132.218.57 On: Tue, 16 Dec 2014 16:10:57

TABLE IX. (*Continued.*)

Band	Exp.	Ref.	Δ,[a] −I, tw[b]	Δ,[a] −II, tw[b]	Δ[a] −1, Ref. 122[c]	Δ[a] −2, Ref. 122[c]	Δ[a] −1, Ref. 19[d]	Δ[a] −2, Ref. 123[d]	Δ[a], Ref. 124	Δ[a], Ref. 125
1	2	3	4	5	6	7	8	9	10	11
$\nu_2+\nu_3+\nu_4(1F_2)$	5823.10	78	−1.59	−3.76	4.50	4.50	8.87	9.34	9.47	
$\nu_2+\nu_3+\nu_4(1F_1)$	5825.42	78	−1.68	−0.42	4.28	4.28	4.91	5.06	5.20	
$\nu_2+\nu_3+\nu_4(1E)$	5832.02	78	−1.90	−1.17	3.89	3.89	3.38	4.19	4.23	
$\nu_2+\nu_3+\nu_4(2E)$	5842.56	78	0.04	0.65	6.37	6.37	4.11	4.64	4.69	
$\nu_2+\nu_3+\nu_4(A_2)$	5843.20	78	1.09	1.09	5.20	5.20	4.72	4.72	4.93	
$\nu_2+\nu_3+\nu_4(2F_2)$	5844.81	78	−0.53	−0.12	4.91	4.91	5.34	5.84	5.89	0.75
$\nu_2+\nu_3+\nu_4(2F_1)$	5847.38	78	1.46	1.43	7.02	7.02	4.67	5.21	5.25	
$\nu_1+\nu_3(F_2)$	5861.49	78	2.63	2.19	−8.47	18.41	7.53	7.90	8.21	
$3\nu_2+\nu_4(1F_2)$	5867.53	78	2.44	2.38	−5.05	−5.05	−4.94	−0.64	−0.85	
$3\nu_2+\nu_4(1F_1)$	5879.76	78	−1.18	−0.89	−5.76	−5.76	−6.39	−1.85	−1.58	
$3\nu_2+\nu_4(2F_2)$	5894.39	78	−1.08	−1.07	−5.75	−5.75	−6.09	−1.68	−0.80	
$\nu_1+2\nu_2(E)$	5952.44	78	−0.24	−0.14	13.27	13.27	2.61	2.88	2.87	
$2\nu_3(A_1)$	5968.15(**)[e]	119	2.04	0.72	48.22	31.76	7.20	7.33	7.84	
$2\nu_3(F_2)$	6004.63(**)[e]	[tw]	0.04	−0.13	41.24	14.36	11.18	11.23	12.25	−0.18
$2\nu_3(E)$	6043.87(**)[e]	132	−2.38	−2.06	15.10	15.10	12.00	12.01	12.60	−0.96
$2\nu_2+\nu_3(1F_2)$	6054.61	[tw]	0.90	0.94	9.66	9.66	6.42	6.67	6.68	−0.37
$2\nu_2+\nu_3(F_1)$	6060.62	78	0.29	0.50	9.84	9.84	5.76	6.17	6.04	
$2\nu_2+\nu_3(2F_2)$	6065.59	78	0.08	−0.26	7.46	7.46	5.53	6.03	5.92	0.63
$5\nu_4(1F_2)$	6377.53[f]	120	6.75	3.92	−19.17	−19.17	−20.39	−20.09		
$5\nu_4(2F_2)$	6450.06[f]	120	−0.52	−0.18	−24.31	−24.31	−19.57	−19.24		
$5\nu_4(3F_2)$	6507.55[f]	120	−5.43	−3.77	−29.45	−29.45	−16.84	−16.49		
$5\nu_4(4F_2)$	6539.18[f]	120	−1.44	0.76	−25.05	−25.05	−17.46	−17.07		
$\nu_1+\nu_3+\nu_4(F_2)$	7156.72[g]	[tw]	1.38	1.98	−15.44	12.43	−0.83	−0.15		
$\nu_2+2\nu_3(F_2)$	7510.34[g]	[tw]	−1.31	−0.99	42.71	15.64	11.51	11.56		
$2\nu_1+2\nu_4(F_2)$	8388.00[g]	[tw]	−0.16	−0.38	−25.48	−5.21				
$\nu_1+\nu_3+2\nu_4(1F_2)$	8421.00[g]	[tw]	−0.16	−0.89	−24.61	5.22				
$\nu_1+2\nu_3(F_2)$	8618.67[g]	[tw]	−0.42	−0.70	−8.61	46.20				
$2\nu_1+\nu_3(F_2)$	8808.95[g]	[tw]	0.13	−0.42	39.93	25.70				
$3\nu_3(1F_2)$	8907.30[g]	[tw]	−0.28	−0.68	112.57	37.90				0.84
$3\nu_3(2F_2)$	9045.96[g]	[tw]	0.30	1.11	50.01	28.59				0.11
$\nu_1+2\nu_3+\nu_4(1F_2)$	9888.47[h]	[tw]	0.15	0.82	−80.03	13.49				
$\nu_1+\nu_2+2\nu_3(F_2)$	10115.67[g]	[tw]	1.69	1.85	−74.43	34.19				
$3\nu_3+\nu_4(2F_2)$	10265.59[g]	[tw]	1.00	1.09	−20.30	21.57				
$2\nu_1+\nu_2+\nu_3(F_2)$	10302.17[g]	[tw]	−1.15	−1.16	47.32	30.77				
$\nu_1+3\nu_3(1F_2)$	11276.31[g]	[tw]	−0.88	−1.06	−235.20	41.27				
N/levels			92	92	92	92	81	81	75	46
d_{rms}/cm^{-1}			1.49	1.34	33.44	15.01	7.12	6.16	4.74	1.34

[a] $\Delta = \nu^{exp.} - \nu^{calc.}$.

[b] Calculation-1 and calculation-2 were made with the parameters from columns 2 and 3 of Table X, respectively (see text for details).

[c] Calculation-1 and calculation-2 were made with the parameters from Ref. 122 without and with resonance interaction parameters F_{1133} and F_{1333}, respectively.

[d] The data presented in columns 8 and 9 are differences between the values of column 2 of Table IX and the corresponding values from Table III of Ref. 19 (Basis I) and Ref. 123 (Basis II), respectively.

[e] Band centers marked by (*) and (**) were used in the first and the second step of the vibrational analysis (see text for details).

[f] Was not used in the Fit-1. As the consequence, the value from column 4 can be considered as a prediction (see text for more details).

[g] Assigned in the recorded 80 K spectrum of the present paper and used in the fit with the weight 1.

[h] Assigned in the recorded 80 K spectrum of the present paper and used in the fit with the weight 1/10.

VII. THE $^{12}CH_4/^{13}CH_4$ ISOTOPE EFFECT AND THE VIBRATIONAL SPECTRUM OF THE $^{13}CH_4$ ISOTOPOMER

In this section we use the experimental results obtained above for $^{12}CH_4$ for a theoretical estimation of the band centers of the $^{13}CH_4$ isotopomer and compare with experimental results for the latter isotopomer. We briefly mention three general equations from Isotopic Substitution Theory (see, e.g., Refs. 84 and 126–129. As shown in Ref. 126, the following three sets of relations can be derived for an arbitrary isotopic substitution in a polyatomic molecule:

1. A set of equations allowing one to determine all harmonic wavenumbers, ω'_ν, of an isotopically substituted molecule as functions of the harmonic wavenumbers, ω_λ, of a mother molecule and a set of coefficients $A_{\lambda\mu}$:

$$\sum_\lambda A_{\mu\lambda}\omega_\lambda^2\alpha_{\lambda\nu} = \alpha_{\mu\nu}\omega_\nu'^2; \tag{40}$$

This article is copyrighted as indicated in the article. Reuse of AIP content is subject to the terms at: http://scitation.aip.org/termsconditions. Downloaded to IP: 129.132.218.57 On: Tue, 16 Dec 2014 16:10:57

TABLE X. Spectroscopic parameters for $^{12}CH_4$ (in cm^{-1}).

Parameter	tw-I[a]	tw-II[b]	Ref. 122	Ref. 123[c]
1	2	3	4	5
$\tilde{\omega}_1$	2929.615(434)	2929.98 (186)	2923.55[d]	2929.010
$\tilde{\omega}_2$	1534.161(479)	1533.706(788)	1533.46[d]	1532.246
$\tilde{\omega}_3$	3025.806(656)	3026.01 (128)	3016.91[d]	3026.078
$\tilde{\omega}_4$	1306.923(428)	1307.172(457)	1308.53[d]	1304.250
x_{11}	− 12.986(677)	− 12.94 (129)	− 12.513	− 14.979
x_{12}	− 14.505(578)	− 14.620(774)	− 18.349	− 12.873
x_{13}	− 51.916(737)	− 52.43 (173)	− 52.746	− 45.082
x_{14}	− 3.283(342)	− 3.204(549)	− 0.764	− 3.299
x_{22}	− 1.175(221)	− 0.835(267)	− 0.332	− 0.472
x_{23}	− 11.989(366)	− 12.019(551)	− 12.843	− 12.972
x_{24}	− 5.564(272)	− 5.765(250)	− 5.231	− 4.309
x_{33}	− 25.709(321)	− 25.682(456)	− 28.469	− 28.173
x_{34}	− 8.465(375)	− 8.669(445)	− 8.249	− 9.083
x_{44}	− 6.523(212)	− 6.472(107)	− 5.831	− 5.026
G_{22}	0.361(135)	0.179(176)	− 0.390	0.311
G_{33}	9.573(222)	9.521(366)	11.606	9.085
G_{34}	− 0.755(299)	− 1.046(429)	− 0.747	− 1.566
G_{44}	5.034(94)	4.899(52)	4.999	4.721
T_{23}	0.366(33)	0.380(51)	0.408	0.377
T_{24}	− 0.901(35)	− 0.924(23)	− 0.906	− 0.904
T_{33}	3.336(74)	3.292(102)	3.266	3.277
T_{34}	0.257(80)	0.410(140)	0.189	0.610
T_{44}	0.542(27)	0.533(18)	0.535	0.525
S_{34}	0.009(89)	− 0.184(144)	0.019	− 0.006
F_{1133}	− 60.581(963)	− 61.93 (275)		− 60.581
F_{1333}	− 220.14(179)	− 218.38(478)		− 220.14
d_{rms}/cm^{-1}	1.49	1.34	33.44	3.03

[a]Obtained from the fit of the present work without using four band centers, $5\nu_4(nF_2)$ (see text for details).
[b]Obtained from the fit in which the four band centers, $5\nu_4(nF_2)$ (see text for details), were included as the fitted data.
[c]Obtained from the fit of "*ab initio*" energy values from Ref. 123. In this case, parameters F_{1133} and F_{1333} have been constrained to the values from the column 2 of this Table (see text for more details).
[d]Re-calculated from the parameters of Ref. 122 in accordance with equation (37).

the $\alpha_{\nu\lambda}$ are additional coefficients which are determined from a solution of a set of equations (40) and additional relations

$$A_{\mu\lambda} = \sum_{\nu} \alpha_{\lambda\nu}\alpha_{\mu\nu}. \quad (41)$$

2. The second set of relations mentioned above has the following form (m_N and m'_N are the masses of atoms before and after isotopic substitution):

$$A_{\lambda\mu} = \delta_{\lambda\mu} - \sum_{N\alpha} \frac{(m'_N - m_N)}{m'_N} l_{N\alpha\lambda} l_{N\alpha\mu}. \quad (42)$$

They determine the $A_{\lambda\mu}$ coefficients via so-called transformation coefficients, $l_{N\alpha\lambda}$, of a main "mother" isotopomer. Often these transformation coefficients are known for some mother isotopomer. In particular, for CH_4 they can be taken from Table 2 of Ref. 130.

3. The third set of relations can be written as

$$l'_{N\gamma\lambda} = \sum_{\alpha\mu} K^e_{\alpha\gamma} \left(\frac{m_N}{m'_N}\right)^{1/2} l_{N\alpha\mu}(\alpha^{-1})_{\lambda\mu}. \quad (43)$$

They give the possibility to calculate the transformation coefficients of a substituted isotopomer as functions of the characteristics of a mother species. Here $K^e_{\alpha\gamma}$ is the matrix which provides a rotation of the molecular equilibrium coordinate axes from a mother species to an isotopically substituted molecule. In Eqs. (40)–(43), α, β, $\gamma = x, y, z$; λ, μ, ν enumerate the vibrational modes (for the CH_4 molecule λ, μ, $\nu = 1$; 2_1, 2_2; 3_x, 3_y, 3_z; and 4_x, 4_y, 4_z).

Because the difference of the $^{12}CH_4$ and $^{13}CH_4$ molecules is in the substitution of only one central atom,

TABLE XI. Illustration of the "local mode" relations for CH_4.

Parameter	Value[a] (cm^{-1})	Value[b] (cm^{-1})
x_{33}	− 25.71	− 25.68
9/5 x_{11}	− 23.37	− 23.29
9/20 x_{13}	− 23.36	− 23.59
−3 G_{33}	− 28.71	− 28.56
−9 T_{33}	− 29.97	− 29.62
(9/20) F_{1133}	− 27.26	− 27.87
(9/80) F_{1333}	− 24.77	− 24.57

[a]Calculated with the set of parameters I from column 2 of Table X.
[b]Calculated with the set of parameters II from column 3 of Table X.

This article is copyrighted as indicated in the article. Reuse of AIP content is subject to the terms at: http://scitation.aip.org/termsconditions. Downloaded to IP: 129.132.218.57 On: Tue, 16 Dec 2014 16:10:57

$^{12}C \rightarrow {}^{13}C$, Eqs. (40)–(43) and the transformation coefficients $l'_{N\gamma\lambda}$ from Ref. 130 lead to the following simple results for the $A_{\lambda\lambda}$ coefficients:

$$A_{11} = A_{2_1 2_1} = A_{2_2 2_2} = 1, \tag{44}$$

$$A_{3_x 3_x} = A_{3_y 3_y} = A_{3_z 3_z} = 1 - \frac{(m'_C - m_C)}{m'_C} \frac{m_C}{m_C + 4m_H} 4\sin^2\gamma, \tag{45}$$

$$A_{4_x 4_x} = A_{4_y 4_y} = A_{4_z 4_z} = 1 - \frac{(m'_C - m_C)}{m'_C} \frac{m_C}{m_C + 4m_H} 4\cos^2\gamma. \tag{46}$$

All the non-diagonal elements in the case of symmetric substitution can be taken as zero. In Eqs. (45) and (46), $\sin\gamma$ is an "ambiguity" parameter for the mother species, which for CH_4 can be estimated to be 0.6036.[131] Consequently, the numerical values of the $A_{3_\alpha 3_\alpha}$ and $A_{4_\alpha 4_\alpha}$ coefficients under the substitution $^{12}C \rightarrow {}^{13}C$ can be estimated as $A_{3_\alpha 3_\alpha} = 0.99299$ and $A_{4_\alpha 4_\alpha} = 0.98776$.

A solution of the set of equations (40) under the substitution $^{12}C \rightarrow {}^{13}C$ also leads to set of very simple relations:

$$A_{\lambda\lambda}^{1/2} = \frac{\omega'_\lambda}{\omega_\lambda}. \tag{47}$$

It is interesting to compare the values of the $A_{\lambda\lambda}$ coefficients obtained above using Eqs. (44)–(46) with the analogous equations obtained using Eq. (47). To do so we make use of the ratios of harmonic wavenumbers for $^{12}CH_4$ and $^{13}CH_4$ obtained from the *ab initio* calculations in Ref. 122. The corresponding results are: $A_{11} = A_{22} = 1.00000$, $A_{33} = 0.99289$, and $A_{44} = 0.98754$, which agrees quite well with the results obtained from the isotopic relations as given above.

Finally, after some mathematical manipulations with the expressions (40)–(47), and the equations which express the vibrational spectroscopic parameters as functions of parameters of an intramolecular potential function, it is possible to

TABLE XII. Spectroscopic parameters of the $^{13}CH_4$ molecule (in cm^{-1}).

Parameter	$^{12}CH_4$-I,[a] tw	Shift-I,[a,b] tw	$^{13}CH_4$-I,[a] tw	$^{12}CH_4$-II,[c] tw	Shift-I,[b,c] tw	$^{13}CH_4$-II,[c] tw	Shift, Ref. 122	$^{13}CH_4$-III,[d] tw
1	2	3	4	5	6	7	8	9
$\tilde{\omega}_1$	2929.615	0.303	2929.918	2929.98	0.306	2930.29	− 1.1	2928.991(743)
$\tilde{\omega}_2$	1534.161	0.114	1534.275	1533.706	0.108	1533.824	0.2	1534.169(189)
$\tilde{\omega}_3$	3025.806	− 10.277	3015.529	3026.01	− 10.275	3015.58	− 9.7	3014.936(472)
$\tilde{\omega}_4$	1306.923	− 7.858	1299.065	1307.172	− 7.867	1299.161	− 8.0	1298.167(369)
x_{11}	− 12.986	0.000	− 12.986	− 12.94	0.000	− 12.94	0.000	− 12.729(254)
x_{12}	− 14.505	0.000	− 14.505	− 14.620	0.000	− 14.620	0.000	− 14.737(470)
x_{13}	− 51.916	0.182	− 51.734	− 52.43	0.187	− 52.24	0.074	− 53.991(808)
x_{14}	− 3.283	0.020	− 3.263	− 3.204	0.020	− 3.184	− 0.812	− 3.818(466)
x_{22}	− 1.175	0.000	− 1.175	− 0.835	0.000	− 0.835	0.000	− 1.193
x_{23}	− 11.989	0.042	− 11.947	− 12.019	0.043	− 11.976	0.148	− 11.936
x_{24}	− 5.564	0.034	− 5.530	− 5.765	0.036	− 5.729	− 0.042	− 5.510
x_{33}	− 25.709	0.180	− 25.529	− 25.682	0.183	− 25.499	0.385	− 24.908(472)
x_{34}	− 8.465	0.082	− 8.383	− 8.669	0.085	− 8.584	0.091	− 8.486
x_{44}	− 6.523	0.080	− 6.443	− 6.472	0.081	− 6.391	0.236	− 6.088(272)
G_{22}	0.361	0.000	0.361	0.179	0.000	0.179	0.000	0.364
G_{33}	9.573	− 0.067	9.506	9.521	− 0.068	9.453	− 0.264	9.710(217)
G_{34}	− 0.755	0.007	− 0.748	− 1.046	0.010	− 1.036	0.012	− 0.641
G_{44}	5.034	− 0.062	4.972	4.899	− 0.061	4.838	− 0.140	5.025(373)
T_{23}	0.366	− 0.001	0.365	0.380	− 0.001	0.379	− 0.001	0.366
T_{24}	− 0.901	0.006	− 0.895	− 0.924	0.006	− 0.918	0.001	− 0.899
T_{33}	3.336	− 0.023	3.313	3.292	− 0.023	3.269	− 0.034	3.298
T_{34}	0.257	− 0.002	0.255	0.410	− 0.004	0.406	0.047	0.242
T_{44}	0.542	− 0.007	0.535	0.533	− 0.007	0.526	− 0.011	0.487(089)
S_{34}	0.009	0.000	0.009	− 0.184	0.002	− 0.182	0.003	0.027
F_{1133}	− 60.581	0.213	− 60.368	− 61.93	0.22	− 61.71		− 60.779
F_{1333}	− 220.14	1.86	− 218.28	− 218.38	1.85	− 216.53		− 210.46(320)

[a]Correspond to the set of parameters (I) from Table X.

[b]The value of the shift is determined by difference, $p(^{13}CH_4) - p(^{12}CH_4)$, where p is frequency, $\tilde{\omega}$, anharmonic parameter, $x_{\lambda\mu}$, or some of the tetrahedral splitting or resonance interaction parameter.

[c]Correspond to the set of parameters (II) from Table X.

[d]Obtained from the fit with the experimental band centers from column 3 of Table V. Values in parentheses are 1σ statistical confidence intervals. Parameters presented without confidence intervals have been constrained to the values of corresponding parameters from column 7 of Table XII.

This article is copyrighted as indicated in the article. Reuse of AIP content is subject to the terms at: http://scitation.aip.org/termsconditions. Downloaded to IP: 129.132.218.57 On: Tue, 16 Dec 2014 16:10:57

show that the following set of relations is fulfilled under the substitution $^{12}C \rightarrow {}^{13}C$:

$$p_{\lambda\mu}(^{13}CH_4) = p_{\lambda\mu}(^{12}CH_4) \times A_{\lambda\lambda}^{1/2} A_{\mu\mu}^{1/2}, \quad (48)$$

where $p_{\lambda\mu}$ is an anharmonic coefficient $x_{\lambda\mu}$, or a tetrahedral splitting coefficient $G_{\dots}$, $T_{\dots}$, or $S_{\dots}$. Equation (47) can be rewritten in more convenient form:

$$p_{\lambda\mu}(^{13}CH_4) = p_{\lambda\mu}(^{12}CH_4) \times \left(\frac{\omega'_\lambda \omega'_\mu}{\omega_\lambda \omega_\mu}\right). \quad (49)$$

We used then Eqs. (47)–(49) and the equations which express vibrational spectroscopic parameters as functions of parameters of an intramolecular potential function, to calculate

TABLE XIII. Isotope shift $\Delta\tilde{\nu} = \tilde{\nu}(^{12}CH_4) - \tilde{\nu}(^{13}CH_4)$).[a]

Level assignment	$\Gamma_v(T_d)$	$n(\Gamma_v)$	$\tilde{\nu}(^{13}CH_4)/cm^{-1}$ exp.	$\Delta\tilde{\nu}/cm^{-1}$ exp.	pred.1	pred.2	CVPT
ν_4	F_2	1	1302.78	7.98	7.98	8.37	7.95
ν_2	E	1	1533.49[b]	−0.16	−0.11	−0.29	−0.16
$2\nu_4$	A_1	1	2572.11[b]	14.93	15.42	16.47	14.89
$2\nu_4$	F_2	1	2598.64	15.62	15.72	15.34	15.56
$2\nu_4$	E	1	2608.74[b]	15.88	15.86	16.26	15.83
$\nu_2 + \nu_4$	F_2	2	2822.45	7.86	7.72	7.62	7.86
$\nu_2 + \nu_4$	F_1	1	2838.20[b]	7.87	7.81	8.02	7.83
ν_1	A_1	2	2915.44[b]	1.04	−0.31	0.78	1.01
ν_3	F_2	3	3009.55	9.95	10.23	9.92	10.00
$2\nu_2$	A_1	3	3063.96[b]	−0.32	−0.22	0.50	−0.32
$2\nu_2$	E	2	3065.46[b]	−0.32	−0.21	−0.23	−0.32
$3\nu_4$	F_2	1	3848.39	22.10	22.98	22.97	21.98
$3\nu_4$	A_1	1	3886.35[b]	22.85	23.43	20.93	22.71
$3\nu_4$	F_1	1	3897.37[b]	23.14	23.57	21.85	23.07
$3\nu_4$	F_2	2	3907.49	23.42	23.70	22.92	23.42
$\nu_2 + 2\nu_4$	E	1	4086.20[b]	15.19	15.24	15.39	14.81
$\nu_2 + 2\nu_4$	F_1	2	4113.19[b]	15.58	15.50	14.35	15.53
$\nu_2 + 2\nu_4$	A_1	2	4117.04[b]	15.82	15.59	15.07	15.88
$\nu_2 + 2\nu_4$	F_2	3	4127.37	15.50	15.59	14.74	15.43
$\nu_2 + 2\nu_4$	E	2	4135.53[b]	15.67	15.70	15.74	15.61
$\nu_2 + 2\nu_4$	A_2	1	4146.04[b]	15.81	15.78	15.87	15.74
$\nu_1 + \nu_4$	F_2	4	4213.82	9.64	7.58	9.76	9.60
$\nu_3 + \nu_4$	F_2	5	4301.30	17.91	18.04	16.90	17.97
$\nu_3 + \nu_4$	E	3	4304.61[b]	17.56	18.05	18.43	17.73
$\nu_3 + \nu_4$	F_1	3	4304.73[b]	17.86	18.06	18.58	17.78
$\nu_3 + \nu_4$	A_1	3	4304.84[b]	17.87	18.06	18.31	17.89
$2\nu_2 + \nu_4$	F_2	6	4340.91	7.81	7.53	7.60	7.79
$2\nu_2 + \nu_4$	F_1	4	4355.88[b]	7.73	7.63	7.62	7.73
$2\nu_2 + \nu_4$	F_2	7	4371.20[b]	7.74	7.73	8.37	7.71
$\nu_1 + \nu_2$	E	4	4434.23[b]	0.89	−0.42	0.60	0.92
$\nu_2 + \nu_3$	F_1	5	4527.88[b]	9.66	10.07	9.44	9.71
$\nu_2 + \nu_3$	F_2	8	4534.05	9.71	10.08	9.66	9.75
$3\nu_2$	E	5	4592.87[b]	−0.84	−0.33	1.65	−0.48
$3\nu_2$	A_2	2	4595.91[b]	−0.65	−0.33	0.16	−0.48
$3\nu_2$	A_1	4	4596.15[b]	−0.65	−0.33	0.16	−0.48
$\nu_3 + 2\nu_4$	F_2	7	5563.42	24.55	25.48	25.83	
$2\nu_3$	F_2	18	5987.05	17.58	18.42	18.48	
$\nu_2 + 2\nu_3$	F_2	41	7493.16	17.18	18.15	17.97	
$\nu_1 + \nu_3 + 2\nu_4$	F_2	36	8393.62	27.38	26.78	28.73	
$2\nu_1 + \nu_3$	F_2	75	8789.70	19.25	16.04	19.34	
$3\nu_3$	F_2	85	8880.87	26.43	26.68	27.15	
$3\nu_3$	F_2	91	9019.59	26.37	29.49	25.12	
$\nu_1 + \nu_2 + 2\nu_3$	F_2	116	10099.81	15.86	15.84	13.98	
$2\nu_1 + \nu_2 + \nu_3$	F_2	143	10284.31	17.86	15.74	19.08	

[a]The shift $\Delta\tilde{\nu}$ is defined as $\tilde{\nu}\left(^{12}CH_4\right) - \tilde{\nu}\left(^{13}CH_4\right)$, where exp. refers to experimentally determined band centers (directly from $J' = 0$ levels, unless otherwise stated), "pred.1" gives predicted shifts using the model described in section VII, "pred.2" is the shift derived from the levels as obtained by the vibrational effective Hamiltonian fit of the present work, "CVPT" gives the shift from the perturbation theory in Ref. 42.

[b]Level position from a fit to an effective ro-vibrational Hamiltonian.[42,44]

This article is copyrighted as indicated in the article. Reuse of AIP content is subject to the terms at: http://scitation.aip.org/termsconditions. Downloaded to IP: 129.132.218.57 On: Tue, 16 Dec 2014 16:10:57

the values of the vibrational spectroscopic parameters of the $^{13}CH_4$ isotopomer on the basis of the corresponding parameters of $^{12}CH_4$. The results of such calculations are summarized in Table XII. In Table XII columns 2 and 5 reproduce the values of parameters of the $^{12}CH_4$ molecule from columns 2 and 3 of Table X. The shifts of parameters after isotopic substitution calculated with Eqs. (47)–(49), are shown in columns 3 and 6. Column 8 presents, for comparison, values of the shifts obtained on the basis of spectroscopic parameters of the $^{12}CH_4$ and $^{13}CH_4$ molecules from *ab initio* calculations in Ref. 122. As one can see, there is at least qualitative agreement between three sets of the shift values, with the exception of the values for x_{14}. If one considers the absolute value of x_{14}, it seems that the *ab initio* value of the shift, -0.812 cm^{-1} in the column 8 is incorrect. Columns 4 and 7 present the values of the spectroscopic parameters of the $^{13}CH_4$ isotopomer which were estimated on the basis of values from columns 2, 3, 5, and 6.

Finally, the parameters from column 4 of Table XII were used to calculate the same band centers for the $^{13}CH_4$ isotopomer as for $^{12}CH_4$. We calculated all the band centers for the polyads $N = 0.5$, 1, 1.5, and 2. For the polyads 2.5, 3, 3.5, and 4 we calculated band centers for the F_2 type bands. The results of these calculation are presented in Table S2 (see Appendix E and the supplementary material[109]), and they were used then as the basis for an assignment of the band centers in the experimental spectrum recorded in the region of 5500–12 000 cm^{-1}. In this way we were able to assign beyond doubt 12 new bands for $^{13}CH_4$ from experimental transitions as presented in column 3 of Table V. Previously assigned bands of $^{13}CH_4$ are also presented in Table V. Columns 5 and 6 of this table give the predicted values of the corresponding band centers. One finds satisfactory agreement between predicted and experimental results, considering that the results for $^{13}CH_4$ are predictions based on parameters derived from $^{12}CH_4$ and not fitted to the experimental results for $^{13}CH_4$. The fit to the experimental results leads to an even better agreement. Table XII provides a summary of the spectroscopic effective Hamilton parameters as obtained by various methods for $^{12}CH_4$ and $^{13}CH_4$ and the corresponding isotope shifts. Only the shifts for $\tilde{\omega}_3$ and $\tilde{\omega}_4$ are really large in absolute values. Table XIII summarizes in a convenient form the measured and predicted isotope shifts for the $^{13}CH_4$ levels derived and discussed in the present work in comparison with the corresponding $^{12}CH_4$ levels. Up to about 8000 cm^{-1}, the isotope shifts follow the simple patterns which would be derived from the shifts of $\tilde{\omega}_3$ and $\tilde{\omega}_4$ by adding the sums of the appropriate multiples of the harmonic shifts. Above 8000 cm^{-1} higher order terms and resonance interactions in the model become more important and both experimental and theoretical shifts deviate from the simple pattern. We compare the shifts in Table XIII also with the shifts predicted from canonical variational perturbation theory (CVPT) in Ref. 42. This theory is slightly more accurate than the simple approach discussed here. One can expect that explicit inclusion of the CH stretching-bending Fermi resonances and some of the higher order terms in the tetrahedral splittings in the effective Hamiltonian would improve the results from the simple model.

VIII. DISCUSSION AND CONCLUSION

Using the strategy[39,40,80–82] of the direct assignment of the $J' = 0$ levels of excited vibrational states of F_2 symmetry in low temperature spectra of $^{12}CH_4$ and $^{13}CH_4$ we have been able in the present work to extend the accurate knowledge for a considerable number of the vibrational level energies for these methane isotopomers up to 12 000 cm^{-1} (about 20 levels in a range where few previous data existed[80,82,119,132]). We have furthermore extended the theoretical formulation for the effective Hamiltonian for the T_d symmetrical isotopomers of methane to cover excitations up to this range. The effective Hamiltonian thus derived here provides a good description of the so far known vibrational energy levels up to 12 000 cm^{-1} including in the fit of the parameters to experiment also very recent and accurate experimental data for the lower polyads up to 6000 cm^{-1} (see Refs. 42, 78, and 96 and literature cited therein). These results can find important applications in the spectroscopy of the earth's atmosphere as well as other planetary and also interstellar objects. The two most abundant isotopomers of methane studied here account for almost 100% of the natural infrared absorption of methane.

More generally, the accurate spectroscopic results up to high vibrational excitations provide an important benchmark for theoretical studies of this important prototype molecule. They can help to further develop and refine potential hypersurfaces for methane based on *ab initio* calculations, a topic of considerable current activity.[9,11–13,16–20,72,123,133–136] They also provide a testing ground for the corresponding quantum dynamical models of intramolecular energy flow in methane isotopomers.[10,137–139]

While it is today possible to carry out full dimensional quantum mechanical calculations for the vibrational levels of the molecules of the size of methane,[135,136,139–142] the effective Hamiltonian description derived in our work has merits in terms of a simple representation of the experimental spectra and for a simple understanding of the most important structures including isotope effects.[129] In conjunction with our previous extensive studies of excited vibrational levels of C_{3v} and C_{2v} symmetrical isotopomers of methane (CH_3D, CHD_3, and CH_2D_2)[39,40] our results can provide also a starting point for a purely empirical anharmonic force-field for methane. Finally, the very complete set of experimental high resolution results obtained in the present work, combined with our first analysis of the vibrational level structure is also a starting point for a more complete rovibrational analysis of the higher polyads, although such work surely requires further long term efforts in the analysis.

ACKNOWLEDGMENTS

Our work is supported financially by the ETH Zürich, the Swiss National Science Foundation (SNF), the European Research Council (ERC), the Swiss-Russian exchange project (Geneva), the project "Leading Russian Research Universities" (Grant No. FTI - 120 of the Tomsk Polytechnic University) and the Deutsche Forschungsgemeinschaft (Grant Nos. BA2176/3-2 and BA2176/4-1). Helpful discussions and correspondence with Vincent Boudon, Irina Bolotova, Tucker

This article is copyrighted as indicated in the article. Reuse of AIP content is subject to the terms at: http://scitation.aip.org/termsconditions. Downloaded to IP: 129.132.218.57 On: Tue, 16 Dec 2014 16:10:57

Carrington, Csaba Fabri, Olga Gromova, Roberto Marquardt, and Xiaogang Wang are gratefully acknowledged.

APPENDIX A: CENTRAL PARTS OF SOME "F_2"-TYPE BANDS OF THE $^{12}CH_4$ AND $^{13}CH_4$ ISOTOPOMERS OF METHANE

The central parts of experimentally observed and assigned "F_2"-type bands of the $^{12}CH_4$ and $^{13}CH_4$ isotopomers of methane are presented in part I of the supplementary material.[109] For all bands the ($J' = 0 \leftarrow J'' = 1$) transitions are marked which were used for determination of the "experimental" band center values. In general, the 24 bands are presented for the $^{12}CH_4$ species (they are $3\nu_4(1F_2)$, $3\nu_4(2F_2)$, $\nu_2 + 2\nu_4(F_2)$, $\nu_1 + \nu_4(F_2)$, $\nu_3 + \nu_4(F_2)$, $2\nu_2 + \nu_4(1F_2)$, $2\nu_2 + \nu_4(2F_2)$, $\nu_2 + \nu_3(F_2)$, $\nu_3 + 2\nu_4(1F_2)$, $2\nu_3(F_2)$, $2\nu_2 + \nu_3(1F_2)$, $\nu_1 + \nu_3 + \nu_4(F_2)$, $\nu_2 + 2\nu_3(F_2)$, $2\nu_1 + 2\nu_4(F_2)$, $\nu_1 + \nu_3 + 2\nu_4(1F_2)$, $\nu_1 + 2\nu_3(F_2)$, $2\nu_1 + \nu_3(F_2)$, $3\nu_3(1F_2)$, $3\nu_3(2F_2)$, $\nu_1 + 2\nu_3 + \nu_4(1F_2)$, $\nu_1 + \nu_2 + 2\nu_3(F_2)$, $3\nu_3 + \nu_4(2F_2)$, $2\nu_1 + \nu_2 + \nu_3(F_2)$, $\nu_1 + 3\nu_3(1F_2)$), and 20 bands are presented for the $^{12}CH_4$ species (they are $\nu_4(F_2)$, $2\nu_4(F_2)$, $\nu_2 + \nu_4(F_2)$, $\nu_3(F_2)$, $3\nu_4(1F_2)$, $3\nu_4(2F_2)$, $\nu_2 + 2\nu_4(F_2)$, $\nu_1 + \nu_4(F_2)$, $\nu_3 + \nu_4(F_2)$, $\nu_2 + \nu_3(F_2)$, $\nu_3 + 2\nu_4(1F_2)$, $2\nu_3(F_2)$, $\nu_2 + 2\nu_3(F_2)$, $\nu_1 + \nu_3 + 2\nu_4(1F_2)$, $2\nu_1 + \nu_3(F_2)$, $3\nu_3(1F_2)$, $3\nu_3(2F_2)$, $\nu_1 + \nu_2 + 2\nu_3(F_2)$, $2\nu_1 + \nu_2 + \nu_3(F_2)$).

APPENDIX B: SYMMETRIZED WAVE FUNCTIONS OF THE DOUBLY DEGENERATE HARMONIC OSCILLATOR

$$|vl = 0A_1\rangle = |v0\rangle,$$

$$|vl = 6pA_1\rangle = \frac{1}{\sqrt{2}}(|v6p\rangle + |v-6p\rangle)p \neq 0,$$

$$|vl = 6pA_2\rangle = -\frac{\mathrm{i}}{\sqrt{2}}(|v6p\rangle - |v-6p\rangle);$$

$$|vl = 6p+1E_1\rangle = \frac{1}{\sqrt{2}}(|v6p+1\rangle - |v-(6p+1)\rangle),$$

$$|vl = 6p+1E_2\rangle = \frac{\mathrm{i}}{\sqrt{2}}(|v6p+1\rangle + |v-(6p+1)\rangle);$$

$$|vl = 6p+2E_1\rangle = \frac{1}{\sqrt{2}}(|v6p+2\rangle + |v-(6p+2)\rangle),$$

$$|vl = 6p+2E_2\rangle = -\frac{\mathrm{i}}{\sqrt{2}}(|v6p+2\rangle - |v-(6p+2)\rangle);$$

$$|vl = 6p+3A_1\rangle = \frac{1}{\sqrt{2}}(|v6p+3\rangle - |v-(6p+3)\rangle),$$

$$|vl = 6p+3A_2\rangle = -\frac{\mathrm{i}}{\sqrt{2}}(|v6p+3\rangle + |v-(6p+3)\rangle);$$

$$|vl = 6p+4E_1\rangle = \frac{1}{\sqrt{2}}(|v6p+4\rangle + |v-(6p+4)\rangle),$$

$$|vl = 6p+4E_2\rangle = \frac{\mathrm{i}}{\sqrt{2}}(|v6p+4\rangle - |v-(6p+4)\rangle);$$

$$|vl = 6p+5E_1\rangle = \frac{1}{\sqrt{2}}(|v6p+5\rangle - |v-(6p+5)\rangle),$$

$$|vl = 6p+5E_2\rangle = -\frac{1}{\sqrt{2}}(|v6p+5\rangle + |v-(6p+5)\rangle).$$

The phases of wave functions are chosen such as to provide real values of the Hamiltonian matrix elements. The value of p is 0, 1, 2, ... The functions $|vl\rangle$ on the right-hand sides are the ordinary eigenfunctions (proportional to Legendre polynomials) of doubly degenerate harmonic oscillators, see Ref. 113.

APPENDIX C: TETRAHEDRAL SPLITTING PARAMETERS FOR CH_4

$$G_{22} = -\frac{1}{2}d_{2222} + \frac{21}{4}\frac{c_{222}^2}{\omega_2} - \frac{1}{4}\frac{c_{122}^2}{(4\omega_2^2 - \omega_1^2)}, \tag{C1}$$

$$G_{33} = -\frac{1}{2}d_{3333_s} + \frac{1}{12}\frac{c_{333}^2}{\omega_3} - \frac{1}{4}\frac{c_{133\omega_1}^2}{(4\omega_3^2 - \omega_1^2)} + B\zeta_3^2 + \frac{2c_{233}^2(6\omega_3^2 - \omega_2^2)}{15\omega_2(4\omega_3^2 - \omega_2^2)} + \frac{c_{334}^2(6\omega_3^2 - \omega_4^2)}{20\omega_4(4\omega_3^2 - \omega_4^2)}, \tag{C2}$$

$$G_{34} = \frac{B}{2}\zeta_{34}^2 + 2B\zeta_3\zeta_4 + \frac{1}{2}\frac{c_{344}^2\omega_4^2}{\omega_3(4\omega_4^2 - \omega_3^2)} + \frac{1}{2}\frac{c_{334}^2\omega_3^2}{\omega_4(4\omega_3^2 - \omega_4^2)} + \frac{1}{2}\frac{c_{134}^2\omega_1\omega_3\omega_4}{(\omega_1+\omega_3+\omega_4)(\omega_1+\omega_3-\omega_4)(\omega_1-\omega_3+\omega_4)(\omega_1-\omega_3-\omega_4)} - \frac{1}{3}\frac{c_{234}^2\omega_2\omega_3\omega_4}{(\omega_2+\omega_3+\omega_4)(\omega_2+\omega_3-\omega_4)(\omega_2-\omega_3+\omega_4)(\omega_2-\omega_3-\omega_4)}, \tag{C3}$$

$$S_{34} = \frac{1}{4}d_{3344_{sb}} - \frac{1}{40}\left[\frac{c_{344}^2\omega_4}{4\omega_4^2 - \omega_3^2} + \frac{c_{334}^2\omega_3}{4\omega_3^2 - \omega_4^2}\right] - \frac{c_{233}c_{244}}{5\omega_2} + \frac{1}{4}B\zeta_{34}^2\frac{\omega_3^2 + \omega_4^2}{\omega_3\omega_4} - \frac{3}{40}\left(\frac{c_{334}c_{444}}{\omega_4} + \frac{c_{333}c_{344}}{\omega_3}\right)$$

This article is copyrighted as indicated in the article. Reuse of AIP content is subject to the terms at: http://scitation.aip.org/termsconditions. Downloaded to IP: 129.132.218.57 On: Tue, 16 Dec 2014 16:10:57

$$-\frac{c_{134}^2\omega_1(\omega_1^2-\omega_3^2-\omega_4^2)}{8(\omega_1+\omega_3+\omega_4)(\omega_1+\omega_3-\omega_4)(\omega_1-\omega_3+\omega_4)(\omega_1-\omega_3-\omega_4)}$$
$$-\frac{c_{234}^2\omega_2\left(\omega_2^2-\omega_3^2-\omega_4^2\right)}{60(\omega_2+\omega_3+\omega_4)(\omega_2+\omega_3-\omega_4)(\omega_2-\omega_3+\omega_4)(\omega_2-\omega_3-\omega_4)}, \quad \text{(C4)}$$

$$T_{34}=d_{3344_t}+\frac{1}{10}\left[\frac{c_{344}^2\omega_4}{4\omega_4^2-\omega_3^2}+\frac{c_{334}^2\omega_3}{4\omega_3^2-\omega_4^2}\right]-\frac{c_{233}c_{244}}{5\omega_2}-\frac{1}{20}\left(\frac{c_{334}c_{444}}{\omega_4}+\frac{c_{333}c_{344}}{\omega_3}\right)$$
$$-\frac{c_{234}^2\omega_2\left(\omega_2^2-\omega_3^2-\omega_4^2\right)}{10(\omega_2+\omega_3+\omega_4)(\omega_2+\omega_3-\omega_4)(\omega_2-\omega_3+\omega_4)(\omega_2-\omega_3-\omega_4)}, \quad \text{(C5)}$$

$$T_{33}=\frac{3}{8}d_{3333_t}+\frac{1}{48}\frac{c_{333}^2}{\omega_3}+\frac{c_{233}^2\left(3\omega_2^2-8\omega_3^2\right)}{20\omega_2\left(4\omega_3^2-\omega_2^2\right)}+\frac{c_{334}^2\left(8\omega_3^2-3\omega_4^2\right)}{80\omega_4\left(4\omega_3^2-\omega_4^2\right)}, \quad \text{(C6)}$$

$$T_{23}=\frac{d_{2233_t}}{8\sqrt{3}}-\frac{\sqrt{3}}{4}\frac{c_{222}c_{233}}{\omega_2}-\frac{c_{233}^2\omega_3}{6\left(4\omega_3^2-\omega_2^2\right)}-\frac{B}{16}\zeta_{23}^2\frac{\omega_2^2+\omega_3^2}{\omega_2\omega_3}$$
$$+\frac{c_{234}^2\omega_4\left(\omega_2^2+\omega_3^2-\omega_4^2\right)}{24(\omega_2+\omega_3+\omega_4)(\omega_2+\omega_3-\omega_4)(\omega_2-\omega_3+\omega_4)(\omega_2-\omega_3-\omega_4)}. \quad \text{(C7)}$$

Coefficients G_{44}, T_{44}, and T_{24} can be obtained by mutual substitution for indices 3 and 4 in Eqs. (C2), (C6), and (C7).

APPENDIX D: TABLES OF TETRAHEDRAL SPLITTINGS OF VIBRATIONAL LEVELS OF A SPHERICAL TOP MOLECULE

The information necessary for calculation of vibrational tetrahedral splittings and vibrational resonance interactions in the $XY_4(C_{3v})$ type molecules is presented in part II of the supplementary material.[109] As was discussed in Sec. V, vibrational tetrahedral splittings are determined by the values $W(v_1v_2v_3v_4n\Gamma_v)$ (see Eq. (7)) which, in turn, are determined as a result of the diagonalization of special matrices. The corresponding matrices which are presented in part II of the supplementary material[109] allow one to calculate tetrahedral splittings for any type of vibrational states for polyads $N \leq 2$. For the polyads $2 < N \leq 4$, matrices presented in part II of the supplementary material[109] allow one to make calculations for the vibrational states of the F_2 symmetry.

APPENDIX E: ENERGY LEVELS OF METHANE E/(hc) FOR $^{12}CH_4$ AND $^{13}CH_4$ IN cm^{-1}

Part III of the supplementary material[109] presents lists of band centers for the $^{12}CH_4$ and $^{13}CH_4$ isotopomers for the polyads $1/2 \leq N \leq 4$ (for the polyads $1/2 \leq N \leq 2$ band centers are presented for the states of all symmetries; for the polyads $5/2 \leq N \leq 4$ only F_2 −type band centers are presented[109]). Band centers of $^{12}CH_4$, which have been calculated with the parameters from columns 2, 3 of Table X are shown in Table S1 of the supplementary material, part III.[109] Band centers of $^{13}CH_4$ are shown in Table S2 (they have been calculated with the parameters from columns 4 and 7 of Table XII).

[1] L. Pauling, *The Nature of the Chemical Bond*, 2nd ed. (Oxford University, London, 1940).
[2] J. H. van't Hoff, *La chimie dans l'espace* (Rotterdam, 1887).
[3] J. H. van't Hoff, *Vorlesungen über theoretische und physikalische Chemie, Band 2* (Vieweg, Braunschweig, 1899).
[4] M. Quack, European Rev. **22**, S50 (2014).
[5] H. Schwarz, Angew. Chem., Int. Ed. Engl. **50**, 10096 (2011).
[6] J. P. Camden, H. A. Bechtel, D. J. A. Brown, and R. N. Zare, J. Chem. Phys. **124**, 034311 (2006).
[7] J. P. Camden, W. F. Hu, H. A. Bechtel, D. J. A. Brown, M. R. Martin, R. N. Zare, G. Lendvay, D. Troya, and G. C. Schatz, J. Phys. Chem. A **110**, 677 (2006).
[8] S. Peyerimhoff, M. Lewerenz, and M. Quack, Chem. Phys. Lett. **109**, 563 (1984).
[9] H. Hollenstein, R. Marquardt, M. Quack, and M. A. Suhm, J. Chem. Phys. **101**, 3588 (1994).
[10] R. Marquardt and M. Quack, J. Chem. Phys. **95**, 4854 (1991).
[11] R. Marquardt and M. Quack, J. Chem. Phys. **109**, 10628 (1998).
[12] R. Marquardt and M. Quack, J. Phys. Chem. A **108**, 3166 (2004).
[13] D. W. Schwenke, Spectrochim. Acta A **58**, 849 (2002).
[14] M. Quack and J. Troe, Ber. Bunsenges. Phys. Chem. **81**, 329 (1977).
[15] M. Quack, J. Phys. Chem. **83**, 150 (1979).
[16] X. G. Wang and E. L. Sibert, J. Chem. Phys. **111**, 4510 (1999).
[17] X. G. Wang and E. L. Sibert, Spectrochim. Acta A **58**, 863 (2002).
[18] X. G. Wang and T. Carrington, J. Chem. Phys. **119**, 94 (2003).
[19] X. G. Wang and T. Carrington, J. Chem. Phys. **119**, 101 (2003).
[20] X. G. Wang and T. Carrington, J. Chem. Phys. **118**, 6260 (2003).
[21] M. A. K. Khalil, Annu. Rev. Energy Environ. **24**, 645 (1999).
[22] P. G. J. Irwin, K. Sihra, N. Bowles, F. W. Taylor, and S. B. Calcutt, Icarus **176**, 255 (2005).
[23] A. Coradini, G. Filacchione, F. Capaccioni, P. Cerroni, A. Adriani, R. H. Brown, Y. Langevin, and B. Gondet, Planet. Space Sci. **52**, 661 (2004).
[24] H. Tran, P. M. Flaud, T. Fouchet, T. Gabard, and J. M. Hartmann, J. Quant. Spectrosc. Radiat. Transfer **101**, 306 (2006).
[25] L. A. Sromovsky and P. Fry, Icarus **193**, 252 (2008).
[26] G. S. Orton, T. Encrenaz, C. Leyrat, R. Puetter, and A. J. Friedson, Astron. Astrophys. **473**, L5 (2007).
[27] A. Coustenis, A. Salama, B. Schulz, E. Lellouch, T. Encrenaz, S. Ott, M. F. Kessler, H. Feuchtgruber, and T. de Graauw, in *Proceedings of the Symposium on the Promise of the Herschel Space Observatory, 12–15 December 2000, Toledo, Spain*, edited by G. L. Pilbratt, J. Cernicharo, A. M. Heras, and R. Harris (ESA Publications Division, Noordwijk, 2001), Vol. SP-460.
[28] C. A. Griffith, P. Penteado, P. Rannou, R. Brown, V. Boudon, K. H. Baines, R. Clark, P. Drossart, B. Buratti, P. Nicholson, C. P. McKay, A. Coustenis, A. Negro, and R. Jaumann, Science **313**, 1620 (2006).
[29] A. Coustenis, A. Negrao, A. Salama, B. Schulz, E. Lellouch, P. Rannou, P. Drossart, T. Encrenaz, B. Schmitt, V. Boudon, and A. Nikitin, Icarus **180**, 176 (2006).
[30] A. Negrão, A. Coustenis, E. Lellouch, J. P. Maillard, P. Rannou, B. Schmitt, C. P. McKay, and V. Boudon, Planet. Space Sci. **54**, 1225 (2006).

This article is copyrighted as indicated in the article. Reuse of AIP content is subject to the terms at: http://scitation.aip.org/termsconditions. Downloaded to IP: 129.132.218.57 On: Tue, 16 Dec 2014 16:10:57

[31] A. Negrão, M. Hirtzig, A. Coustenis, E. Gendron, P. Drossart, P. Rannou, M. Combes, and V. Boudon, J. Geophys. Res.: Planets **112**, E02S92, doi:10.1029/2005JE002651 (2007).
[32] J. A. Stansberry, J. R. Spencer, B. Schmitt, A. I. Benchkoura, R. V. Yelle, and J. I. Lunine, Planet. Space Sci. **44**, 1051 (1996).
[33] V. Formisano, S. Atreya, T. Encrenaz, N. Ignatiev, and M. Giuranna, Science **306**, 1758 (2004).
[34] M. R. Swain, G. Vasisht, and G. Tinetti, Nature **452**, 329 (2008).
[35] M. J. M. Pepper, I. Shavitt, P. v. Ragué Schleyer, M. N. Glukhovtsev, R. Janoschek, and M. Quack, J. Comput. Chem. **16**, 207 (1995).
[36] A. Bakasov, T. K. Ha, and M. Quack, J. Chem. Phys. **109**, 7263 (1998).
[37] O. N. Ulenikov, E. S. Bekhtereva, S. V. Grebneva, H. Hollenstein, and M. Quack, Phys. Chem. Chem. Phys. **7**, 1142 (2005).
[38] O. N. Ulenikov, E. S. Bekhtereva, S. V. Grebneva, H. Hollenstein, and M. Quack, Mol. Phys. **104**, 3371 (2006).
[39] O. N. Ulenikov, E. S. Bekhtereva, S. Albert, S. Bauerecker, H. Hollenstein, and M. Quack, J. Phys. Chem. A **113**, 2218 (2009).
[40] O. N. Ulenikov, E. S. Bekhtereva, S. Albert, S. Bauerecker, H. Hollenstein, and M. Quack, Mol. Phys. **108**, 1209 (2010).
[41] H.-M. Niederer, Doctoral dissertation, ETH Zürich, 2012.
[42] H.-M. Niederer, X.-G. Wang, T. Carrington, Jr., S. Albert, S. Bauerecker, V. Boudon, and M. Quack, J. Mol. Spectrosc. **291**, 33 (2013).
[43] S. Albert, S. Bauerecker, V. Boudon, L. Brown, J.-P. Champion, M. Loëte, A. Nikitin, and M. Quack, Chem. Phys. **356**, 131 (2009).
[44] H. M. Niederer, S. Albert, S. Bauerecker, V. Boudon, J. P. Champion, and M. Quack, Chimia **62**, 273 (2008).
[45] J. Tyndall, Philos. Trans. R. Soc. London **152**, 59 (1862).
[46] K. J. Angström, Öfversigt af Kongl. Vetenskaps-Akad. Förh. **47**, 331 (1890).
[47] W. W. Coblentz, *Investigations of Infra-Red Spectra* (Publications of the Carnegie Institution, Washington, 1905).
[48] J. P. Cooley, Astrophys. J. **62**, 73 (1925).
[49] A. H. Nielsen and H. H. Nielsen, Phys. Rev. **48**, 864 (1935).
[50] H. A. Jahn, Proc. R. Soc. London, Ser. A **168**, 469 (1938).
[51] H. A. Jahn, Proc. R. Soc. London, Ser. A **168**, 495 (1938).
[52] W. H. J. Childs and H. A. Jahn, Proc. R. Soc. London, Ser. A **169**, 451 (1939).
[53] H. A. Jahn, Proc. R. Soc. London, Ser. A **171**, 450 (1939).
[54] G. Herzberg, *Molecular Spectra and Molecular Structure, II. Infrared and Raman Spectra of Polyatomic Molecules* (Krieger Publishing Company, Malabar, Florida, USA, 1991).
[55] H. C. Allen and E. K. Plyler, J. Chem. Phys. **26**, 972 (1957).
[56] E. K. Plyler, E. D. Tidwell, and L. R. Blaine, J. Res. Natl. Bur. Stand., Sect. A **64**, 201 (1960).
[57] K. T. Hecht, J. Mol. Spectrosc. **5**, 355 (1960).
[58] K. T. Hecht, J. Mol. Spectrosc. **5**, 390 (1960).
[59] J. Moret-Bailly, J. Mol. Spectrosc. **15**, 344 (1965).
[60] J. Moret-Bailly, L. Gautier, and J. Montagutelli, J. Mol. Spectrosc. **15**, 355 (1965).
[61] J. Moret-Bailly, Cahiers de Physique **15**, 237 (1961).
[62] F. Michelot, J. Moret-Bailly, and K. Fox, J. Chem. Phys. **60**, 2606 (1974).
[63] K. Fox, J. Quant. Spectrosc. Radiat. Transfer **10**, 1335 (1970).
[64] B. Bobin and K. Fox, J. Chem. Phys. **58**, 1771 (1973).
[65] J. P. Champion and H. Berger, J. Phys. France **36**, 135 (1975).
[66] H. Berger, J. Mol. Spectrosc. **66**, 55 (1977).
[67] M. Oldani, A. Bauder, J. C. Hilico, M. Loete, and J. P. Champion, Europhys. Lett. **4**, 29 (1987).
[68] J. P. Champion, G. Pierre, F. Michelot, and J. Moret-Bailly, Can. J. Phys. **55**, 512 (1977).
[69] J. P. Champion, Can. J. Phys. **55**, 1802 (1977).
[70] F. Merkt and M. Quack, "Molecular quantum mechanics and molecular spectra, molecular symmetry, and interaction of matter with radiation," in *Handbook of High-Resolution Spectroscopy*, edited by M. Quack and F. Merkt (John Wiley & Sons, Ltd., Chichester, 2011), Vol. 1, Chap. 1, pp. 1–55.
[71] S. Albert, K. Keppler Albert, and M. Quack, "High resolution fourier transform infrared spectroscopy," in *Handbook of High-Resolution Spectroscopy*, edited by M. Quack and F. Merkt (John Wiley & Sons, Ltd, Chichester, 2011), Vol. 2, Chap. 26, pp. 965–1019.
[72] R. Marquardt and M. Quack, "Global analytical potential energy surfaces for high resolution molecular spectroscopy and reaction dynamics," in *Handbook of High-Resolution Spectroscopy*, edited by M. Quack and F. Merkt (John Wiley & Sons, Ltd., Chichester, 2011), Vol. 1, Chap. 12, pp. 511–549.
[73] M. Snels, V. Horká-Zelenková, H. Hollenstein, and M. Quack, "High resolution FTIR and diode laser spectroscopy of supersonic jets," in *Handbook of High-Resolution Spectroscopy*, edited by M. Quack and F. Merkt (John Wiley & Sons, Ltd., Chichester, New York, 2011), Vol. 2, Chap. 27, pp. 1021–1067.
[74] M. Quack, "Fundamental symmetries and symmetry violations from high resolution spectroscopy," in *Handbook of High-Resolution Spectroscopy*, edited by M. Quack and F. Merkt (Wiley, Chichester, New York, 2011), Vol. 1, pp. 659–722.
[75] V. Boudon, J.-P. Champion, T. Gabard, M. Lote, M. Rotger, and C. Wenger, "Spherical top theory and molecular spectra," in *Handbook of High-Resolution Spectroscopy*, edited by M. Quack and F. Merkt (John Wiley & Sons, Ltd., Chichester, 2011), Vol. 3, Chap. 39, pp. 1437–1460.
[76] M. Lewerenz and M. Quack, J. Chem. Phys. **88**, 5408 (1988).
[77] M. Quack, J. Chem. Phys. **82**, 3277 (1985).
[78] A. V. Nikitin, V. Boudon, C. Wenger, S. Albert, L. R. Brown, S. Bauerecker, and M. Quack, Phys. Chem. Chem. Phys. **15**, 10071 (2013).
[79] M. Quack, Mol. Phys. **34**, 477 (1977).
[80] M. Hippler and M. Quack, J. Chem. Phys. **116**, 6045 (2002).
[81] M. Quack, Chimia **57**, 147 (2003).
[82] C. Manca Tanner and M. Quack, Mol. Phys. **110**, 2111 (2012).
[83] O. N. Ulenikov, E. S. Bekhtereva, S. Albert, S. Bauerecker, H. M. Niederer, and M. Quack, "Survey of the high resolution spectroscopy and vibrational dynamics of methane $^{12}CH_4$ and $^{13}CH_4$ extended towards 12 000 cm^{-1}," in *Proceedings of the 22nd Colloquium on High-Resolution Spectroscopy, Université de Bourgogne, Dijon, August 29–September 2, 2011*, edited by V. Boudon (Presses Universitaires de Bourgogne, Dijon, 2011), p. 359.
[84] O. Ulenikov, E. Bekhtereva, S. Albert, S. Bauerecker, H.-M. Niederer, and M. Quack, "The infrared spectrum of methane up to 12 000 cm^{-1}," in *Proceedings of the 19th Symposium on Atomic, Cluster and Surface Physics (SASP 2014), University Center Obergurgl, Austria, 8–14 February 2014*, edited by D. Stock, R. Wester, and R. Scheier (Innsbruck University Press, 2014), pp. 240–243.
[85] S. Albert, K. K. Albert, and M. Quack, Trends Opt. Photonics **84**, 177 (2003).
[86] S. Albert and M. Quack, ChemPhysChem **8**, 1271 (2007).
[87] S. Albert, K. Keppler Albert, P. Lerch, and M. Quack, Faraday Discuss. **150**, 71 (2011).
[88] S. Albert, P. Lerch, R. Prentner, and M. Quack, Angew. Chem., Int. Eng. **52**, 346 (2013).
[89] S. Albert, P. Lerch, and M. Quack, ChemPhysChem. **14**, 3204 (2013).
[90] S. Albert, S. Bauerecker, M. Quack, and A. Steinlin, Mol. Phys. **105**, 541 (2007).
[91] S. Bauerecker, M. Taraschewski, C. Weitkamp, and H. K. Cammenga, Rev. Sci. Instrum. **72**, 3946 (2001).
[92] S. Bauerecker, F. Taucher, C. Weitkamp, W. Michaelis, and H. K. Cammenga, J. Mol. Struct. **348**, 237 (1995).
[93] S. Bauerecker, Phys. Rev. Lett. **94**, 033404 (2005).
[94] A. Maki and S. Wells, *Wavenumber Calibration Tables from Heterodyne Frequency Measurements* (NIST Special Publication 821, USA, 1991).
[95] L. S. Rothman, I. E. Gordon, A. Barbe, D. C. Benner, P. F. Bernath, M. Birk, V. Boudon, L. R. Brown, A. Campargue, J. P. Champion, K. Chance, L. H. Coudert, V. Dana, V. M. Devi, S. Fally, J. M. Flaud, R. R. Gamache, A. Goldman, D. Jacquemart, I. Kleiner, N. Lacome, W. J. Lafferty, J. Y. Mandin, S. T. Massie, S. N. Mikhailenko, C. E. Miller, N. Moazzen-Ahmadi, O. V. Naumenko, A. V. Nikitin, J. Orphal, V. I. Perevalov, A. Perrin, A. Predoi-Cross, C. P. Rinsland, M. Rotger, M. imeckov, M. A. H. Smith, K. Sung, S. A. Tashkun, J. Tennyson, R. A. Toth, A. C. Vandaele, and J. Vander Auwera, J. Quant. Spectrosc. Radiat. Transfer **110**, 533 (2009).
[96] L. R. Brown, K. Sung, D. C. Benner, V. M. Devi, V. Boudon, T. Gabard, C. Wenger, A. Campargue, O. Leshchishina, S. Kassi, D. Mondelain, L. Wang, L. Daumont, L. Rgalia, M. Rey, X. Thomas, V. G. Tyuterev, O. M. Lyulin, A. V. Nikitin, H. M. Niederer, S. Albert, S. Bauerecker, M. Quack, J. J. O'Brien, I. E. Gordon, L. S. Rothman, H. Sasada, A. Coustenis, M. A. H. Smith, T. Carrington, Jr., X. G. Wang, A. W. Mantz, and P. T. Spickler, J. Quant. Spectrosc. Radiat. Transfer **130**, 201 (2013).
[97] G. Herzberg, *Molecular Spectra and Molecular Structure* (Van Nostrand, Toronto, 1966), Vol. III.
[98] J. T. Hougen, J. Chem. Phys. **37**, 1433 (1962).
[99] H. C. Longuet-Higgins, Mol. Phys. **6**, 445 (1963).

This article is copyrighted as indicated in the article. Reuse of AIP content is subject to the terms at: http://scitation.aip.org/termsconditions. Downloaded to IP: 129.132.218.57 On: Tue, 16 Dec 2014 16:10:57

[100]E. R. Cohen, T. Cvitas, J. G. Frey, B. Holstrom, K. Kuchitsu, R. Marquardt, I. Mills, F. Pavese, M. Quack, J. Stohner, H. L. Strauss, M. Takami, and A. J. Thor, *Quantities, Units and Symbols in Physical Chemistry* (The Royal Society of Chemistry, 2007).
[101]J. T. Hougen, J. Chem. Phys. **55**, 1122 (1971).
[102]M. Hamermesh, *Group Theory and Its Application to Physical Problems* (Addison-Wesley, Reading, MA, 1962).
[103]A. Amrein, M. Quack, and U. Schmitt, J. Phys. Chem. **92**, 5455 (1988).
[104]H. M. Niederer, S. Albert, S. Bauerecker, V. Boudon, G. Seyfang, and M. Quack, Faraday Discuss. **150**, 128 (2011).
[105]K. F. Bonhoeffer and P. Harteck, Z. Phys. Chem. **4**, 113 (1929).
[106]W. Heisenberg, Z. Phys. **41**, 239 (1927).
[107]J. P. Champion, J. C. Hilico, and L. R. Brown, J. Mol. Spectrosc. **133**, 244 (1989).
[108]J. Susskind, J. Chem. Phys. **56**, 5152 (1972).
[109]See supplementary material at http://dx.doi.org/10.1063/1.4899263 for the tables of data as briefly discussed in Appendices A, D, and E of the present paper.
[110]D. Papousek and M. R. Aliev, *Molecular Vibrational Rotational Spectra* (Elsevier, Amsterdam, 1982).
[111]U. Fano and G. Racah, *Irreducible Tensorial Sets* (Academic Press, New York, 1959).
[112]E. P. Wigner, *Quantum Theory of Angular Momentum* (Academic Press, New York, 1965).
[113]H. H. Nielsen, Rev. Mod. Phys. **23**, 90 (1951).
[114]D. A. Varshalovitch, A. N. Moskalev, and V. K. Khersonsky, *Quantum Theory of Angular Momentum* (Nauka, Leningrad, 1975).
[115]R. Zare, *Angular Momentum: Understanding Spatial Aspects in Chemistry and Physics* (Wiley, New York, 1988).
[116]A. E. Cheglokov, V. N. Saveliev, and O. N. Ulenikov, J. Phys. B: At., Mol. Opt. Phys. **19**, 3687 (1986).
[117]A. E. Cheglokov and O. N. Ulenikov, J. Mol. Spectrosc. **110**, 53 (1985).
[118]Y. S. Makushkin and O. N. Ulenikov, J. Mol. Spectrosc. **68**, 1 (1977).
[119]R. Georges, M. Herman, J. C. Hilico, and O. Robert, J. Mol. Spectrosc. **187**, 13 (1998).
[120]A. Nikitin, X. Thomas, L. Regalia, L. Daumont, P. Von der Heyden, V. Tyuterev, L. Wang, S. Kassi, and A. Campargue, J. Quant. Spectrosc. Radiat. Transfer **112**, 28 (2011).
[121]I. M. Mills and A. G. Robiette, Mol. Phys. **56**, 743 (1985).
[122]T. J. Lee, J. M. L. Martin, and P. R. Taylor, J. Chem. Phys. **102**, 254 (1995).
[123]J. M. Bowman, T. Carrington, and H. D. Meyer, Mol. Phys. **106**, 2145 (2008).
[124]H. G. Yu, J. Chem. Phys. **121**, 6334 (2004).
[125]E. Venuti, L. Halonen, and R. G. Della Valle, J. Chem. Phys. **110**, 7339 (1999).
[126]A. D. Bykov, Y. S. Makushkin, and O. N. Ulenikov, J. Mol. Spectrosc. **85**, 462 (1981).
[127]A. D. Bykov, Y. S. Makushkin, and O. N. Ulenikov, J. Mol. Spectrosc. **93**, 46 (1982).
[128]A. D. Bykov, Y. S. Makushkin, and O. N. Ulenikov, Mol. Phys. **51**, 907 (1984).
[129]O. N. Ulenikov, E. S. Bekhtereva, A. L. Fomchenko, A. G. Litvinovskaya, C. Leroy, and M. Quack, Mol. Phys. **112**, 2529 (2014).
[130]A. E. Cheglokov, O. N. Ulenikov, A. S. Zhilyakov, V. N. Cherepanov, Y. S. Makushkin, and A. B. Malikova, J. Phys. B: At., Mol. Opt. Phys. **22**, 997 (1989).
[131]Y. S. Makushkin, O. N. Ulenikov, A. E. Cheglokov, V. N. Cherepanov, A. S. Zhilyakov, and A. B. Malikova, J. Phys. B: At., Mol. Opt. Phys. **23**, 1149 (1990).
[132]A. De Martino, R. Frey, and F. Pradere, Mol. Phys. **55**, 731 (1985).
[133]A. V. Nikitin, M. Rey, and V. G. Tyuterev, Chem. Phys. Lett. **501**, 179 (2011).
[134]D. W. Schwenke and H. Partridge, Spectrochim. Acta A **57**, 887 (2001).
[135]M. Rey, A. V. Nikitin, and V. G. Tyuterev, J. Chem. Phys. **136**, 244106 (2012).
[136]X. G. Wang and T. Carrington, J. Chem. Phys. **141**, 154106 (2014).
[137]R. Marquardt, M. Quack, and I. Thanopulos, J. Phys. Chem. A **104**, 6129 (2000).
[138]R. Marquardt and M. Quack, "Energy redistribution in reacting systems," in *Encyclopedia of Chemical Physics and Physical Chemistry. Volume 1: Fundamentals*, edited by J. Moore and N. Spencer (IOP Publ., Bristol, 2001), pp. 897–936.
[139]M. Quack, Chimia **55**, 753 (2001).
[140]T. Carrington, Jr., "Using iterative methods to compute vibrational spectra," in *Handbook of High-Resolution Spectroscopy*, edited by M. Quack and F. Merkt (John Wiley & Sons, Ltd., Chichester, 2011), Vol. 1, Chap. 14, pp. 573–585.
[141]J. Tennyson, "High accuracy rotation - vibration calculations on small molecules," in *Handbook of High-Resolution Spectroscopy*, edited by M. Quack and F. Merkt (John Wiley & Sons, Ltd., Chichester, 2011), Vol. 1, Chap. 13, pp. 551–571.
[142]A. G. Csaszar, C. Fabri, T. Szidarovszky, E. Matyus, T. Furtenbacher, and G. Czako, Phys. Chem. Chem. Phys. **14**, 1085 (2012).
[143]G. Pierre, J. C. Hilico, C. Debergh, and J. P. Maillard, J. Mol. Spectrosc. **82**, 379 (1980).
[144]J.-M. Jouvard, B. Lavorel, and J.-P. Champion, J. Mol. Spectrosc. **150**, 201 (1991).
[145]R. Z. Martinez, D. Bermejo, J. Santos, J. P. Champion, and J. C. Hilico, J. Chem. Phys. **107**, 4864 (1997).

This article is copyrighted as indicated in the article. Reuse of AIP content is subject to the terms at: http://scitation.aip.org/termsconditions. Downloaded to IP: 129.132.218.57 On: Tue, 16 Dec 2014 16:10:57